THYRISTOR CONTROLLERS FOR SLIPRING INDUCTION MOTOR

A Thesis Submitted
In Partial Fulfilment of the Requirements
for the Degree of
DOCTOR OF PHILOSOPHY

By
NAVIN S WANI

to the

DEPARTMENT OF ELECTRICAL ENGINEERING
INDIAN INSTITUTE OF TECHNOLOGY KANPUR
MARCH 1978

POST GRADUATE OFFICE
IIT Kanpur
Submitted on 14-3-79
RL

C E R T I F I C A T E

It is certified that this work, "Thyristor Controllers for Slipring Induction Motors" by N. S Wani, has been carried out under my supervision and that this work has not been submitted elsewhere for a degree.

M.Ramamoorty

(M.RAMAMOORTY)
Professor,
Department of Electrical Engg.,
Indian Institute of Technology,
Kanpur, India.

POST GRADUATE OFFICE
This thesis has been approved
for the award of the Degree of
[illegible]
in accordance with the
regulations of the Indian
Institute of Technology Kanpur
Dated 14 9 79 RL

EE-1979-D-WAN-THY

Class
Acc. No. 55765.

Thesis
621.4162
W186t

- 8 NOV 1979

ACKNOWLEDGEMENTS

I express my deep sense of gratitude to Dr. M. Ramamoorty for suggesting the research problems discussed in this thesis, and for his kind, valuable and encouraging guidance at all stages of this work.

My thanks are due to many of my teachers, colleagues and staff of Electrical Engineering Dept. of I.I.T.Kanpur, but for their help on various occasions the completion of this work would have been impossible.

I wish to thank the authorities of Research and Development Centre, SAIL, Ranchi for granting me leave to complete my thesis work.

I wish to acknowledge the research facilities provided by the authorities of I.I.T.Kanpur and the fast and skilful typing of Mr. K.N. Tewari.

IIT-Kanpur
March, 1978

Navin S. Wani

TABLE OF CONTENTS

LIST OF FIGURES

SYNOPSIS

N.S.WANI
Ph.D.
Department of Electrical Engineering
Indian Institute of Technology, Kanpur
January, 1978

THYRISTOR CONTROLLERS FOR SLIPRING INDUCTION MOTOR

From the beginning of industrial revolution, the trend has been toward automation of various industrial operations. In the recent past developments in solid-state electronic circuits have accelerated the automation trend at various levels. Simultaneous growth in the field of power semiconductors made the industrial drives amenable to the application of signal and power modulation techniques so far associated with data processing and communication equipments only.

Most of the industrial drives are induction motors due to their economy and ruggedness compared to dc drives. However, dc shunt motor is still the champion in terms of breadth of application in adjustable speed drives due to the easiness in speed control. But it has its age-old commutator arcing and maintenance problems. This has led to the development of variable speed controllers for ac synchronous and induction motors. Speed control of synchronous motor requires variable voltage and variable frequency source.

The conventional methods of induction motor speed control are as follows.

i) Stator voltage control

ii) Stator voltage and frequency control

iii) Rotor power control

iv) Rotor resistance control.

The first method is simple but inefficient for low speed operation and gives poor starting torque. The second method gives wide range speed variation with very good efficiency. However, the complexity of this scheme makes it uneconomical for low power applications. The third and fourth methods are applicable to slipring induction motors only. Speed-torque characteristic of slip power controlled drive is similar to that of DC shunt motor. Method of rotor resistance control is simple and economical in nature, though it suffers from poor efficiency at low speeds.

The aim of the present thesis is to study the third and fourth methods of speed control techniques applicable to the slipring induction motor, and propose mathematical models of the drive system for the analysis of steady-state and dynamic performance.

The principle of slip power recovery from the rotor circuit has been commonly utilized in rotating Scherbius and Kramer cascade systems. In recent years solid state frequency converters have been used in place of rotating

auxiliary machines, providing compact, high efficiency, variable speed static drives with better dynamic response and good control characteristics.

Feeding rotor power to line poses a difficult problem since the rotor power has both a variable voltage and variable frequency. The variable frequency problem is overcome by rectifying the rotor output in which case only a line commutated inverter is required to feed variable voltage dc power into constant voltage ac line.

In this thesis, problems associated with slip power control are discussed, and it is pointed out that slip power control is economical only for sub-synchronous operation. Super-synchronous operation requires that both the converters should be fully controlled bridges. Moreover, designing firing circuits for wide variations in slip frequency requires elaborate firing circuits and/or rotating transducers mounted on the same shaft.

Though various techniques for power factor improvement are available such as asymmetrical triggering or forced commutation, these methods give increased distortion in line current. Hence these methods were not attempted here.

A sub-synchronous slip power recovery controller was designed for 3 HP slip-ring motor. The power circuit comprises a diode bridge, a fully controlled thyristor

bridge, a smoothing inductor, and a bleeder resistor. This arrangement is capable of only returning slip power from rotor circuit to ac line and not vice-versa. The appropriate values of smoothing inductor and resistor help in maintaining continuous current in dc path and hence linear operation of line commutated converters.

DC circuit model is developed and comparison of speed-torque characteristics obtained from this model is made with that of experimentally obtained results.

The co-sine comparator arrangement is used in firing circuits. This gives linear relation between average output voltage and control voltage to firing circuit. Hence, thyristor converter is treated as a linear, switching mode power amplifier.

A closed loop controller is designed to obtain improved speed regulation. The scheme is as follows:

A PI controller is used for speed control loop. This loop contains another inner loop with PI controller for current control. The output of speed controller which has adjustable saturation level provides reference signal for current control loop. Because of this arrangement, during starting and under overload condition motor current and hence torque is limited to preset value, corresponding to saturation level of speed controller

output. Moreover, current control loop maintains constant current against disturbances in supply voltage. The closed loop speed-torque characteristics of the drive are almost flat giving speed regulation better than 0.5 percent.

The complete transient analysis of induction motor is quite difficult. The presence of bridge rectifier and inverter makes it all the more difficult. Therefore, it is not possible to derive analytically a transfer function that will be valid under all conditions. However, transfer function that will be valid under certain simplifying assumptions is derived.

If voltage drop across stator impedance and voltage loss due to commutation is ignored, relation between motor torque and rotor current becomes linear. It is shown that this assumption is valid almost upto full load rotor current. Moreover, it is mentioned earlier that thyristor converter could be considered as linear amplifier. Based on these assumptions transfer functions for motor and controller are developed. It is shown that these transfer functions hold good over a wide range.

These transfer functions are used to study the transient response of the drive for step-input signals. The design of PI controllers is also based on the same transfer functions.

Comparison of motor speed and rotor current transient response computed from these transfer functions with experimentally obtained response is given. The Chapters 2 and 3 cover in detail the slip power recovery scheme mentioned above. The other method of speed control of slipring motor discussed in the thesis, is by rotor resistance control.

Conventionally, the rotor resistance is controlled manually and in discrete steps. Using thyristors, the conventional resistance control scheme can be eliminated either by using a 3-phase rectifier bridge and a chopper controlled external resistance, or phase controlled thyristors in the rotor circuit. Use of phase controlled thyristors require no commutation circuit, however, obtaining synchronizing signal corresponding to variable frequency rotor voltage is somewhat difficult. Hence wide range speed control using this method requires rotating sensors mounted on the shaft. A chopper is a power switch electronically monitored by a control circuit, The equivalent rotor resistance is altered by changing the duty cycle of the chopper. A simple arrangement of switching resistor gives discontinuity in rotor currents and hence excessive harmonic losses. This problem is solved by introducing a filter in the rotor circuit. This improvement gives continuous ripple

free dc in the rotor circuit, and permits application of motor with almost 90 percent derating factor.

The chopper control scheme for variable speed control of slipring induction motor is discussed in Chapters 4 and 5. It has been shown that using a simple L-R filter restricts the external resistance to a very small value resulting in not so wide variation in the speed-torque characteristics. A superior scheme of using a second order, i.e., L-C-R, filter in the rotor circuit is suggested. This arrangement permits very high value (even removal) of external resistance, which gives wide variations in the characteristics. It is shown that use of high speed thyristors will permit operation at higher frequency and hence reduction in filter component size. Design considerations for second order filter are also given.

DC circuit model for this scheme is derived. Comparison of speed-torque characteristics based on this model and experimental results is also given.

With 2nd order filter it is not easy to get closed form solution for rotor current for the following reasons:

1. Each switching operation introduces transients - and it is a tedious job to determine boundary values under steady state condition.

2. Presence of leakage reactance on the ac side makes it all the more difficult.

Hence, iterative procedure is adapted to determine the steady state current wave form and thereby average current and torque developed for the given motor speed.

The rotor resistance controlled slipring motor has very poor speed regulation with open loop cntrol. In many industrial applications, very good speed regulation of the drive is essential. Precision closed loop regulator for conventional rotor resistance control is impractical. However, with thyristor chopper precision speed control could be obtained.

Design of closed loop controller is same as that of slip power recovery scheme. The closed loop controller used for chopper controlled drive also incorporates speed and current feedbacks. Speed regulation is better than 0.5 percent.

Since for a chopper circuit without filter,current wave form could be highly distorted, derivation of average current feedback signal did pose a problem. To reduce the ripple amplitude in such current feedback signal would require a filter with large time constant, particularly when the chopper frequency is low. Moreover, filter time constants would be different for different chopper frequency,

and also for different parameters of chopper filter. A simple filter in the current feedback path may have adverse effect on the dynamic performance of the drive. To overcome these problems a novel high speed average current sensing circuit is developed. This circuit samples and holds the minimum and maximum values of rotor current for each cycle and outputs the average value for that cycle. It is shown that since the nature of current increase or decrease is almost linear, the output signal corresponds to the average value of rotor current.

For 'chopper controlled slipring motor' rotor winding currents and dc equivalent circuit are similar to that of slip power recovery. Hence, the voltage drop across stator impedance and voltage loss due to commutation could be ignored under light load for this scheme also. This assumption simplifies analysis by making torque and rotor current relation linear. Moreover, rotor circuit time constants during 'ON' and 'OFF' modes are not equal. This results in highly nonlinear relation between rotor current and chopper duty cycle. However, transfer functions that will be valid for small perturbations are derived, the parameters being dependent on the given steady-state operating point.

These transfer functions are used to study the dynamic performance of the drive. The design of closed loop controller is also based on these transfer functions. Comparison of experimental and computed results based on these transfer functions is also given.

CHAPTER 1

INTRODUCTION

In the recent past developments in the area of power semiconductors and electronic circuits have given way to the revolutionary approach to the control of industrial drives. Thyristor controllers, the outcome of these developments, are rapidly replacing the conventional motor control devices like rotating amplifiers, mercury arc converters and motor-generator sets due to their superiority in operation, maintenance and amenability to signal and power modulation techniques associated so far with communication and data-processing equipments only.

Most of the industrial drives are induction motors due to their economy and ruggedness compared to dc drives. However, dc shunt motor is still the most commonly used motor for adjustable speed drives due to the easiness in speed control. But it has its age-old commutator arcing and maintenance problems. This has led to the development of variable speed controllers for ac motors. Though the thyristor controller like variable voltage and variable frequency controller for cage motor (Section 1.2) involves complex and expensive

circuitry it works out one of the most competitive controller for high power drives used in hazardous environment Moreover, it is expected that future developments in power transistors and gate turn-off thyristors will make these controllers far more reliable and economical for low and medium power drives.

The conventional methods of induction motor speed control are as follows

i) Stator voltage control
ii) Stator voltage and frequency control
iii) Slip power control
iv) rotor resistance control.

A brief discussion of these methods is given in the following sections.

1.1 STATOR VOLTAGE CONTROL

From induction motor theory, it is known that the torque developed by motor at a given speed is proportional to the square of the airgap voltage. Therefore, motor torque can be varied by adjusting stator voltage. The corresponding variation in speed-torque characteristics is given in Figure 1.1. It is observed from the speed torque characteristics that this method of control gives poor speed regulation, reduced pullout torque, and

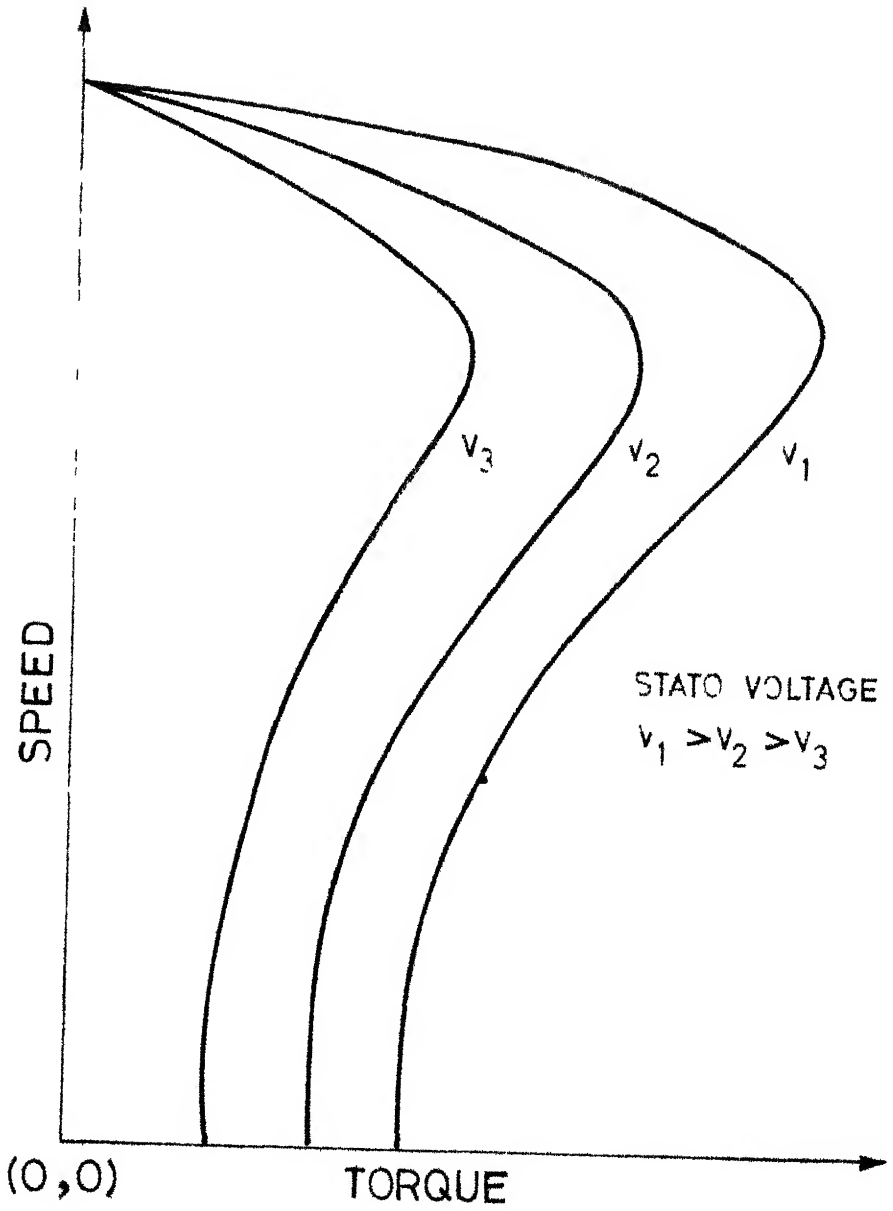

FIG.1.1 SPEED-TORQUE CHARACTERISTICS-
STATOR VOLTAGE CONTROL

also lower starting torque for reduced voltages. These limitations in speed torque characteristics make this speed control technique suitable for fan type loads only, where load torque is proportional to the square of the speed. For constant load torque this method will give speed control over limited range.

Conventionally, variable voltage is obtained by using variac or tape-changing transformer. Solid state alternatives comprise of thyristors, triacs, or reverse conducting thyristors used in different configurations to control the rms voltage across stator [1,2,3]. The stator voltage is controlled by controlling the firing angle of these devices and the nature of commutation is natural (line) commutation. However, forced commutation is also used when power factor improvement is essential.

The phase control scheme with natural commutation is the simplest method of controlling induction motor. The major drawbacks of this method are its poor efficiency at low speeds and reduced torque for low voltages. This technique is commonly used for controlling small capacity drives like portable machine tools, fans etc.

1.2 VARIABLE VOLTAGE AND VARIABLE FREQUENCY CONTROL [4,5]

The method of stator voltage and frequency control is ideally suitable for induction motor speed control.

The speed torque characteristics obtained with this method are similar to that of variable voltage control of dc separately excited motor. The slip power recovery scheme (Section 1.3) also gives similar speed torque characteristics. However, this scheme is not applicable to cage induction motor, which is most commonly used.

For induction motor synchronous speed is proportional to supply frequency. And operating speed is slightly less than the synchronous (no-load) speed of the motor. Hence motor speed can be controlled by varying supply frequency. However, a reduction in supply frequency will increase the air-gap flux and magnetizing current and it may even saturate the core resulting in excessive stator winding currents. Therefore, variable frequency control is always accompained by variable voltage control in order to keep voltage to frequency ratio (V/F) constant, and hence constant air-gap flux throughout the operating range. Consequently, this scheme maintains constant pullout torque for the sub-synchronous operation of the motor. For the supply frequencies higher than the rated frequency, it is not possible to keep (V/F) ratio constant due to limitations of the motor.

Conventionally, this scheme was implemented by using variable speed/frequency rotating generators for driving the induction motor. By now large number of thyristor inverter configurations are available as variable voltage and frequency source required for induction motor control. No doubt, thyristors have played an important role in popularizing this method. A typical controller scheme consists of a phase controlled rectifier followed by variable frequency inverter feeding the induction motor. The firing angle and frequency are adjusted to obtain the required characteristics. The availability of high voltage thyristors gave rise to the development of current source inverters. These inverters are capable of providing regenerative braking of the motor.

At present only points against inverter circuits are their low reliability compared to controlled rectifiers, elaborate commutation circuits, and high cost. It is expected that future developments in power transistors and gate turn-off SCR's will solve these problems for low and medium power drives.

1.3 SLIP POWER CONTROL

It is known that the secondary electrical power for induction motor is proportional to slip. Hence,

continuous low speed operation is inherently inefficient. Thus if slip power is recovered from the secondary instead of dissipating it in the rotor winding and external resistance, if any, then the overall efficiency of the system can be improved drastically. In a slip power recovery scheme, the slip power is either returned to the supply lines or is used to drive an auxiliary motor coupled to the same shaft. This principle has been commonly utilized in rotating Scherbius and Kramer cascade systems. This method, like stator voltage and frequency control, also gives speed torque characteristics similar to that of dc separately excited motor with armature voltage control.

The problem of transferring power between a constant voltage and constant frequency supply line, and a variable voltage, variable frequency source at slipring can be solved either by providing (1) a 3-phase to 3-phase cycloconverter, or (2) by rectifier/inverter connections. In either of these schemes, if slip power is recovered and fedback to the supply, speed control for sub-synchronous motoring and super-synchronous regenerative braking are obtained. If additional power is injected into the rotor circuit, speed control for super-synchronous motoring and sub-synchronous regenerative braking are obtained. The four quadrant operation of such controllers is explained in Figure 1.2.

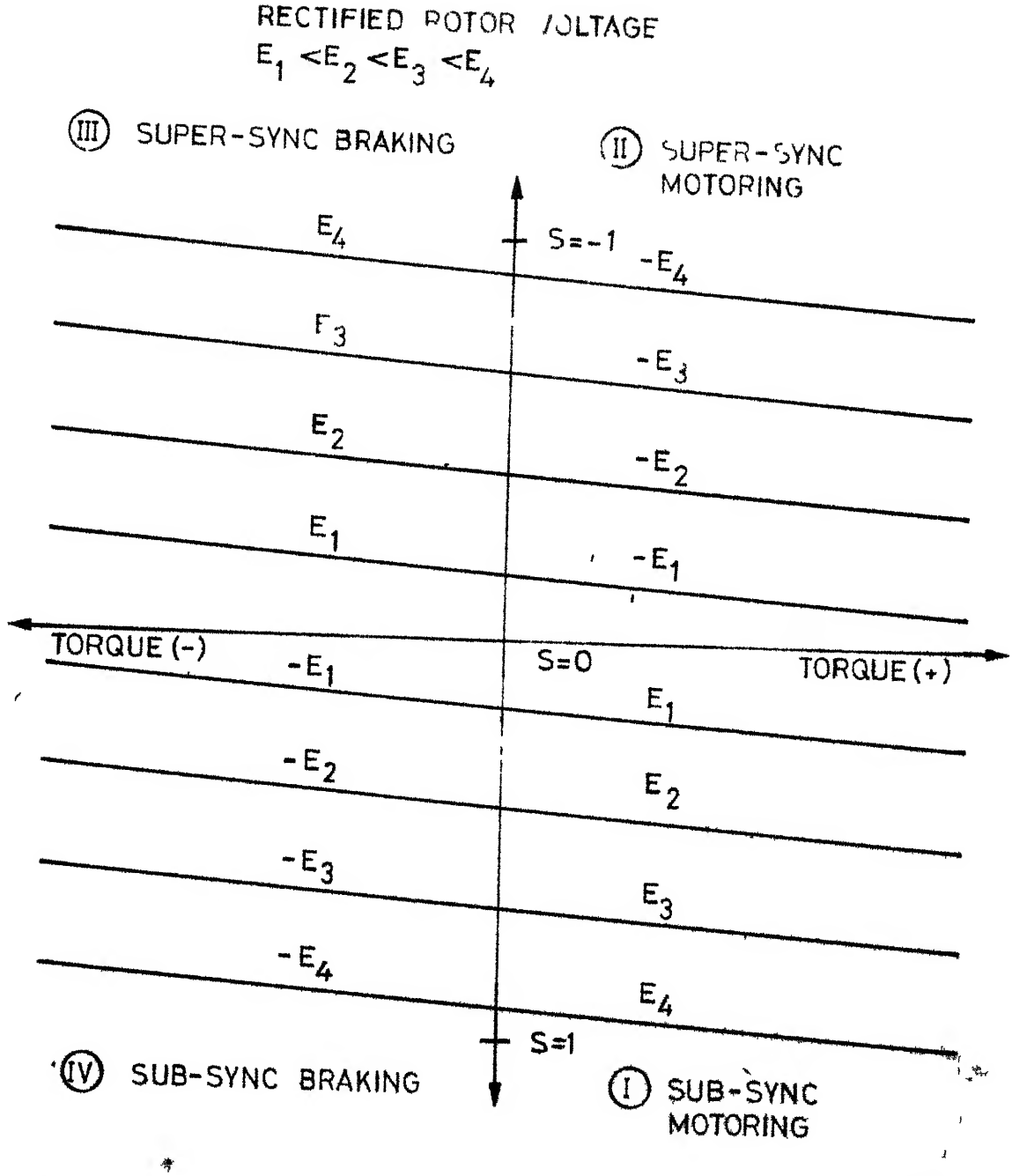

FIG 1.2 SPEED-TORQUE CHARACTERISTICS-SLIP POWER CONTROL

In a cycloconverter scheme, 50 Hz constant voltage supply is converted to rotor voltage at slip frequency. The power-flow direction is controlled by adjusting phase difference (or polarity) between the rotor induced voltage and cycloconverter output

In the second method two fully controlled bridges are used (refer Figure 2.1) and depending on the mode of control of these bridges either rotor power is recovered from or fed into the rotor circuit. When uncontrolled bridge (rectifier) on slipring side and a line commutated inverter on supply side are used, only sub-synchronous motoring and super-synchronous regenerative braking are possible with this scheme. When both the converters are fully controlled, the converter on the slipring side requires elaborate control circuits. Moreover, expenditure on two controllers may be prohibitive in many applications. However, the scheme with only one fully controlled bridge and an uncontrolled rectifier is a highly economical alternative for controlling high power drives (100 KW and above) in sub-synchronous range.

The notable feature of slip power control scheme is super-synchronous motoring is possible, unlike stator voltage and frequency controller, without any reduction

in torque developed, and at the same time electrical parameters of the drive are within specified limits.

1.4 ROTOR RESISTANCE CONTROL

At a given speed, torque developed by induction motor can be varied by changing the effective rotor resistance. This technique is commonly used for starting the slipring motor. When this method is applied for speed control of slipring motor its major drawback, like stator voltage control, is poor efficiency at low speed. Therefore, this method is used for low or medium power drives only. The advantages of this scheme over stator voltage control are

i) wide range speed control is possible, irrespective of the load speed torque characteristics, and
ii) pullout torque is independent of rotor resistance (refer Figure 1.3).

Conventionally, external resistance connected in the rotor circuit is controlled manually in descrete steps. Using power semiconductors, the conventional resistance control can be eliminated by using 3-phase rectifier bridge and chopper controlled external resistance. The simple arrangement of resistance and chopper in the rotor circuit cause highly distorted waveforms of rotor winding currents. The filter

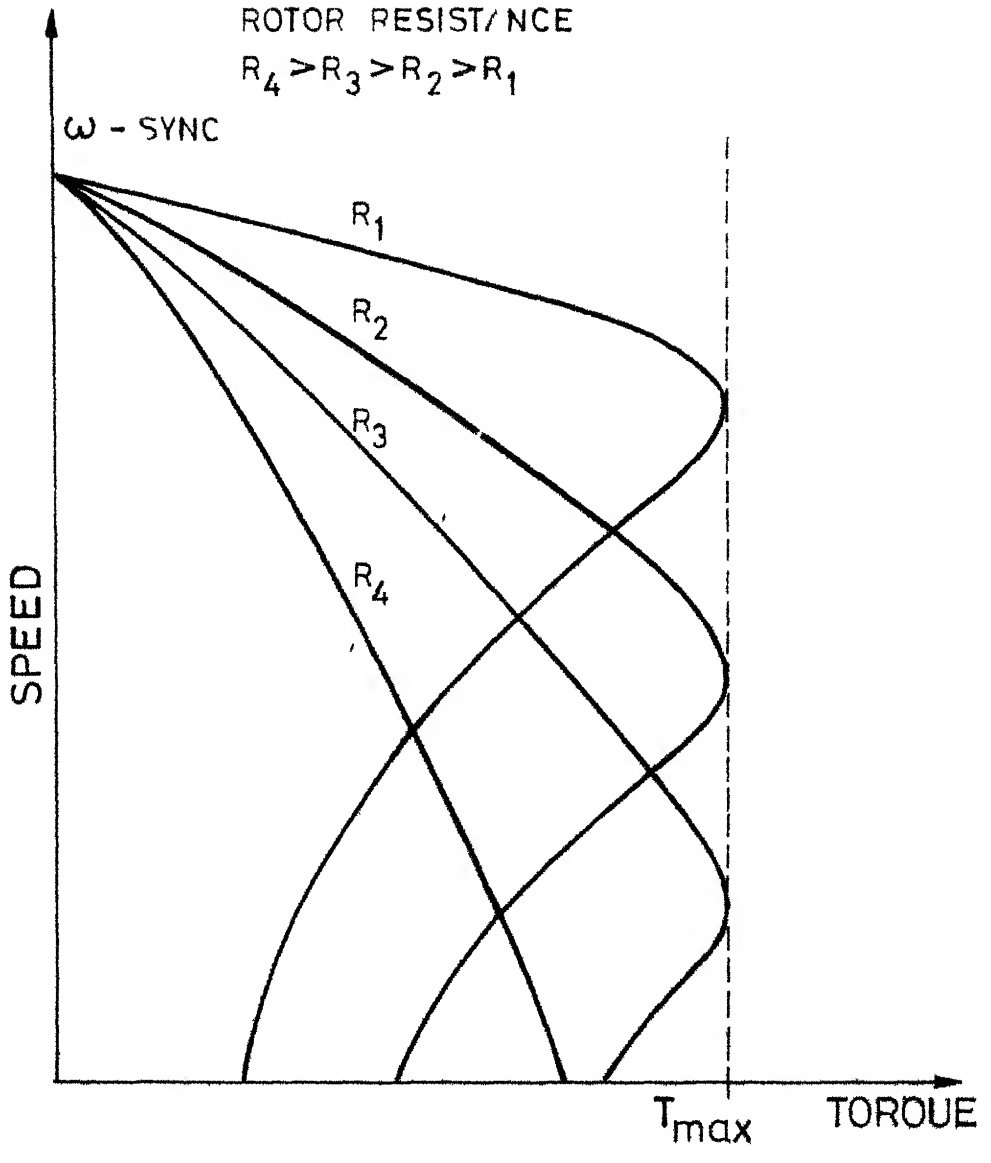

FIG.1.3 SPEED-TORQUE CHARACTERISTICS
ROTOR RESISTANCE CONTROL

circuit between 3-phase rectifier and chopper is incorporated to solve this problem.

The other alternatives of controlling effective rotor resistances are i) short circuiting rotor circuit through phase controlled thyristors or ii) using controlled bridge rectifier with external R-L load on dc side. Since both of these circuits operate on variable frequency source from sliprings, the wide range phase angle control requires elaborate firing circuits and/or rotating transducer mounted on the motor shaft.

The chopper control scheme is simple and also economical for small and medium power slipring motor.

1.5 THESIS OUTLINE

The aim of the present thesis is to study the last two methods of speed control namely, slip power recovery and rotor resistance control, applicable to the slipring induction motor, and propose mathematical models of the drive system for the analysis of steady state and dynamic performance.

In Chapter 2, problems associated with slip power control are discussed and it is pointed out that slip power control is economical only for sub-synchronous operation. Though various techniques for power factor

improvement are available such as asymmetrical triggering or forced commutation, these methods give increased distortion in line current. Hence these methods are not attempted here. In the same chapter, DC circuit model is developed for slip power recovery controlled drive and comparison of speed torque characteristics obtained from this model is made with that of experimentally obtained results.

A sub-synchronous slip power controller is designed for 3 HP slipring motor. The cosine comparator arrangement used for firing circuit for converters gives linear relationship between average output voltage of converter and control voltage to firing circuit.

A closed loop controller is designed to obtain improved speed regulation. This scheme comprises of a PI controller for speed control loop, and another inner loop with PI controller for current control. The speed controller outputs with adjustable saturation level, is used as reference signal for current control loop. This arrangement limits motor current and hence torque developed during starting and overload conditions to preset value determined by speed controller output.

In Chapter 3, a dynamic model for slip power recovery scheme, based on certain simplifying assumptions is derived. Thyristor controller is treated

as a linear, switching mode power amplifier. It is shown that almost upto full load rotor current, the relation between motor torque and rotor current is linear. Based on these assumptions transfer functions are developed. It is shown that these transfer functions are valid over a wide range of motor speed and torque

Chapter 3 also gives complete transient analysis of the drive for step-input reference signals applied to open loop controller, current loop, and speed control loop. The closed loop controller design based on these transfer functions is also given. Comparison of motor speed and rotor current transient response computed from these transfer functions with experimentally obtained response is given.

The chopper control scheme for variable speed control of slipring induction motor is discussed in detail in Chapter 4. It has been shown that using a simple L-R filter restricts the external resistance to a very small value resulting in not so wide variation in the speed torque characteristics. A superior scheme of using a second order filter in the rotor circuit is suggested. This arrangement theoretically permits wide variations in the speed torque characteristics of the drive.

A D C. circuit model, assuming that rotor current in dc path is continuous and ripple free, is developed. Comparison of experimental and computed speed torque characteristics, using this model, is given. The presence of rotor leakage reactance and periodic transients in each cycle of chopper operation makes it difficult to obtain closed form solution for rotor current waveform. Hence iterative procedure is adapted to determine the steady-state current waveform and thereby average current and torque developed for the given motor speed.

The design of closed loop speed controller for chopper controlled slipring motor given in Chapter 4 is similar to that of slip power controller given in Chapter 2. A novel high speed average current sensing circuit is developed for current feedback. This circuit samples and holds the minimum and maximum values of rotor current for each cycle and outputs the average value for that cycle. The effective time constant of this circuit is independent of chopper filter component size or rotor current waveform. Since output of this circuit is ripple free it does not require any additional filter. This circuit is superior compared to other alternatives, when rotor current waveform is highly distorted. The comparatively small time constant of this circuit gives superior dynamic performance of the drive.

Chapter 5 gives dynamic model and transient response of chopper controll slipring motor. In Chapter 4, it is pointed out that the rotor circuit time constants during ON and OFF modes of chopper are not equal. And it is observed that this results in highly nonlinear relation between rotor current and duty cycle. However, transfer functions that will be valid for small perturbations are derived, the parameters being dependent in the given steady state operating point. The rest of the simplifying assumptions are same as the assumptions given in Chapter 3 for slip power control. Moreover, a dynamic analysis and closed loop controller design based on these transfer functions are given in this chapter. Comparison of computed and experimentally obtained results is also given.

Concluding remarks are given in Chapter 6

CHAPTER 2

SLIP POWER RECOVERY SCHEME

2.1 INTRODUCTION

The principle of slip power recovery from the rotor circuit has been commonly utilized in rotating Scherbius and Kramer cascade systems. In recent years solid-state frequency converters have been used in place of rotating auxiliary machines, providing compact, high efficiency variable speed static drives with a better dynamic response and good control characteristics [6,7].

From the induction motor theory, it is known that the secondary electrical power is proportional to slip. Hence continuous high slip (low speed) operation is inherently inefficient. Therefore, the speed control of Induction Motor by variable voltage at constant frequency or by variation of external rotor resistance is inefficient. Moreover, variable voltage and constant frequency control at low voltage suffers from the further disvantages of

1. the rapid temperature rise caused by excessive winding current,
2. reduced torque at low speeds

Thus if the slip power is recovered from the secondary instead of dissipating it in the rotor winding and external resistance, if any, then the overall efficiency of the system can be improved drastically. In a slip power recovery scheme, the slip power is either returned to the supply lines or is used to drive an auxiliary motor coupled to the shaft.

The design of slip power controlled drive, complete with speed and current feedback is given in this chapter.

2.2 STATIC SLIP POWER CONTROL SCHEME

The slip power control scheme requires that the voltage at slip frequency is injected in the rotor circuit to absorb the slip power when motor is running at subsynchronous speeds, and to feed power when it is running at super-synchronous speeds. With the use of thyristors it has become possible to implement this technique without using auxiliary machines or commutator machine.

The problem of transferring power between a constant voltage and constant frequency supply line, and a variable voltage, variable frequency source at sliprings can be solved either by providing [8,9]

1 a 3-phase to 3-phase cycloconverter,

or 2 by a rectifier and a line commutated inverter.

In a cycloconverter scheme 50 Hz constant voltage supply is converted to rotor voltage at slip frequency The power flow direction is controlled by adjusting phase difference (or polarity) between the rotor induced voltage and cycloconverter output. Hence it is possible to obtain sub-synchronous and also super-synchronous speeds with the same arrangement.

The second scheme using line commutated converters is given in Figure 2.1. The converters I and II are fully controlled bridges. Assuming 'voltage drop' across inductor $L_d \simeq 0$, output voltage of Converter II is equal to that of Converter I.

For this scheme, no load slip

$$S_o = \frac{V_2 \cos \alpha}{E_2 \cos \beta} \qquad (2.1)$$

where V_2 - secondary supply voltage/phase

E_2 - rotor induced voltage/phase for slip S=1

α, β - firing angles for Converters I and II respectively.

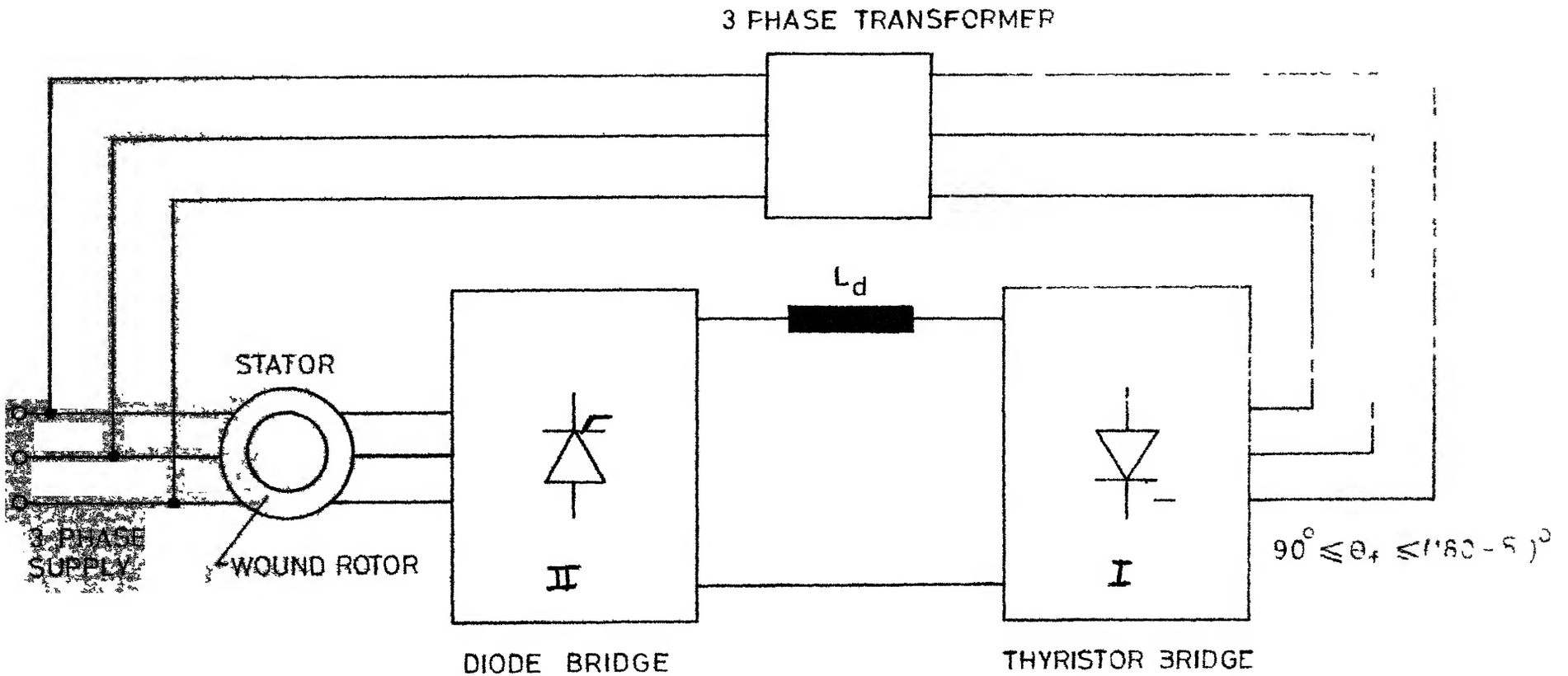

FIG. 2.1 THYRISTOR CONTROLLER FOR SLIPRING INDUCTION MOTOR-SLIP POWER RECOVERY SCHEME

From eqn (2.1), it is observed that by controlling firing angles α and β, it is possible to control the no-load slip of the motor. The power flow in both the directions is possible only when both the converters are fully controlled type. For power flow from rotor to supply, Converter II should function as rectifier i.e., $0 \leq \beta \leq \pi/2$, and Converter I as inverter i.e., $\pi-\delta \geq \theta_f \geq \pi/2$, where δ is commutation angle.

At this stage, it should be pointed out that controlling firing angle β for Converter II is not easy, since no synchronising signal is directly available from the rotor circuit. In the literature [8,9] various methods of controlling β are suggested where elaborate firing circuits and/or rotating sensors mounted on the same shaft are used. However, for Converter I it is easy to control firing angle as synchronising signal is available from the supply. Now, even if the problem of controlling Converter II is solved, use of two full controlled converters will make the cost of slip power controller uneconomical. On the other hand, when Converter II is uncontrolled, i.e. diode bridge, the whole control unit becomes quite simple and economical. Of course, now it has many limitations, one of them is motoring operation at synchronous speed is not possible. However, with this

simple arrangement following 3-modes of control are possible

i) motoring for $1 \geq S \geq 0$

ii) regenerative braking for $S < 0$

iii) dynamic braking for $1 \geq S \geq 0$, where S is motor slip.

The dynamic braking requires switching of stator from ac to dc supply.

2.3 POWER FACTOR IMPROVEMENT

The normally used line commutated converter is of symmetrically triggered type This has the serious drawback of poor power factor, particularly when firing angle is near 90°. When line commutated inverter is used in the rotor circuit, power fed to the supply has leading power factor since firing angle varies between 90° to 180°. Consequently, reactive component drawn from the supply is lagging. This makes overall power factor of the slip power recovery scheme poor. For large capacity drive this decrease in power factor becomes objectionable, particularly for higher speeds, i.e., when inverter firing angle is near 90°. The amount of lagging power drawn from the supply can be reduced considerably when asymmetrical triggering of thyristors is used. With asymmetrical triggering converter has two distinct modes

of operation viz., rectifier/inverter operation depending on firing angle of the positive half cycle side thyristors, and free-wheeling operation. For inverter operation firing angle of positive side thyristors is kept close to 180° and duration of free-wheeling operation is controlled by varying firing angle of negative side thyristors between 180° to 360°. Such inverters due to their free-wheeling mode of operation are known as through-pass inverters.

Miljanic [10] has suggested a method in which forced commutation is used for turning-off thyristors on the negative side of the converter. With this technique the usual limitation on firing angle for line commutated converter that $\theta_f \leq 180-\delta$, is no longer necessary and firing angle is always kept beyond 180°. Hence this type of converter draws leading power from the supply, and help in improving the overall power factor of the drive. The major drawback of both the schemes is considerable increase in distortion of line current waveforms Hence these techniques were not attempted here.

2.4 SLIP POWER RECOVERY FOR SUB-SYNCHRONOUS MODE

Figure 2.2 gives the power circuit for sub-synchronous slip power control using thyristor converters. The system consists of a 3-phase diode bridge

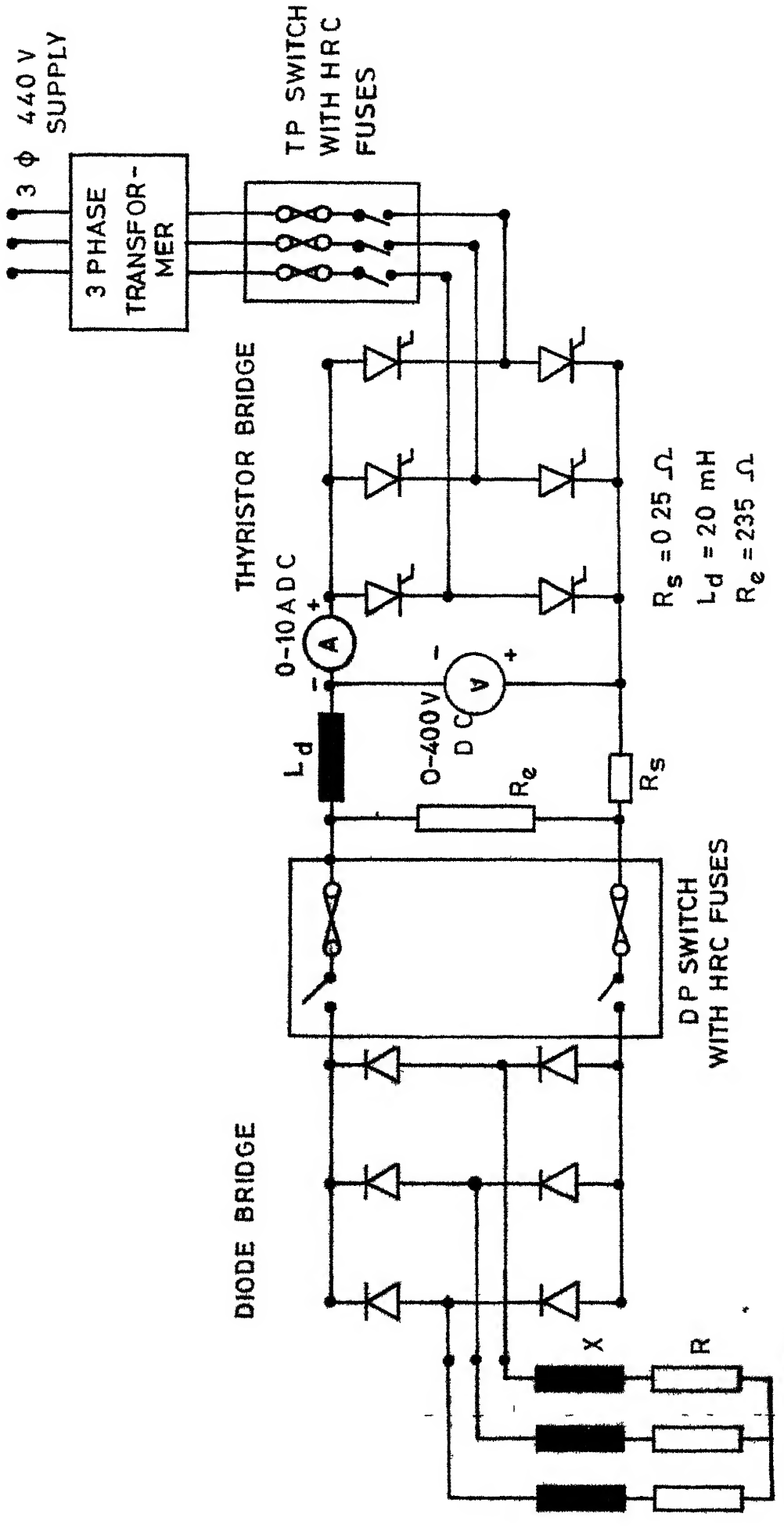

FIG.2.2 POWER CIRCUIT-SLIP POWER RECOVERY SCHEME

rectifier which operates at slip frequency and feeds rectified slip power through the smoothing inductor L_d to the line commutated thyristor inverter, which in turn, returns the rectified slip power to the ac power supply. In sub-synchronous range slip is always positive and the slip power is recovered from the rotor circuit.

The external resistance R_e across the diode bridge ensures continuous current flow through the choke. The absence of resistance will result in discontinuous conduction and hence a speed increase at very light loads The smoothing inductor L_d in dc path is necessary to maintain continuous conduction under normal loading conditions, and also to reduce ripple content in winding and supply side currents However, the larger values of L_d will have adverse effect on the dynamic performance of the drive A reasonably high value of R_e helps in continuous conduction even under very light loads. The design considerations for the inductor L_d are given in [12].

A 3-phase transformer is used for inverter ac supply. The reason for using transformer is discussed below.

In this scheme, since Converter II is a diode bridge, eqn. (2.1) becomes,

$$\text{no load slip } S_o = \frac{V_2 \cos \alpha}{E_2} .$$

From this relation, it is obvious that for $V_2 = E_2$, no load slip could be set between $S_o = 0$ to $S_o = 1$, depending on the Converter I firing angle α. As a result inverter side power factor will vary between zero lagging to unity. A higher value of V_2 will result in reduced power factor even for $S_o = 1$. Hence proper matching of V_2 with reference to E_2 will improve the average power factor over the given speed control range. It is obvious from the same relation that for braking in reverse direction, i.e. for $S > 1$, V_2 should be higher than E_2.

From this discussion, for sub-synchronous motoring operation transformer is not necessary if stator/rotor turns ratio is unity However, most of the slipring motors have stator/rotor turns ratio greater than unity. Hence, it is necessary to incorporate transformer on the rotor side to obtain better power factor over the given speed control range.

2.5 MODEL DEVELOPMENT [10,13]

For slipring motor exact analysis is tedious, involving the phasor calculations for motor fundamental and harmonic quantities, and step-by-step analysis of

nonlinearities in the rectifier inverter circuits. However, it has been found possible to develop a circuit model from which a good prediction can be made. In the literature [13,14] attempts have been made to use ac, and also dc equivalent circuit model for the slip power recovery scheme The ac circuit model derived is the per-phase equivalent circuit model, while dc circuit model is derived for 3-phase system.

However, it is observed that it is difficult to incorporate the effect of commutation phenomenon, in the ac circuit model for the following reasons.

It is not possible to correlate bridge rectifier terminal voltage drop and phase shift introduced in the fundamental component of the rotor winding current - due to commutation overlap - with the equivalent voltage drop on the ac side and phase shift in the line current introduced by equivalent impedance Such obvious discripancy in ac circuit model makes it less accurate compared to the dc circuit model discussed below.

If for the given firing angle of the Converter I, smoothing inductor L_d is chosen such that ripple in the rectified current I_d is negligible the rotor current is composed of alternating square phase of $2\pi/3$ duration.

Rotor rms current I_2 is given by

$$I_2 = \sqrt{(\frac{2}{3})} I_d \qquad (2\ 2)$$

where I_d is the average value of the rectified rotor current

Figure 2 3(a) shows the per-phase equivalent circuit of induction motor referred to the rotor side. In developing a dc circuit model, the effect of stator and rotor winding parameters on the performance of the dc converters is taken into account. Since, injected emf is obtained from step-down transformer, it is necessary to consider the effect of transformer parameters also. The voltage drop across slipring brushes and diodes cause a reduction in terminal voltage of the bridge rectifier Similarly voltage drop across thyristor is also taken into account. The presence of leakage reactance in the motor windings causes voltage drop due to commutation overlap. Similarly, on the inverter side, there is voltage drop due to transformer leakage reactance.

The system is represented by the dc equivalent circuit as shown in Figure 2 3(b). Rectified output on slipring side and opposing voltage from inverter are represented by equivalent dc sources, effect of ripple being negligible. The winding resistance and equivalent

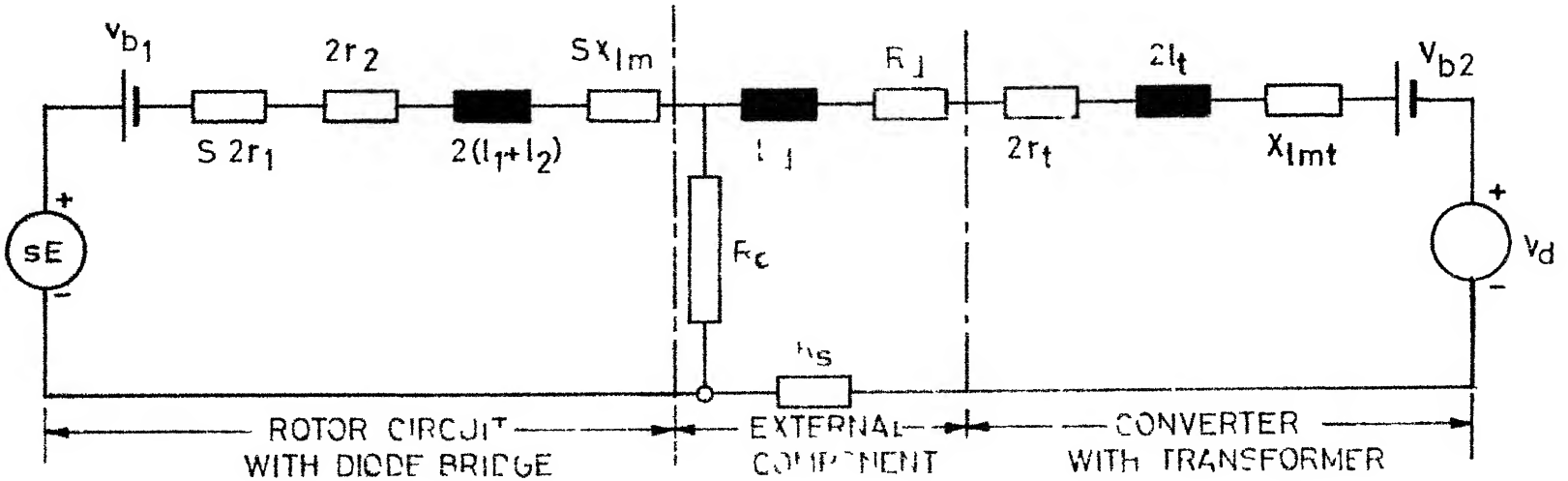

FIG 2 3 (b) D C CIRCUIT MODEL WITH RECTIFIER AND CONVERTER

$2r_1 = 0\ 464\ \Omega$
$2r_2 = 1\ 185\ \Omega$
$r_d = 0\ 8\ \Omega$
$2r_t = 0\ 5\ \Omega$
$R_s = 0\ 25\ \Omega$

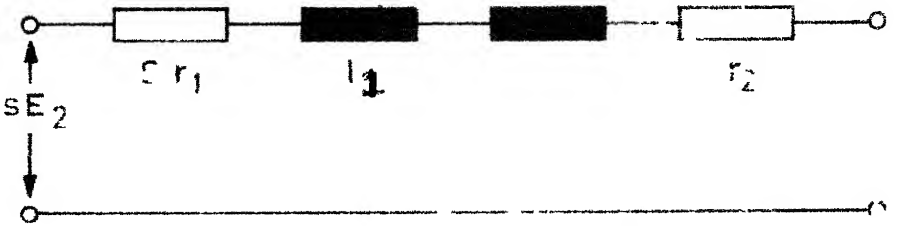

$L_d = 50\ 0$ mH
$2(l_1+l_2) = 5\ 0$ mH
$2l_t = 6\ 0$ mH
$V_{b1} + V_{b2} = 4\ 2$ V

FIG 2 3 (a) PER PHASE A C CIRCUIT REFERRED TO ROTOR SIDE

resistance representing voltage drop due to commutation are shown in series with respective sources. The separate representation of leakage reactances helps in the transient analysis of the circuit. And the presence of external components in the equivalent circuit is self-explanatory. The steady state voltage balance equation for this circuit model is given by

$$SE = V_d + V_b + [S(2r_1 + X_{\ell m}) + 2r_2]\, I_d + (2r_t + X_{\ell t})I_d + (R_s + R_d)\, I_d \qquad (2.3)$$

where E - average value of rectified rotor voltage

$$= \frac{3\sqrt{6}}{\pi} E_2$$

E_2 - rotor voltage per phase in rms at stand-still

$(\ell_1 + \ell_2)$ - total leakage inductance of motor per phase referred to rotor

r_1 - stator resistance per phase referred to rotor

r_2 - rotor resistance per phase

$X_{\ell m} = \frac{3\,\omega_s}{\pi}(\ell_1 + \ell_2)$

ω_s - supply frequency

$\omega = S.\ \omega_s$

L_d - smoothing inductor

R_d - resistance of L_d

R_e - external resistance to ensure continuous condition

r_t - equivalent resistance of transformer per phase

l_t - equivalent inductance of transformer per phase

$X_{\ell t} = \frac{3\omega_s}{\pi} \ell_t$

$v_b = v_{b1} + v_{b2}$

v_{b1} - voltage drop across two numbers of slipring brushes and two numbers of diodes.

v_{b2} - voltage drop across two numbers of thyristors

$V_d = \frac{3\sqrt{6}}{\pi} V_2 \cos \theta_f$

V_2 = ac side voltage per phase in rms for Converter I

θ_f = firing angle for converter I

R_s = dc current sensing resistance (for closed loop control only)

In writing voltage balance equation following simplifications are made.

1. Since $R_e >> (R_d + R_s + 2r_t)$, and also $>> (2r_1 + 2r_2)$

   its effect on motor characteristics is not considered.

2. For ripple free dc current, commutation voltage drop for diode bridge is

$$\frac{3\omega}{\pi}(\ell_1 + \ell_2) I_d.$$

It should be noted that this relation is based on the assumption that series resistance on ac side of the bridge is negligible compared to the series reactance. For slip power recovery scheme the diode bridge is supplied by variable frequency source, and for low frequency, reactance value becomes comparable to that of winding resistance, and hence above mentioned relation will not hold good. It has been established by Moltgen [15] that this relation will hold good for

$$\frac{\omega_s (\ell_1 + \ell_2)}{r_1 + \frac{r_2}{S}} > 3.0$$

Hence the model developed here holds good only for higher values of slip.

In the following section speed-torque relation, using this dc equivalent circuit is derived. In deriving torque current relation, effect of torque produced by harmonics is ignored. It has been established by [13] that effect of harmonic currents on motor torque is negligibly small

From eqn. (2.3) and equivalent circuit of Figure 2.3(b), rotor electric power is given by

$$SP_2 = (SE - SX_{\ell m} I_d) I_d - S\, 2r_1 I_d^2 ,$$

where $(SE-S X_{\ell m} I_d)$ is the effective dc voltage

available in the rotor circuit. While $SX_{\ell m} I_d$ is only reduction in voltage due to commutation and it does not account for power loss in the rotor circuit.

Therefore, Torque in synchronous watts,

$$P_2 = [E - (X_{\ell m} + 2r_1) I_d]I_d \qquad (2.4)$$

where I_d is given by eqn. (2.3). The power fedback to the supply is given by

$$[V_d + X_{\ell t} I_d] I_d$$

2.6 SLIP POWER CONTROLLER - CONTROL SCHEME

The power circuit is given in Figure 2.2. The Converter II is a 3-phase diode bridge and Converter I is a fully controlled thyristor bridge. A step-down transformer is used for converter I ac supply. The controller is fabricated for 3-HP, slipring motor. The machine details are given in Appendix A.

The smoothing inductor

$L_d \approx 50$ mH with $R_d = 0.8$ ohms

and external resistance $R_e = 230$ ohms were connected in the dc path of the rotor circuit Both of these components help in maintaining continuous conduction and inverter operation over a wide range of load variations.

Obtaining synchronising signal for the Converter I was not a problem. Power transformer secondary output was used to derive synchronising signals for this three phase converter.

2.7 FIRING AND CONTROL CIRCUITS

A conventional cosine comparator scheme which gives linear relationship between average output voltage and input signal was used for generating pulses [16]. Figure 2.4 gives the waveforms for synchronising signal, comparator output, and firing pulse which is the output of a monostable circuit. A firing pulse of 5.0 mS width is provided to take care of highly inductive and/or back emf type of loads This scheme gives firing angle variation from $\theta_f = 0$ to π. However, for line commutated converter it is necessary that

$$\theta_f \leq \pi - \delta ,$$

where δ is commutation overlap angle + thyristor turn-off period.

Secondly, as this controller is designed only for sub-synchronous operation of motor, the additional restriction on firing angle, i.e. $\theta_f \geq \pi/2$ is required. For $\theta_f \leq \pi/2$ there will be short circuit across the diode bridge terminals. From the dc circuit analysis given in the previous section it is clear that due to voltage drops

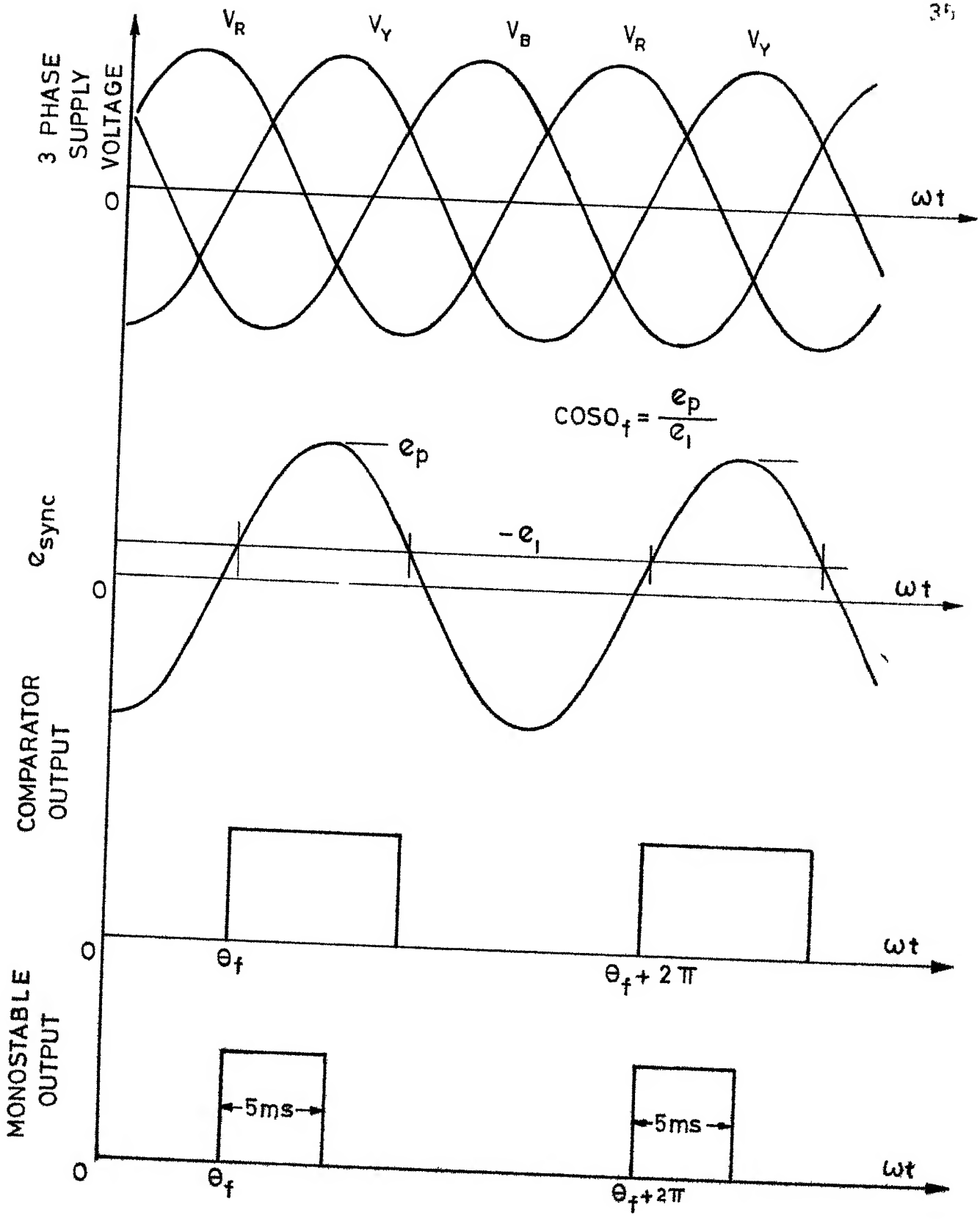

FIG. 2 4 CO-SINE COMPARATOR FIRING SCHEME

across slipring brushes, diodes and thyristors, even for $_d$ = 0,'no load'slip will not be zero. If these voltage drops are compensated by making $V_d = -v_b$, no load slip will become zero.

Taking into account these considerations a clamping circuit is incorporated in the control circuit which limits e_1 such that

$$\frac{\pi}{2} - \sigma \leq \theta_f \leq \pi - \delta$$

where

$$v_b = \frac{3\sqrt{6}}{\pi} V_2 \cos(\frac{\pi}{2} - \sigma)$$

A block diagram of firing scheme for one of the phases is given in Figure 2 5(a). A low-pass filter between synchronising voltage and comparator is required to eliminate higher order harmonics For 3-phase circuit it is convenient to adjust the phase shift of this filter to 60^o at 50 Hz, and remaining 30^o phase shift required for cosine comparator scheme is obtained by Δ/Y connections of synchronising transformers It has been observed that 60^o phase shift filter eliminates frequencies higher than 100 Hz. This arrangement prevents the false triggering of thyristors due to distortions noise in the supply voltage waveform. The control signal e_1 determines the firing angle θ_f. And monostable gives 50 mS width pulse at the desired firing angle.

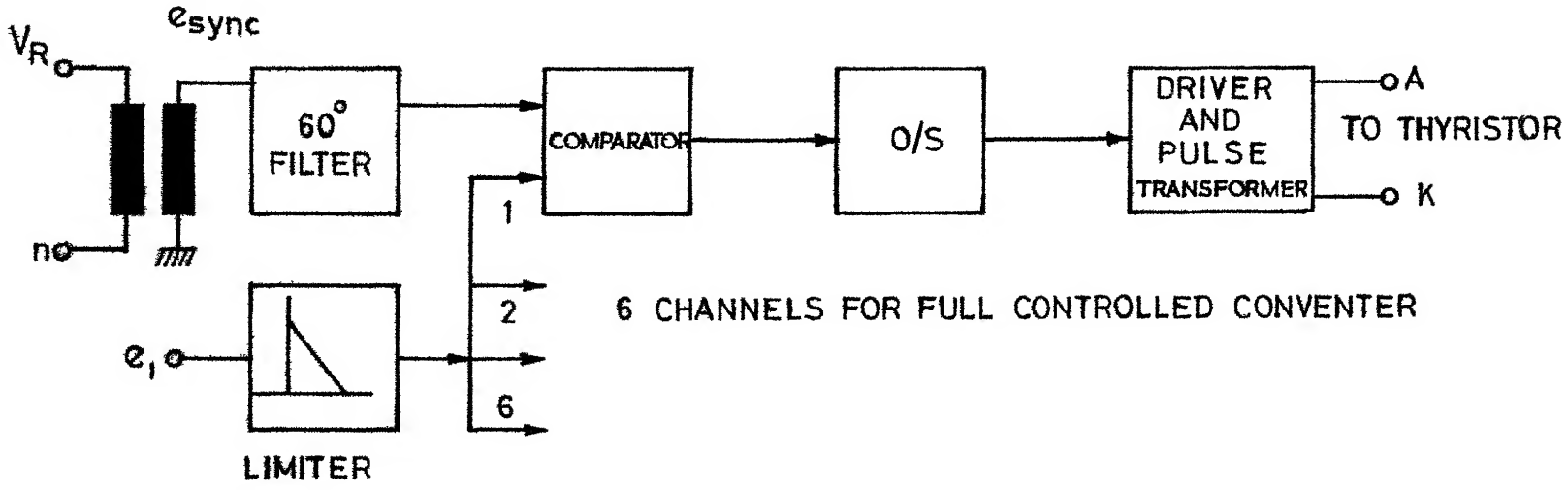

FIG 2.5 (a) FIRING CIRCUIT SCHEMATIC

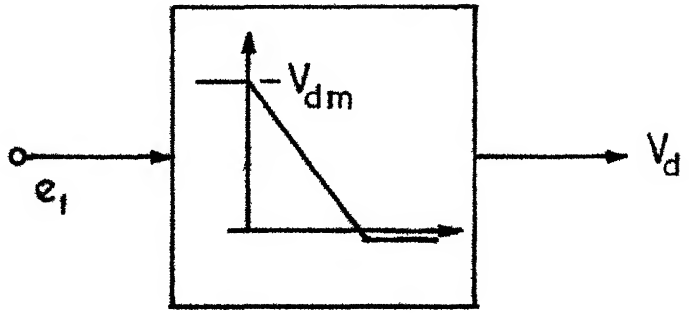

FIG.2.5 (b) TRANSFER CHARACTERISTIC-CONVERTER AND CONTROL CIRCUIT

A modulated carrier frequency (5 KHz) is used to trigger the thyristors This provides isolation between control circuits and gate-cathode terminals of thyristors, at the same time it is possible to apply maintained gate signal [16]

A precision bridge limiter is used to ensure that inverter firing angle is within limits. The overall transfer characteristics of the converter with firing and clamping circuits is given in Figure 2.5(b). The composite transfer characteristic of converter, firing and clamping circuits gives

$$V_d = V_{dm} - k_r\ e_1$$

where

$$V_{dm} = V_d \Big|_{e_1=0}$$

and k_r = incremental gain of the converter.

2.8 CLOSED LOOP SPEED CONTROL

In many industrial applications, speed regulation given by open loop slip power control (see Figure 2.10) is undesirable. In such cases it becomes necessary to go for closed loop speed control. The closed loop speed control scheme with current feedback is duscussed below.

2.8.1 System Description:

Figure 2.6 gives a block diagram of the complete speed control system. A diode bridge on rotor side and

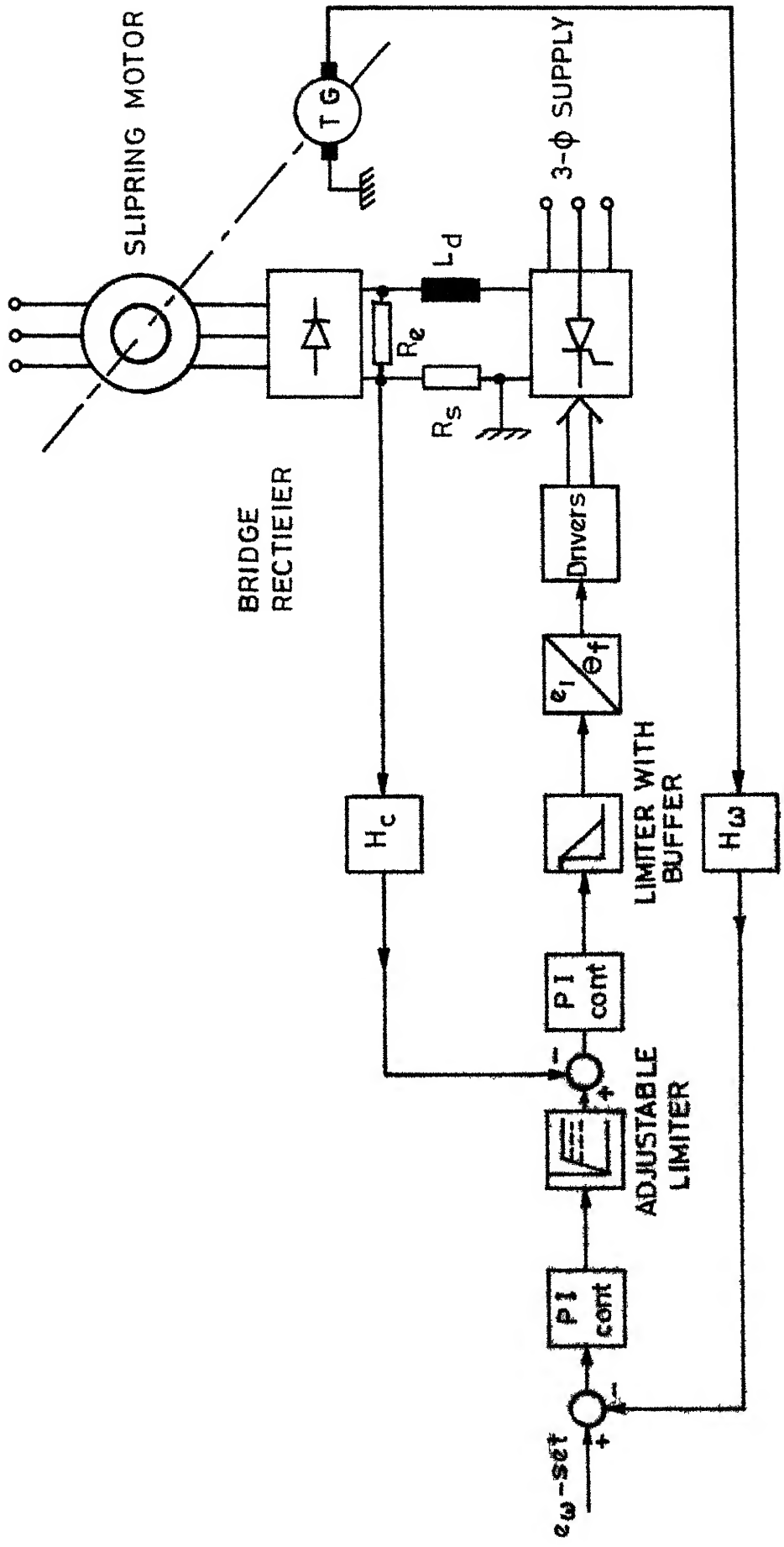

FIG.2.6 SLIP ROWER RECOVERY SCHEME- BLOCK DIAGRAM OF CLOSED LOOP CONTROL

a full controlled bridge on the 3-phase supply side are connected as shown in the diagram. A smoothing inductor, and resistance across diode bridge are connected in the dc path. A permanent magnet tacho-generator mounted on the same shaft is used to obtain speed feedback signal. The rotor current is sensed by connecting a small resistance on the dc circuit. The converter voltage is controlled by varying e_1, the output of current controller. An eddy-current brake connected to the shaft (not shown in the diagram) is used as load. The motor details and its equivalent circuit are given in Appendix A and Figure 2.9 respectively.

A simple arrangement of proportional speed control with current limit will also give improved speed regulation with protection against excessive currents during starting and under over-load conditions. However, the scheme shown in the block diagram uses a PI controller The PI i.e., proportional plus integral controller gives zero steady state error due to integrating effect of the controller and proportional part of the gain helps in improving the transient response. The speed controller output which is used as reference for current loop, has adjustable saturation level.

There is a second PI controller for current control loop. The output of this PI controller is given to the limiter circuit followed by firing circuits. The function of this limiter circuit, as discussed earlier (section 2 7), is to maintain firing angle within permissible limits for the satisfactory operation of the converter. During starting and under over-load condition, output of speed controller saturates and limits rotor current to a preset value. The starting current and hence starting torque can be set by adjusting the saturation level of speed controller output Moreover, this arrangement of providing inner current control loop maintains constant current against supply voltage disturbances, and provides fast response compared to current limit arrangement [17,18].

2.9 SPEED CONTROLLER

A permanent magnet dc tacho-generator is used to obtain a speed feedback signal. There could be a cheaper arrangement of disc with holes on the circumference mounted on the same shaft with a magnetic or photo pick-up, giving a train of pulses. The frequency of these pulses is proportional to the shaft speed. However, tacho-generator arrangement was preferred because its output is dc with ripple of very small amplitude. The tacho-generator used in this set-up has a ripple of 50 Hz

at about 750 rpm, the reason being the presence of commutator segments in dc machine. To reduce the effect of this ripple a first order filter is used in the feedback path. The filter cut-off frequency is kept half of the ripple frequency corresponding to the lowest operating speed say, 500 rpm. A potential divider arrangement is used to make feedback voltage levels compatible with the available reference voltage levels. This gives 6.0 V (approx) at 1500 rpm, and corresponding transfer function for speed feedback path is

$$H_{\omega}(s) = \frac{0.0386}{1+s\ T_g}$$

where T_g - filter time constant

= 62 mS.

Figure 2.7 gives the circuit diagram of speed controller. It is essential that output of speed controller should be unidirectional and with well defined saturation level. Besides this, to make current limit adjustable, it is desirable to make this saturation level rather than the feedback factor adjustable This is achieved by using a precision 1/2 bridge limiter with adjustable limiting level. Output of this limiter is the reference for the current control loop.

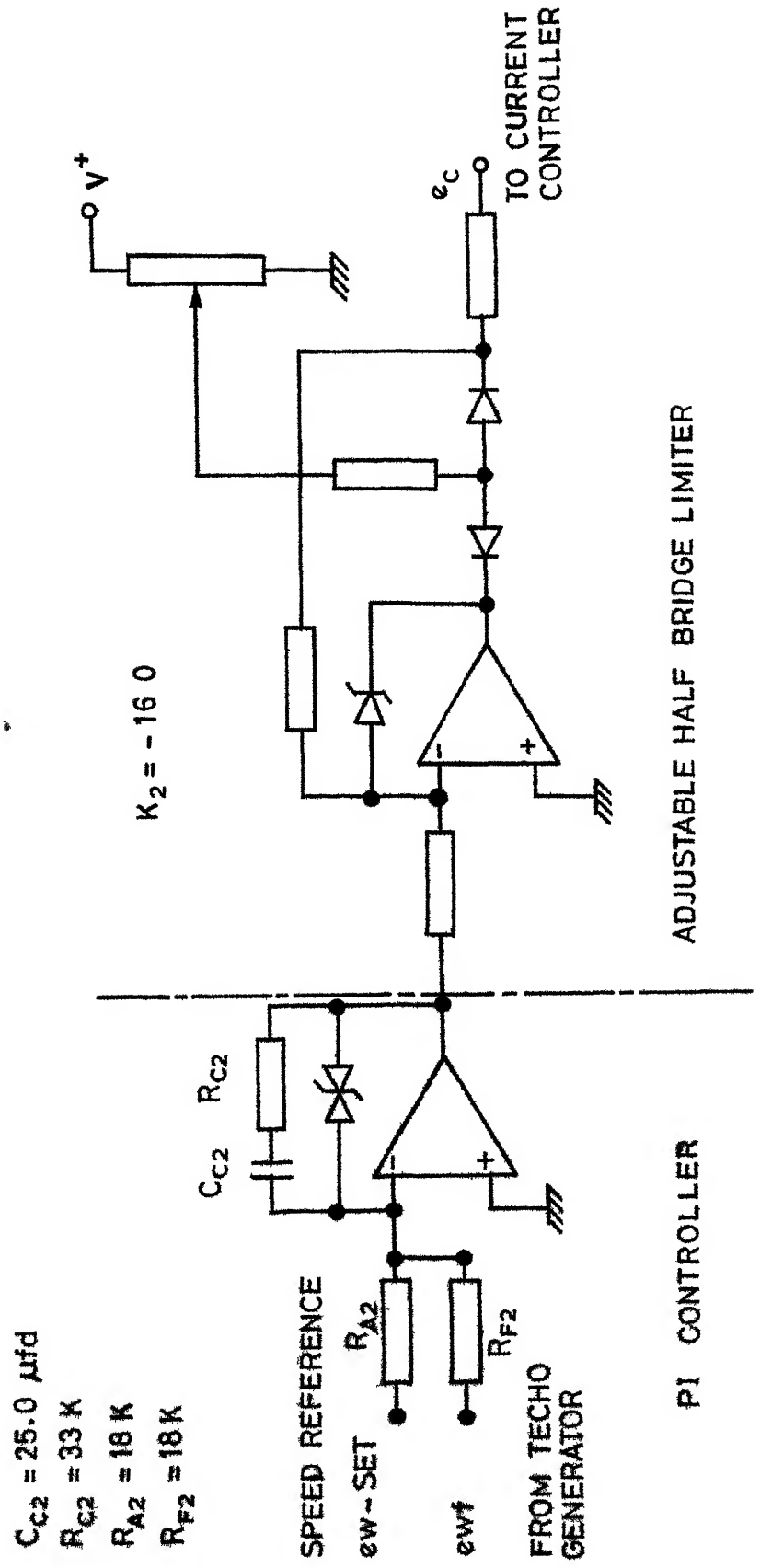

FIG. 2.7 SLIP POWER RECOVERY-SPEED CONTROLLER

A PI controller is used to obtain zero steady state error in the speed control loop Design procedure is more or less same as current controller (see Sec 3.8). The transfer function of PI controller is given by

$$G_{\omega c} = \frac{k_2(1 + S\,T_{c2})}{S^s},$$

where $T_{c2} = C_{c2}\,R_{c2}$,

$$k_2 = \frac{\text{gain of limiter}}{R_{2f}\,C_{c2}}$$

The procedure of determining k_2 and T_{c2} is given in Chapter 3.

In ideal case PI controller is supposed to give zero steady state error. However, because of OP-AMP bias current and leakage resistance of capacitors there is non-zero steady state error (regulation 0.5 percent). Moreover, it is very difficult to obtain stable dc level as reference source Use of PLL (phase locked loop) will overcome these drawbacks of PI controller. Here the reference source is a train of pulses with constant frequency. The scheme of comparing reference frequency with feedback frequency and giving the d.c level proportional to phase difference as output works as an integrator in the forward path. Hence this scheme gives absolutely zero steady-state error. Moreover, it is easy to obtain a

highly stable frequency source. However, in the present scheme the conventional PI controller is used since a regulation of about 0.5 percent is not objectionable.

2.10 CURRENT CONTROLLER

A Hall-effect transducer or dc current transformer can be used on the dc side of the rotor circuit to sample the rotor current I_d. Since the rotor circuit is isolated, there was no need of having a transducer which must provide isolation between the power circuit and the control circuit. The common cathode terminal of the Converter I is connected to control circuit common (ground) point, and a resistance of 0 25 ohm is connected between ground, and negative terminal of the bridge rectifier The voltage across this resistance is proportional to the instantaneous current in the rotor circuit. It was observed that the ripple amplitude of rotor current, under light load condition with firing angle near 90^{o}, is considerably high. In order to reduce the effect of this ripple component a first order filter is used in the feedback path. The steady-state current feedback is adjusted such that feedback signal level is comparable to that of reference signal for current loop. The procedure for determining filter time constant is discussed in Chapter 3. This arrangement gives, current feedback factor

$$H_c(s) = \frac{0.15}{1+S\,T_s}$$

where T_s is filter time constant.

The circuit diagram of current controller is given in Figure 2.8. A bridge type limiter is used between a PI controller and firing circuits. The limiter function is discussed in Section 2.7.

The PI controller is used to give zero steady state error. A reference signal e_c for current controller is obtained from the output of speed controller. The speed controller output has adjustable saturation level. The voltage across R_s, after filtering out ripple, is used as current feedback signal e_{cf}. During starting output of speed controller will saturate because of large error in the speed feedback loop, and this limits the starting current and hence motor torque to the preset value. Under overload condition also similar action takes place.

The current control loop provides fast response against supply voltage disturbances or parameter variations in the current loop. A simple current limit arrangement will not respond that fast, because under normal load conditions only speed feedback is effective, and the mechanical time constant has its effect on the system response [19].

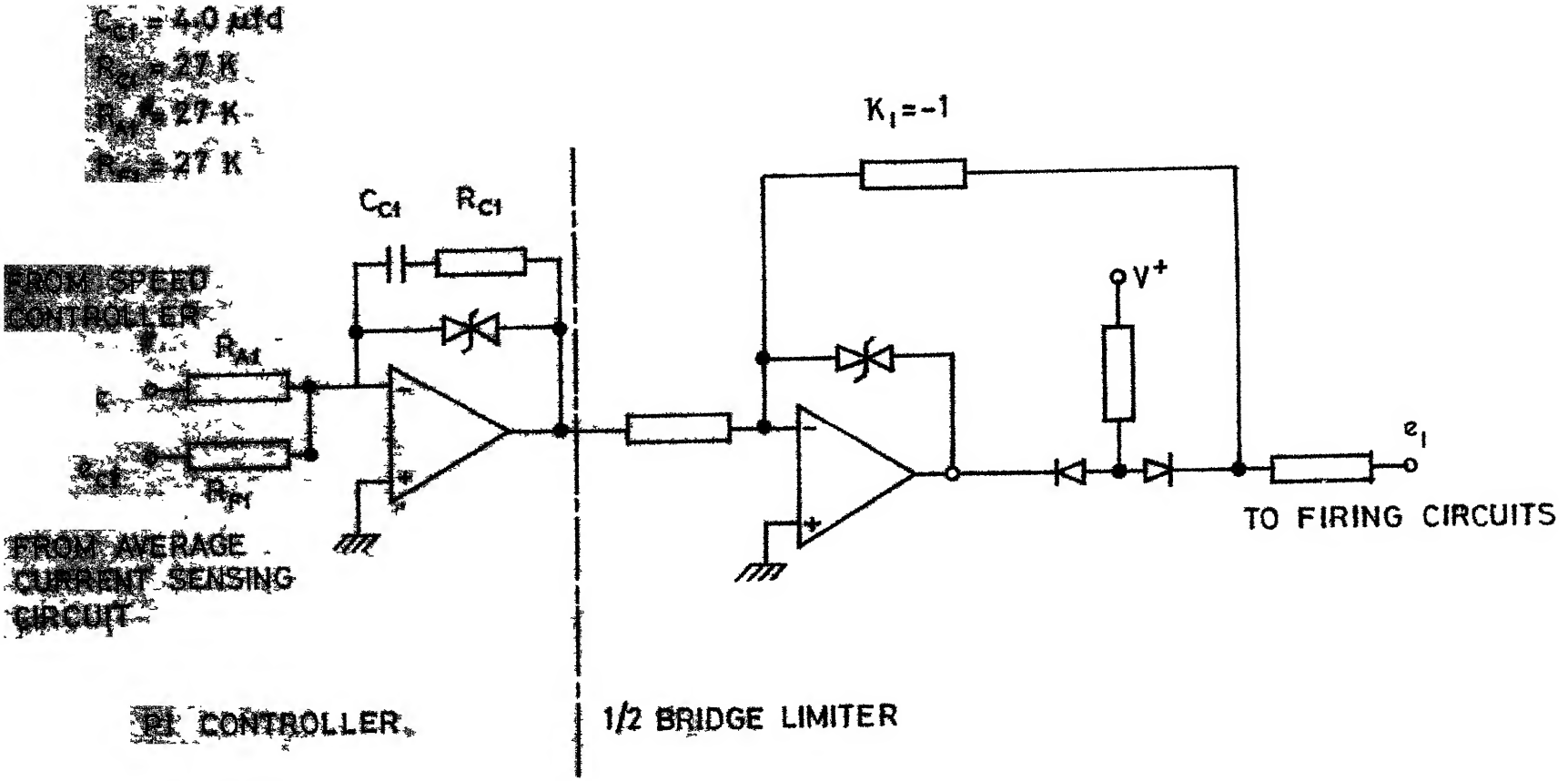

FIG.2.8 SLIP POWER RECOVERY-CURRENT CONTROLLER

Though an integrator tends to slow down the response, adjustment of the transfer function zero and gain of the controller can give reasonably fast response. The transfer function of current controller is given by

$$G_{cc}(s) = \frac{k_1(1 + s\,T_{c1})}{s}$$

where

$$T_{c1} = C_{c1} \cdot R_{c1} \quad ms$$

and

$$k_1 = \frac{\text{gain of limiter}}{R_{f1} \cdot C_{c1}}$$

The design procedure for this controller is discussed in Chapter 3.

2.11 EXPERIMENTAL INVESTIGATIONS

A 3 HP slipring induction motor was used for experimental investigations. The values of power circuit components are given in Figure 2 2. The details of the motor are given in Appendix A. Figure 2.9 gives the per phase equivalent circuit of motor referred to rotor.

The loading arrangement constitutes a separately excited dc generator and eddy-current brake. These machines are directly coupled to the motor shaft. A permanent magnet tacho-generator is used to provide speed feedback. A resistance connected in the dc

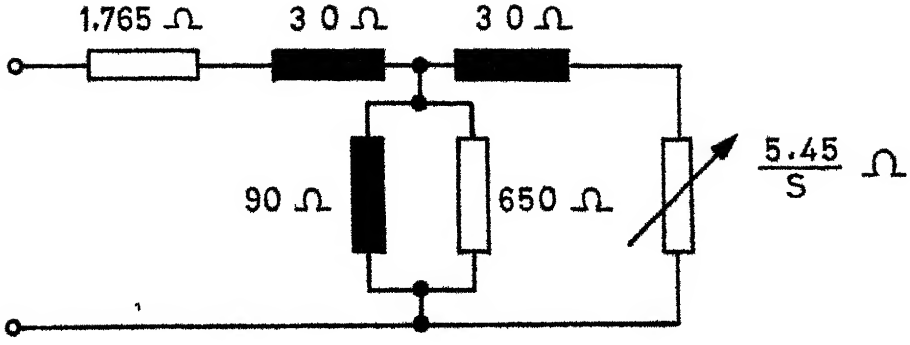

FIG.2.9(a) EQUIVALENT CIRCUIT REFERRED TO STATOR

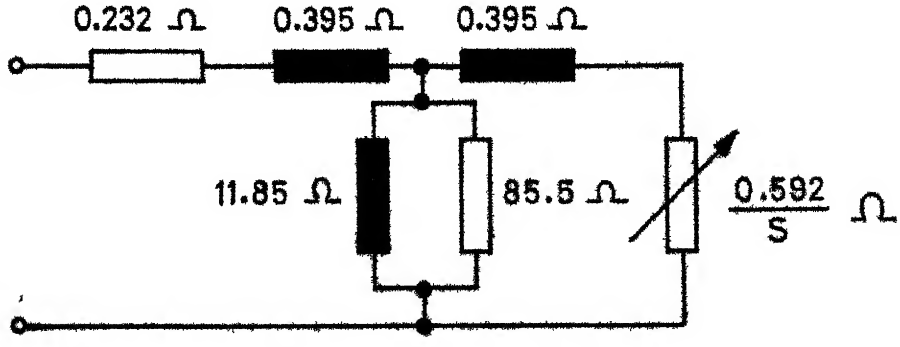

FIG2.9(b) EQUIVALENT CIRCUIT REFERRED TO ROTOR

path of the rotor circuit is used to obtain rotor current feedback signal.

Figures 2.10 and 2.11 give the open loop speed versus torque and speed versus current characteristics respectively. The computed characteristics, based on the dc circuit model given in Section 2.5, are also given for the sake of comparison. The steady state speed torque characteristics with closed loop system are found to be almost flat for various set speeds and currents. The transient response of the drive is given in Chapter 3.

2.12 CONCLUSION

The slip power recovery scheme overcomes the inherent disadvantages at low-speed operation with variable stator voltage or variable rotor resistance control methods. The recovered rotor power causes overall reduction in the motor power factor. However, alternative arrangements giving improved power factor, give higher distortion factor.

Open loop speed torque characteristics are similar to that of dc shunt motor. Sub-synchronous slip power control is simple and economical compared to equivalent dc motor control. Excellent drive characteristics can be obtained with closed loop control.

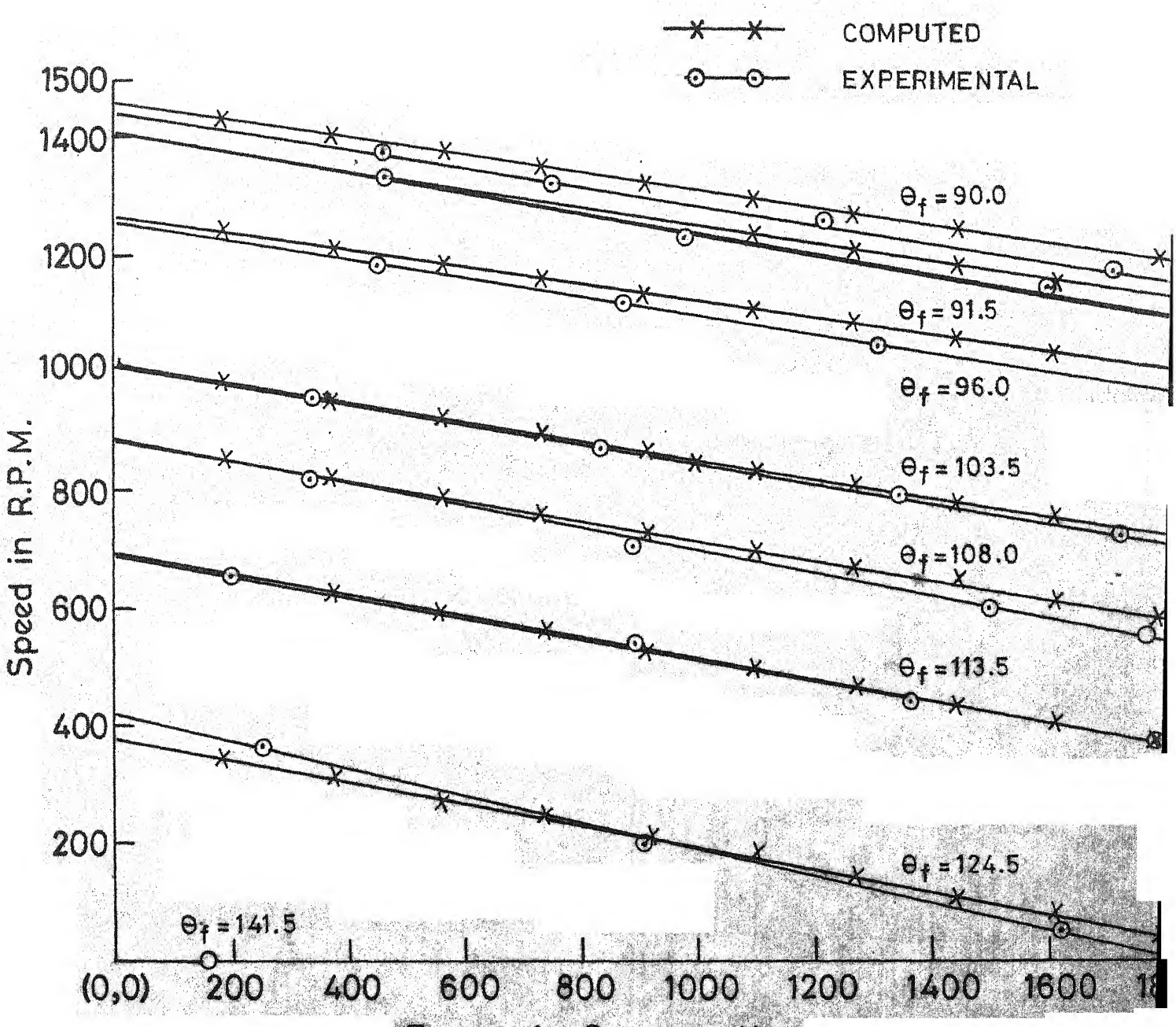

FIG.2.10 SPEED-TORQUE CHARACTERISTICS-SLIP POWER RECOVERY

CENTRAL LIBRARY
Acc. No. 35705

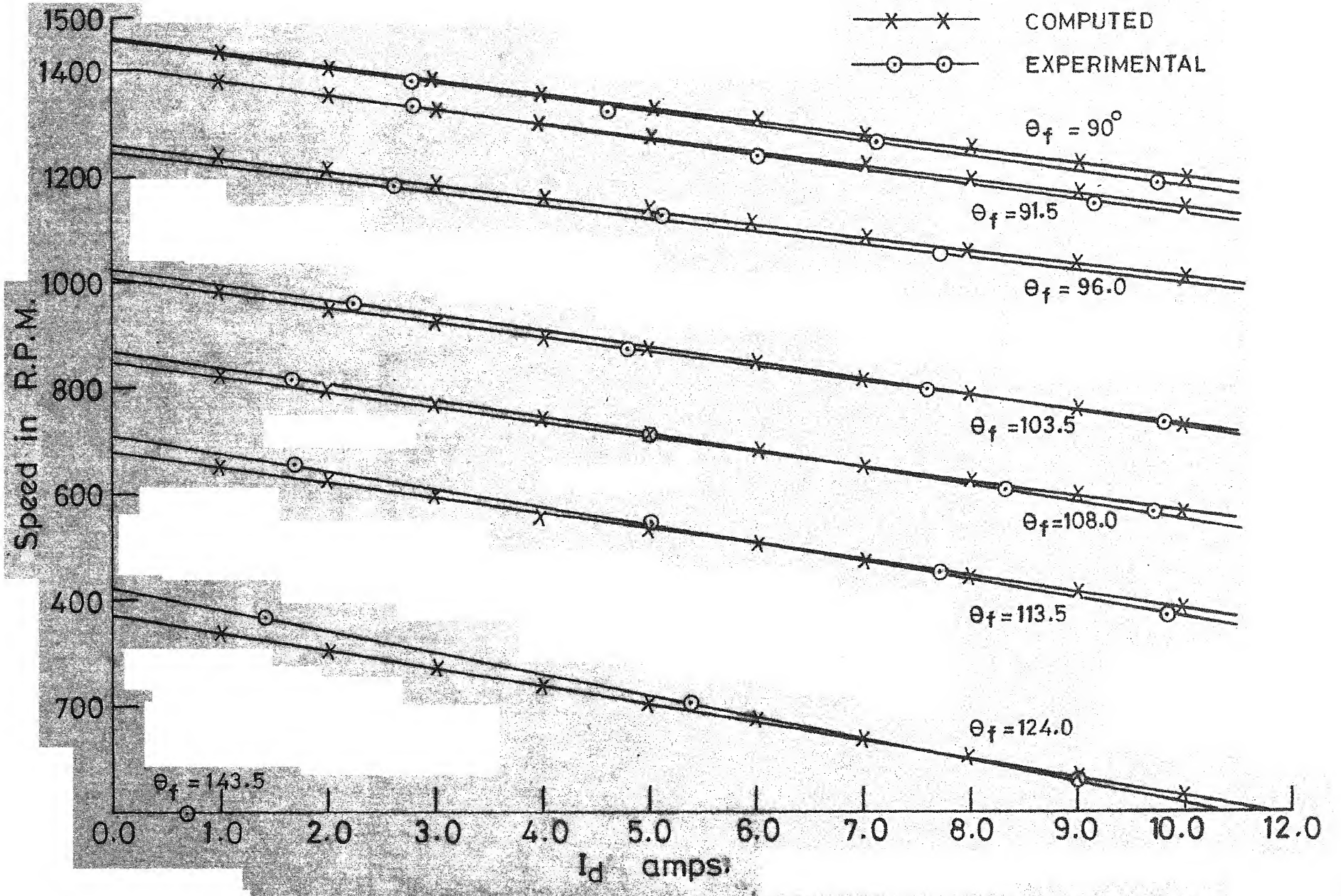

FIG.2.11 SPEED-I_d CHARACTERISTICS-SLIP POWER RECOVERY

CHAPTER 3

THE TRANSIENT RESPONSE OF SLIP POWER RECOVERY SCHEME

3.1 INTRODUCTION

In this chapter, a dynamic model for slip power recovery is developed. The speed-torque characteristics of slip power recovery controller is similar to that of dc shunt motor over a wide range of operation (see Sec.2.5). Hence it is possible to derive a transfer function which holds good over a wide range of speed and torque.

A block diagram is developed for the motor from which transfer functions are derived to predict the transient response of the drive. It has been shown that these transfer functions can be used for designing the various feedback loops.

However, it should be noted that sub-synchronous slip power recovery scheme given in Chapter 2 does not have the provision to provide braking torque for sub-synchronous range of operation, unless dynamic braking is used. Since dynamic braking requires switching of stator from ac to dc supply [10], it was not implemented.

For this scheme, when negative step input of small amplitude is applied in order to reduce motor speed, inverter voltage increases, rotor current drops, and motor decelerates to new steady state speed. However, if the negative step signal is large enough to make increased voltage of inverter greater than the no-load voltage output of rectifier, rotor current drops to zero very rapidly. Hence motor is not able to provide braking torque and motor decelerates depending on the mechanical load and time constant of the set-up. Obviously, during this period, linear transfer functions developed here will not be valid.

With closed loop control such situation can arise even when positive step input is applied as speed or current reference, if system response is highly oscillatory.

3.2 DEVELOPMENT OF SMALL SIGNAL MODEL

The complete transient analysis of conventional induction motor is quite difficult. The presence of bridge rectifier and inverter makes it all the more difficult. Therefore it is not possible to derive analytically a transfer function that will be valid under all conditions. However, transfer functions that

functions that will be valid over a sub-synchronous motoring range of operation may be derived under certain simplifying assumptions [20].

The following simplifying assumption is made in the dc circuit model given in Section 2.5.

The voltage drop across stator impedance and voltage loss due to commutation is negligible. With this assumption the torque developed by motor under steady state becomes

$$T = \frac{E\, I_d}{\omega_s} \qquad (3.1)$$

From this equation, torque is the linear function of I_d. This will hold good only when motor is not heavily loaded. The open loop speed torque and speed current characteristics given in Figures 2.10 and 2.11, respectively indicate the linear behaviour, at least, upto 10.0 Amps of rotor current I_d. This establishes that the above mentioned assumption and eqn.(3.1) are valid under normal loading conditions.

The transfer characteristics of the inverter with control circuit is given by

$$V_d = V_{dm} - k_r\, e_1, \qquad \text{from Figure 2.5(b)},$$

where

$$V_{dm} = V_d \Big|_{e_1=0}$$

$-k_r$ = incremental gain of the converter

Since voltage drops due to commutation of the converters and stator impedance are neglected

$$I_d = \frac{S\,E - V_d}{R} \quad \text{(under steady state)}$$

where

R = total resistance in the rotor circuit

S = motor slip.

Therefore,

$$\Delta I_d = \frac{\Delta S\,E + k_r \Delta e_1}{R} \quad \text{(under steady state)} \quad (3.2)$$

where ΔI_d, ΔS and Δe_1 are incremental changes in I_d, S and e_1 respectively. Since

$$S = \frac{\omega_s - \omega}{\omega_s}$$

where ω - motor speed.

Therefore,

$$\Delta S = - \frac{\Delta \omega}{\omega_s} \quad .$$

Substituting this in eqn.(3 2) gives

$$\Delta I_d = (k_r - \Delta e_1 - \frac{E}{\omega_s} \Delta\omega)/R \quad \text{(under steady state)} \tag{3.3}$$

Now,

$$\Delta T = \frac{E}{\omega_s} \Delta I_d, \quad \text{(from eqn.(3 1))}$$

where ΔT is incremental change in motor torque If the perturbation in load torque T_L is $\Delta T_L = 0$, the perturbation in motor speed is given by

$$\Delta\omega = \frac{\Delta T}{f} = \frac{E.\Delta I_d}{\omega_s f} \quad \text{(under steady-state)} \tag{3.4}$$

where

f - coefficient of linear (viscous) friction of load.

Substituting the value of ΔI_d from eqn.(3.2) gives

$$\Delta\omega = \frac{E}{\omega_s f R}[k_r \Delta e_1 - \frac{E}{\omega_s} \Delta\omega] \tag{3.5}$$

From equations (3.3), (3 4) and (3.5), under steady-state

$$\frac{\Delta I_d}{\Delta e_1} = \frac{k_r/R}{(1+k_{eb})},$$

$$\frac{\Delta\omega}{\Delta e_1} = \frac{E}{\omega_s f} \cdot \frac{k_r/R}{(1+k_{eb})} \tag{3.6}$$

where $k_{eb} = \dfrac{E^2}{\omega_s^2 f R}$

represents the effect of internal speed feedback.

3.3 BLOCK DIAGRAM AND TRANSFER FUNCTIONS

Before developing a block diagram the presence and effect of various time constants in the system will be discussed.

3.3.1 Converter Time Constant [15,21]

In a line commutated converter, although the average voltage is proportional to e_1, the triggering of thyristors is not instantaneously corrected. There is certain delay in the actual change in the average voltage and change in the control signal. Hence, this system should be treated as sampled data system. The triggering of thyristor corresponds to sampling of e_1. The amplitude of e_1 at that instant determines the corresponding average voltage. And converter does not respond to any changes in e_1 till the next firing pulse. This corresponds to zero-order hold arrangement. Analysis can be simplified by considering it as simple first-order system with a time constant, $T_c = t_p/2$. Where t_p is the interval between two consecutive firing pulses. For 3-phase, 50 Hz, full controlled converter, $T_c = 1.66$ mS. This gives

$$\Delta V_d(s) = \frac{-k_r \Delta e_1(s)}{1+s T_c} \qquad (3.7)$$

where s - Laplace operator.

3 3.2 DC Circuit Time Constant

The inductor L_d is connected in the rotor circuit mainly to reduce the heating of rotor windings and also to give continuous conduction operation of line commutated converter. This smoothing inductor L_d along with winding leakage reactances of motor and transformer introduces a single time constant in the dc circuit of this scheme. This time constant is expressed as (refer Figure 2.3).

$$T_d = \frac{L_d + 2(\ell_1 + \ell_2) + 2\ell_t}{R_d+R_s+2r_2+2r_t + S\ 2r_1}$$

where effect of 'R_e' is neglected. Since

$$(R_d + R_s + 2r_2 + 2r_t) >> S\ 2r_1$$

$$T_d = \frac{L_d + 2(\ell_1+ \ell_2) + 2\ell_t}{R_d + R_s + 2r_2 + 2r_1} \qquad (3.8)$$

This simplified expression of time constant is independent of motor slip at the operating point

The converter time constant T_c comes into picture only when we are considering the change in e_1. However, dc circuit time constant T_d is to be considered for changes in ω and also in e_1. Considering these time constants equations (3.3) and (3.4) could be rewritten as

$$\Delta I_d(s) = \frac{k_r/R}{(1+sT_c)(1+sT_d)} \Delta e_1(s) - \frac{E}{\omega_s R(1+s\ T_d)} \Delta\omega\ (s) \qquad (3\ 9)$$

Considering the perturbations in speed and torque

$$\Delta\omega = \frac{\Delta T - \Delta T_L}{f(1+s\ T_m)} ,$$

where $T_m = J/f$ - mechanical time constant of load and motor,

J - moment of inertia of load and motor.

If $\Delta T_L = 0$

$$\Delta\omega(s) = \frac{(E/\omega_s)\,\Delta I_d(s)}{f(1+s\ T_m)} \qquad (3.10)$$

Block diagram corresponding to equations (3.9) and (3.10) is given in Figure 3.1.

3.4 DERIVATION OF $\Delta I_d(s)/\Delta e_1(s)$ AND $\Delta\omega(s)/\Delta e_1(s)$:

From the block diagram of Figure 3.1

$$\frac{\Delta I_d}{\Delta e_1}(s) = \frac{(k_r/R)(1 + s\ T_m)}{(1+s.T_c)[(1+sT_d)(1+sT_m)+k_{eb}]}$$

where $k_{eb} = E^2/(\omega_s^2\ f\ R)$

$$\frac{\Delta I_d}{\Delta e_1}(s) = \frac{(k_r/R)(1+s\ T_m)}{T_d T_m[s^2+(\frac{1}{T_d} + \frac{1}{T_m})s+ \frac{1}{T_d T_m}(1+k_{eb})](1+sT_c)} \qquad (3.11)$$

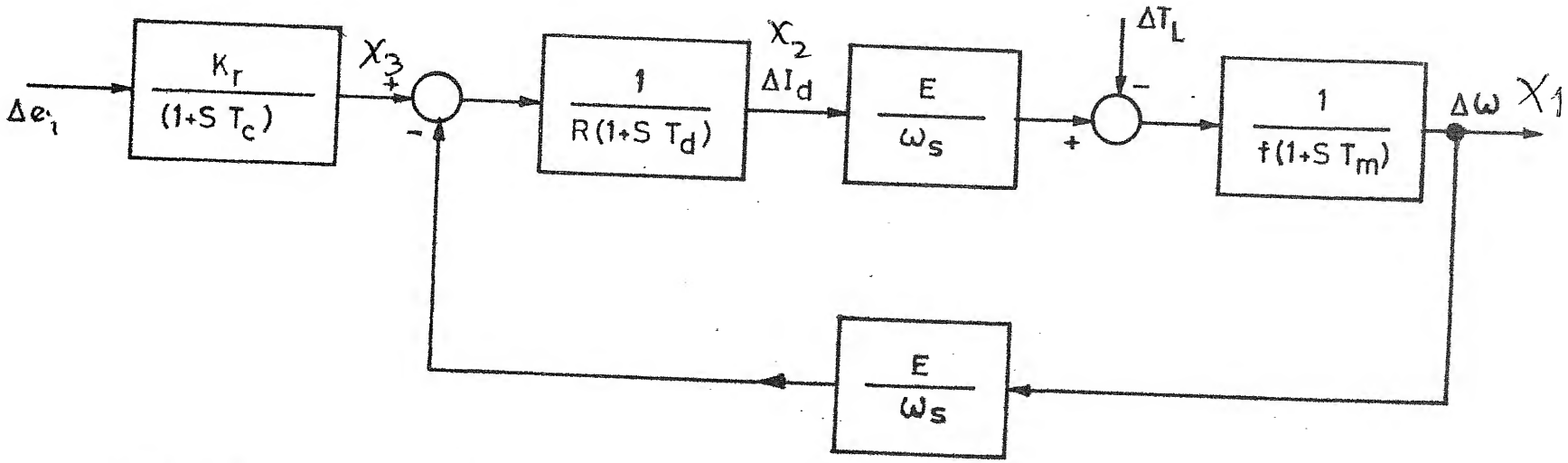

FIG. 3.1 SLIP POWER RECOVERY-SMALL SIGNAL BLOCK DIAGRAM

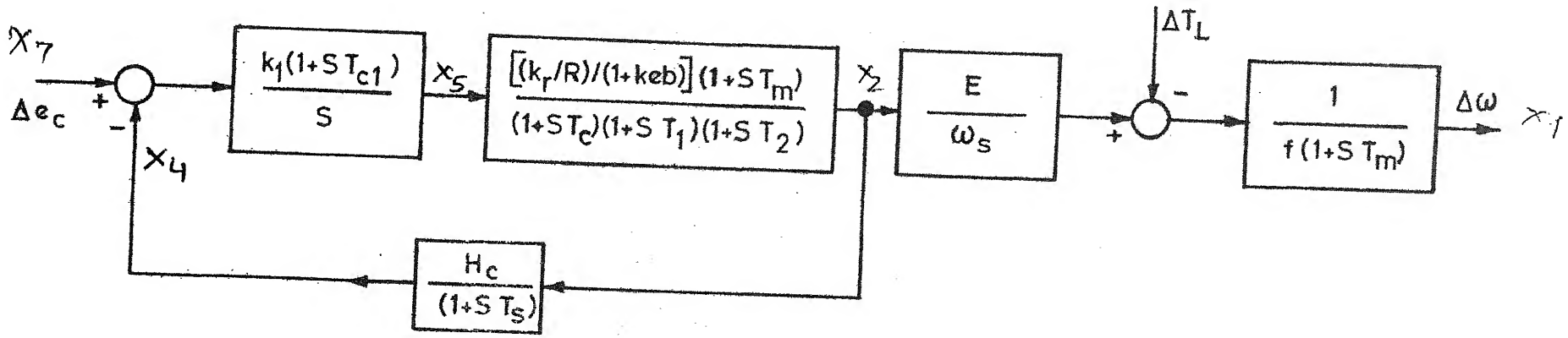

FIG. 3.2 SLIP POWER RECOVERY-CURRENT CONTROL LOOP BLOCK DIGRAM

The roots of

$$s^2+(\frac{1}{T_d} + \frac{1}{T_m})s + \frac{1}{T_d T_m}(1+k_{cb}) = 0$$

are given by

$$s_{1,2} = -\frac{1}{2}(\frac{1}{T_d} + \frac{1}{T_m}) \pm \sqrt{[\frac{1}{4}(\frac{1}{T_d} + \frac{1}{T_m})^2 - \frac{1}{T_d T_m}(1+k_{cb})]} \qquad (3.12)$$

Let, $T_1 = -\frac{1}{s_1}$ and $T_2 = -\frac{1}{s_2}$.

Substituting this in eqn.(3.11) gives

$$G_c(s) = \frac{\Delta I_d}{\Delta e_1}(s) = \frac{[(k_r/R)/(1+k_{eb})](1+sT_m)}{(1+sT_1)(1+sT_2)(1+sT_c)} \qquad (3.13)$$

Now

$$\frac{\Delta\omega}{\Delta e_1}(s) = \frac{\Delta I_d}{\Delta e_1}(s)\frac{E}{\omega_s f(1+sT_m)}, \quad \text{from the block diagram .}$$

From eqn.(3.12),

$$\frac{\Delta\omega}{\Delta e_1}(s) = \frac{(E/\omega_s f)[(k_r/R)/(1+k_{eb})]}{(1+sT_1)(1+sT_2)(1+sT_c)} \qquad (3.14)$$

Effect of ΔT_L.

From the block diagram if $T_L \neq 0$,

$$\frac{\Delta\omega}{\Delta T_L}(s) = \frac{(1/f)(1 + s T_d)}{(1+sT_d)(1+sT_m)+k_{eb}}$$

$$= \frac{(1+sT_d)[1/f(1+k_{eb})]}{(1+sT_1)(1+sT_2)(1+sT_c)} \qquad (3.15)$$

Equations (3.13)-(3.15) are the transfer functions for the perturbations around the given operating point.

From the block diagram developed here, the following statements could be made

i) It is the internal feedback factor k_{eb} that tends to make current response oscillatory

ii) If $k_{eb}\ll 1$, $T_1 \simeq T_m$ and $T_2 \simeq T_d$ with this approximation

$$\frac{\Delta I_d}{\Delta e_1}(s) = \frac{k_r/R}{(1+s\,T_d)(1+s\,T_c)} \qquad (3.16)$$

and

$$\frac{\Delta\omega}{\Delta T_L}(s) = \frac{1/f}{(1+s\,T_m)} \qquad (3.17)$$

3.5 TRANSFER FUNCTIONS - CLOSED LOOP SYSTEM

The open loop transfer functions and a block diagram are given in the previous section. To study the transient response of closed loop system around the given operating point, the same transfer functions can be used. The closed loop control scheme for sub-synchronous slip power recovery, complete with speed and current feedback, is given in Figure 2.6. In this section block diagrams, and transfer functions for the same scheme will be developed. Subsequent sections give the design of various blocks of the closed loop controller.

3 5.1 Current Control Loop

In the linear analysis of current control loop it is assumed that

i) The limiter in the current loop is operating in the linear mode.

ii) The limiter in the speed control loop is in the saturated mode. This makes speed feedback ineffective.

Figure 3 2 gives the block diagram of current loop. The PI controller transfer function is

$$G_{cc}(s) = \frac{k_1(s + T_{c1})}{s}$$

where,

$$T_{c1} = C_{c1} R_{c1}$$

$$K_1 = \frac{\text{gain of limiter}}{C_{c1} R_{f1}}$$

A first order filter is incorporated in the current feedback path. This is necessary to reduce the effect of current ripples on the average current feedback signal. The transfer function of current feedback path is given by

$$H_c(s) = \frac{H_c}{1+s T_s}$$

where T_s is the filter time constant.

This gives loop gain

$$G_c\ G_{cc}\ H_c(s) = -\frac{[(k_r/R)/(1+k_{eb})](1+sT_m)(1+sT_{cl})k_1 H_c}{s(1+sT_c)(1+sT_1)(1+sT_2)(1+s\ T_s)} \qquad (3.18)$$

If some of the time constants from this expression could be ignored in favour of the dominating time constants, derivation of loop gain for speed control loop will become very easy.

Now, from eqn.(3.12) T_1 and T_2 are functions of k_{eb}, T_d and T_m. For the slip power recovery scheme, normally $K_{eb} << 1$ and $T_m >> T_d$. This gives

$$T_1 \simeq T_m \text{ , from eqn.(3.12) .}$$

Secondly, T_s, being current sensing circuit time constant, is kept as small as possible (refer to Section 3.8), and T_c is 3 phase converter time constant. This makes T_s and T_c negligible compared to T_1 or T_2. The validity of these assumptions is shown in Section 3.8. With these assumptions

$$G_c\ G_{cc}\ H_c(s) = \frac{[k_1\ H_c(k_r/R)/(1+k_{eb})](1+sT_{cl})}{s(1+s\ T_2)} \qquad (3.19)$$

The closed loop transfer function for current loop, is given by

$$G_c^*(s) = \frac{\Delta I_d}{\Delta e_c}(s) = \frac{G_c\, G_{cc}(s)}{1 + G_c G_{cc} H_c(s)}$$

where Δe_c is input to the current control loop.

From eqn. (3.19)

$$G_c^*(s) = \frac{\Delta I_d}{\Delta e_c}(s)$$

$$= \frac{[k_1(\frac{k_r}{R})/(1+k_{eb})](1 + s\, T_{c1})}{s(1+sT_2)+[k_1(k_r/R)H_c/(1+k_{eb})](1+ST_{c1})}$$

$$= \frac{(1/H_c)(1 + s\, T_{c1})}{(1+sT_a)(1 + sT_b)} \qquad (3.20)$$

where $-1/T_a$, and $-1/T_b$ are the roots of equation

$$s^2+s[\frac{1}{T_2} + \frac{k_1 H_c(k_r/R)}{1 + k_{eb}} \frac{T_{c1}}{T_2}] + \frac{k_1+H_c(k_r/R)}{(1+k_{eb})T_2} = 0$$

3.5.2 Speed Control Loop:

While analyzing the behaviour of speed control loop, it is assumed that both the limiters are operating in the linear mode.

The speed control loop block diagram given in Figure 3.3 incorporates the approximate transfer function given by eqn.(3.20). In the block diagram

$$G_{\omega c}(s) = \frac{k_2(1 + s\, T_{c2})}{s}$$

is PI controller transfer function. Where

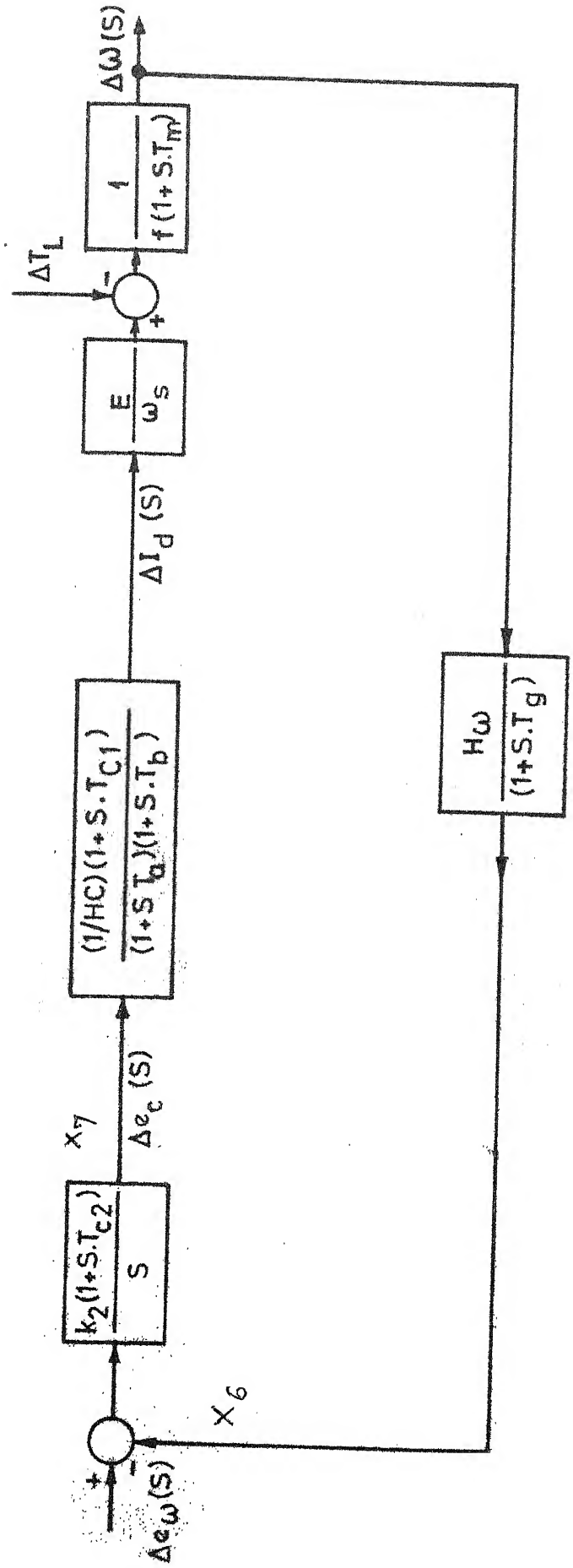

FIG.3.3 SLIP POWER RECOVERY-SPEED CONTROL LOOP BLOCK DIAGRAM

$$T_{c2} = R_{c2} C_{c2}$$

and $$k_2 = \frac{\text{gain of limiter}}{C_{c2} R_{f2}}$$

The transfer function in speed feedback path is

$$H_\omega(s) = \frac{H_\omega}{1 + s T_g}$$

where H_ω is steady state feedback factor and T_g is filter time constant. A first order filter in the speed feedback path was necessary to reduce the effect of ripples in the tacho-generator output. From Figure 3.3, loop gain

$$G_{\omega c}(s) = \frac{\Delta I_d}{\Delta e_c}(s) \frac{E}{\omega_s} \frac{1}{f(1+s T_m)} \frac{H_\omega}{(1 + sT_g)}$$

$$= \frac{[k_2 E/\omega_s f H_c](1 + s T_{c1})(1 + s T_{c2})}{s(1 + s T_a)(1 + s T_b)(1 + s T_m)} \quad (3.21)$$

3.6 DETERMINATION OF OPERATING POINT

The open loop speed-torque and speed I_d characteristics given in Figures 2.10 and 2.11 respectively indicate that these characteristics are definitely linear for rotor current $I_d \leq$ 10.0 A. This establishes that the eqn.(3.1) is valid in this region. Hence the various transfer functions and block diagrams are also valid for any operating point in this range.

For studying transient response experimentally, the following operating point was selected.

Motor speed N_o	= 900 rpm
Corresponding slip S_o	= 0.4
Rotor current in dc path I_{do}	= 4 1 Amps
Converter firing angle θ_{fo}	= 103 5^o

The controller power circuit and rotor circuit parameters are given in Figures 2.2 and 2.3 respectively. The machine parameters and load characteristics are given in Appendix A. This information is used to determine the open loop transfer functions of the drive.

3.7 TRANSFER FUNCTION EVALUATION - OPEN LOOP

From Figure 2 3, total resistance in the rotor circuit,

$$R = 2r_2 + r_d + 2r_t + R_s$$

$$= 2.88 \text{ ohms.}$$

Total inductance in the rotor circuit,

$$L = L_d + 2(\ell_1 + \ell_2) + 2\ell_t$$

$$= 61 \text{ mH.}$$

This gives dc circuit time constant

$$T_d = L/R = 21.8 \text{ mS}$$

and converter time constant is given by

$$T_c = 1.66 \text{ mS}, \text{ from Section 3 3 1}$$

The field current of loading generator was adjusted such that

$$f = 4.0 \text{ watts-sec}^2.$$

The motor and load moment of inertia is

$$J = 1.75 \text{ Kg-m}^2.$$

From these value of J and f, mechanical time constant of the set up is

$$T_m = \frac{J}{f} \; 437.5 \text{ mS}.$$

For line commutated converter

$$V_d = V_{dm} - k_r \, e_1$$

where $-k_r$ is incremental gain of the converter, depends on the amplitude of e_{sync} - synchronising signal converter supply voltage V_2 and input resistances connected to the comparator. For $e_{sync} = 5.0 \; V_{rms}$, $V_2 = 180 \; V_{rms}$, input resistances are adjusted such that

$$k_r = 48.6.$$

Consequently,

$$k_r/R = 16.88.$$

Since,

$$\omega_s = 2\pi \times 50 = 157 \text{ rad/sec} ,$$

and $E = 190$ V for the stator supply of 400 Volts line-to-line.

$$k_{eb} = (E/\omega_s)^2 \frac{1}{R_f} = 0.127 ,$$

$$(k_r/R)/(1+k_{eb}) = 14.98.$$

Substituting the values of T_d, T_m and K_{eb} in characteristic equation

$$s^2 + (\frac{1}{T_d} + \frac{1}{T_m})\, s + \frac{1}{T_d T_m}(1 + k_{eb}) = 0$$

gives

$$T_1 = 385 \text{ mS}, \quad T_2 = 21.32 \text{ mS}$$

where $-1/T_1$, $-1/T_2$ are the roots of the characteristic equation. Therefore, from equations (3.13) and (3.14),

$$G_c(s) = \frac{\Delta I_d}{\Delta e_1}(s) = \frac{14.98(1 + s\, T_m)}{(1+s\, T_1)(1+s\, T_2)(1 + s\, T_c)} \qquad (3.22)$$

$$\frac{\Delta\omega}{\Delta e_1}(s) = 4.53/[(1+s\, T_1)(1+s\, T_2)(1+s\, T_c)] \qquad (3.23)$$

Similarly, from eqn.(3.14)

$$\frac{\Delta\omega}{\Delta T_L}(s) = \frac{0.222(1+s\,T_d)}{(1+s\,T_1)(1+s\,T_2)} \qquad (3.24)$$

where

$T_1 = 385$ mS , $T_2 = 21.32$ mS ,

$T_m = 437.5$ mS, $T_c = 1.66$ mS, and

$T_d = 21.18$ mS.

3.8 TRANSFER FUNCTION EVALUATION -CLOSED LOOP

In the previous section open loop transfer functions of the drive are given with numerical values of various parameters. These transfer functions depend on motor and load parameters, and the only design parameter is the converter gain k_r. The converter firing circuit is designed such that output voltage swings from maximum to zero for 0-5.0V variation of e_1.

~~While~~ The design of closed loop controller requires the determination of gain and time constants of PI controllers and filters used in the feedback path.

The transfer function of the first order filter used in the current feedback path is

$$H_c(s) = \frac{0.15}{1+ s\,T_s}$$

where $T_s = 8.32$ mS.

The steady state feedback factor of 0.15V/Amp is chosen to keep feedback voltage level comparable to that of reference voltage to current control loop The filter time constant T_s is kept large enough to reduce ripple amplitude and small enough to keep cut-off frequency $1/T_s$ greater than the cut-off frequency $1/T_2$ of $G_c(s)$ (refer Figure 3.4).

The transfer function of PI controller in this loop is

$$G_{cc}(s) = \frac{k_1(1 + s\,T_{c1})}{s}$$

where T_{c1} = 108 mS, and

k_1 = 9.26, includes the gain of a limiter.

Normally, PI controller 'zero' i.e., $1/T_{c1}$ for current controller is chosen small enough such that system phase shift is not affected near the gain cross-over point[19]. At the same time it should not be very small, such that system response becomes sluggish. In this case PI controller gain k_1 is chosen to keep phase margin of at least 45°. With the help of Nicols chart it was observed that maximum rotor current overshoot is approximately 0.1 db. This ensures that system response is not highly oscillatory. The Bode plots of $G_c(s)$ and $G_{cc}\,H_c(s)$ are given in Figure 3.4. Since $T_1 \simeq T_m$, from

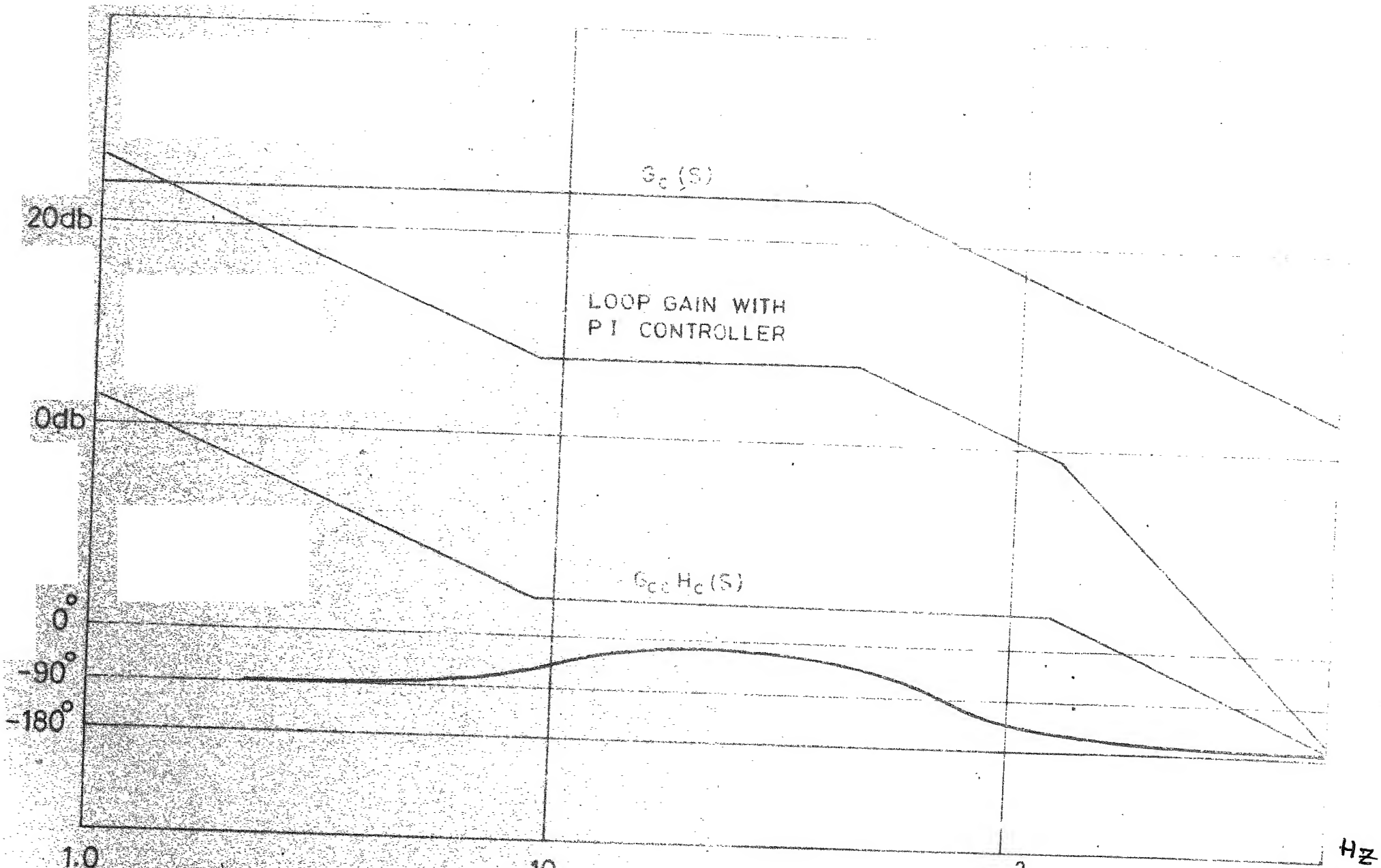

FIG. 3.4 SLIP POWER RECOVERY-FREQUENCY RESPONSE-CURRENT CONTROL LOOP

Section 3.7, cut-off frequencies at $1/T_1$ and $1/T_m$ are not indicated in the Bode plots. Similarly eqn (3.21) is rewritten as

$$G_c(s) = \frac{\Delta I_d}{\Delta e_1}(s) \simeq 14.98/[(1+sT_2)(1+sT_c)] \qquad (3\ 25)$$

Consequently, loop gain

$$G_c G_{cc} H_c(s) = \frac{20.8(1 + s\ T_{cl})}{s(1+s\ T_2)(1 + s\ T_c)(1 + s\ T_s)} \qquad (3.26)$$

The Bode plot of loop gain is also given in Figure 3.4.

The closed loop transfer function of current loop is given by

$$G_c^*(s) = \frac{\Delta I_d}{\Delta e_c}(s) = \frac{G_c\ G_{cc}(s)}{1 + G_c\ G_{cc}\ H_c(s)}$$

Since T_c and T_s are very small compared to T_2 or T_{cl}, they are ignored while calculating the transfer function $G_c^*(s)$. With this simplification, from eqn.(3.20),

$$G_c^*(s) = \frac{6.66(1+sT_{cl})}{(1 + s\ T_a)(1 + s\ T_b)} \qquad (3.27)$$

where $-1/T_a$ and $-1/T_b$ are the roots of equation

$$s^2 + \frac{1}{T_2}(1 + 20.8\ T_{cl})s + \frac{20.8}{T_2} = 0.$$

This gives

$$T_a = 149.3 \text{ mS}$$

and

$$T_b = 6.87 \text{ mS}.$$

Speed Control Loop.

The simplified transfer function $G_c^*(s)$ of current loop will be used for designing the speed control loop. This loop has PI controller with transfer function

$$G_{\omega c}(s) = \frac{k_2(1 + s\, T_{c2})}{s} \qquad (3.28)$$

where

$$T_{c2} = 8.25 \text{ mS}$$

and $k_2 = 35.5$ includes the gain of a limiter.

The design procedure for k_2 and T_{c2} is similar to that of current control loop. And the speed feedback transfer function is

$$H_\omega(s) = 0.0386/(1 + s\, T_g)$$

where

$$T_g = 62 \text{ mS}.$$

The design procedure for $H_\omega(s)$ is given in Section 2.8.

The transfer function

$$G_\omega(s) = \frac{\Delta\omega}{\Delta I_d}(s) = \frac{B}{\omega_{sf}} \frac{1}{(1+s\, T_{c2})} = \frac{0.303}{(1 + s\, T_m)} \qquad (3.29)$$

Consequently, loop gain

$$G_{\omega c} G_c^* G_\omega H_\omega(s) = \frac{35.5(1+sT_{c2})}{s} \frac{6.66(1+sT_{c1})}{(1+sT_a)(1+sT_b)}$$

$$\frac{0.303}{(1+sT_m)} \frac{0.0386}{(1+sT_g)} \qquad (3.30)$$

Expressing for the sake of convenience, loop gain

$$= A(s).\, B(s)$$

where

$$A(s) = \frac{2.0(1 + s\, T_{c1})}{(1+sT_a)(1+sT_b)(1+sT_m)(1+sT_g)} \qquad (3.31)$$

and

$$B(s) = \frac{35.5 \times 0.0386(1 + s\, T_{c2})}{s} \qquad (3.32)$$

Figure 3.5 gives Bode plots of A(s), B(s) and A(s).B(s). From Bode plots it is observed that the cut-off frequency, $1/T_g$ of $H_\omega(s)$ is greater than the gain cross-over frequency of the system. This ensures that it does not affect system performance. The loop gain plot indicates that the system has phase margin of 55° at the gain of cross-over frequency of 5.4 rad/sec. With the help of Nicols chart it was observed that the system is stable and response is not highly oscillatory.

3.9 EXPERIMENTAL INVESTIGATIONS

The loading and testing arrangement for the drive is same as given in Section 2.9. Details of Induction

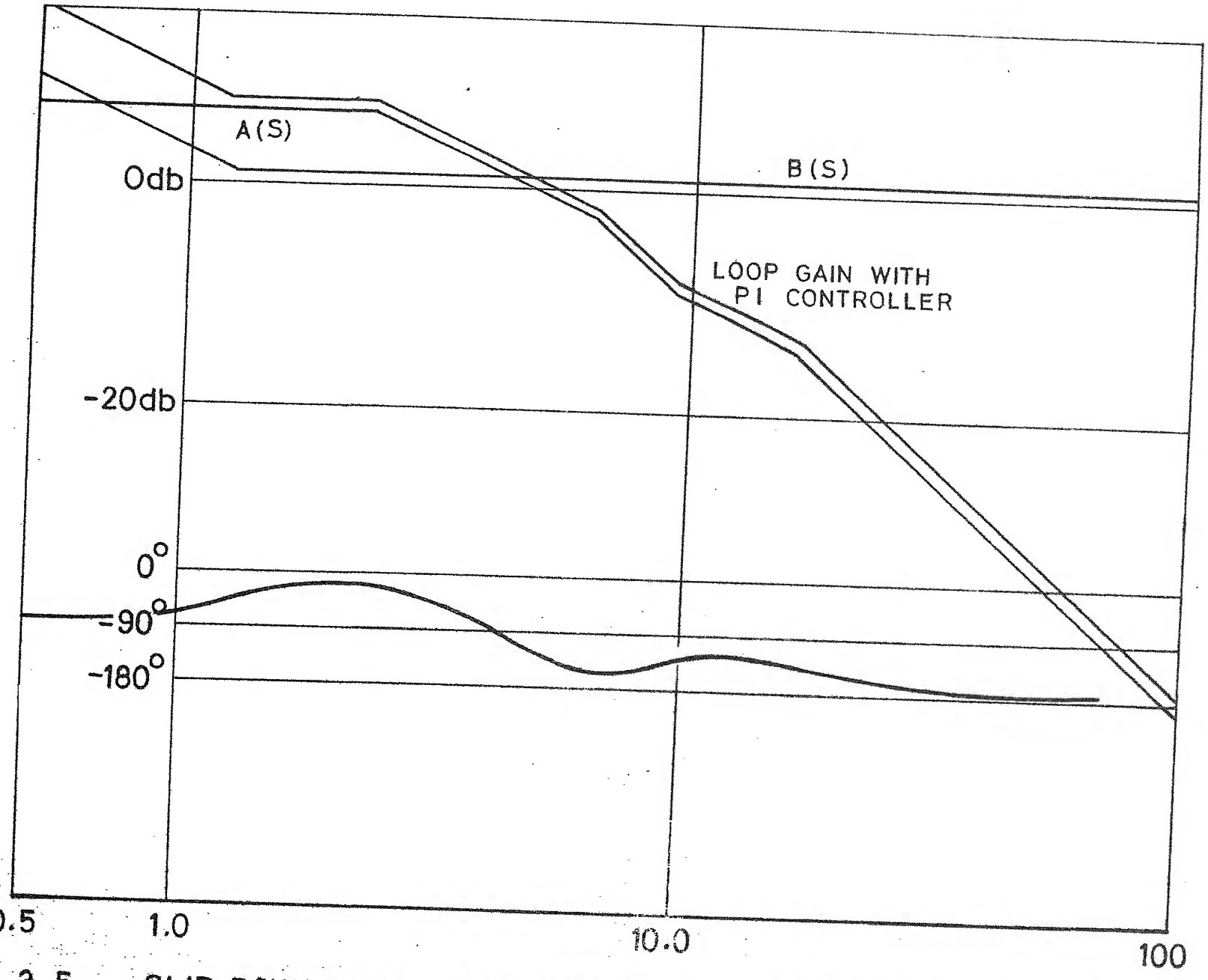

FIG. 3.5 SLIP POWER RECOVERY-FREQUENCY RESPONSE-SPEED CONTROL LOOP

Motor are given in Appendix A. The steady state characteristics are given in Figures 2.10 and 2.11.

The initial condition of the drive is kept same as the operating point given in Section 3.6. And a step input is applied to the controller at different input points to obtain transient response of the speed and rotor current. The response is recorded on the strip-chart recorder.

The open loop speed and current responses for +1.0V change in control signal are given in Figure 3.6.

Similarly Figure 3.7 gives the closed loop transient response with current feedback only. The step change in the current loop reference signal is $\Delta e_c = +0.5V$.

The transient response with speed and current feedbacks are given in Figure 3.8. The step change in the speed loop reference signal is $\Delta e_\omega = 0.05V$.

Since the controller does not have the provision to provide braking torque during retardation, only positive step inputs are applied as test signals.

3.10 DIGITAL COMPUTER PROGRAM

After labelling the appropriate current, speed and controller output voltages as state variables (refer

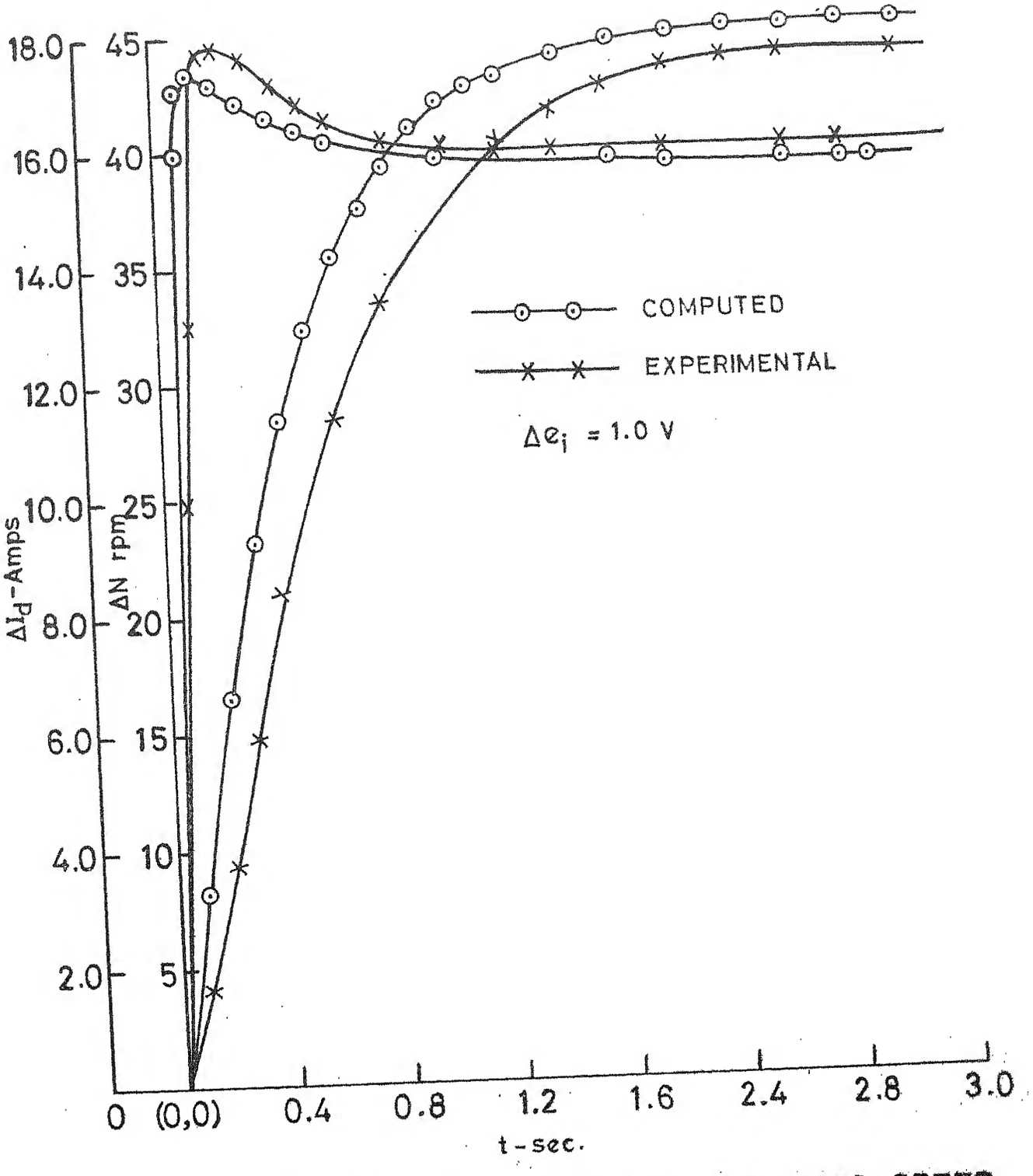

FIG. 3.6 SLIP POWER RECOVERY-OPEN LOOP SPEED AND CURRENT RESPONSE

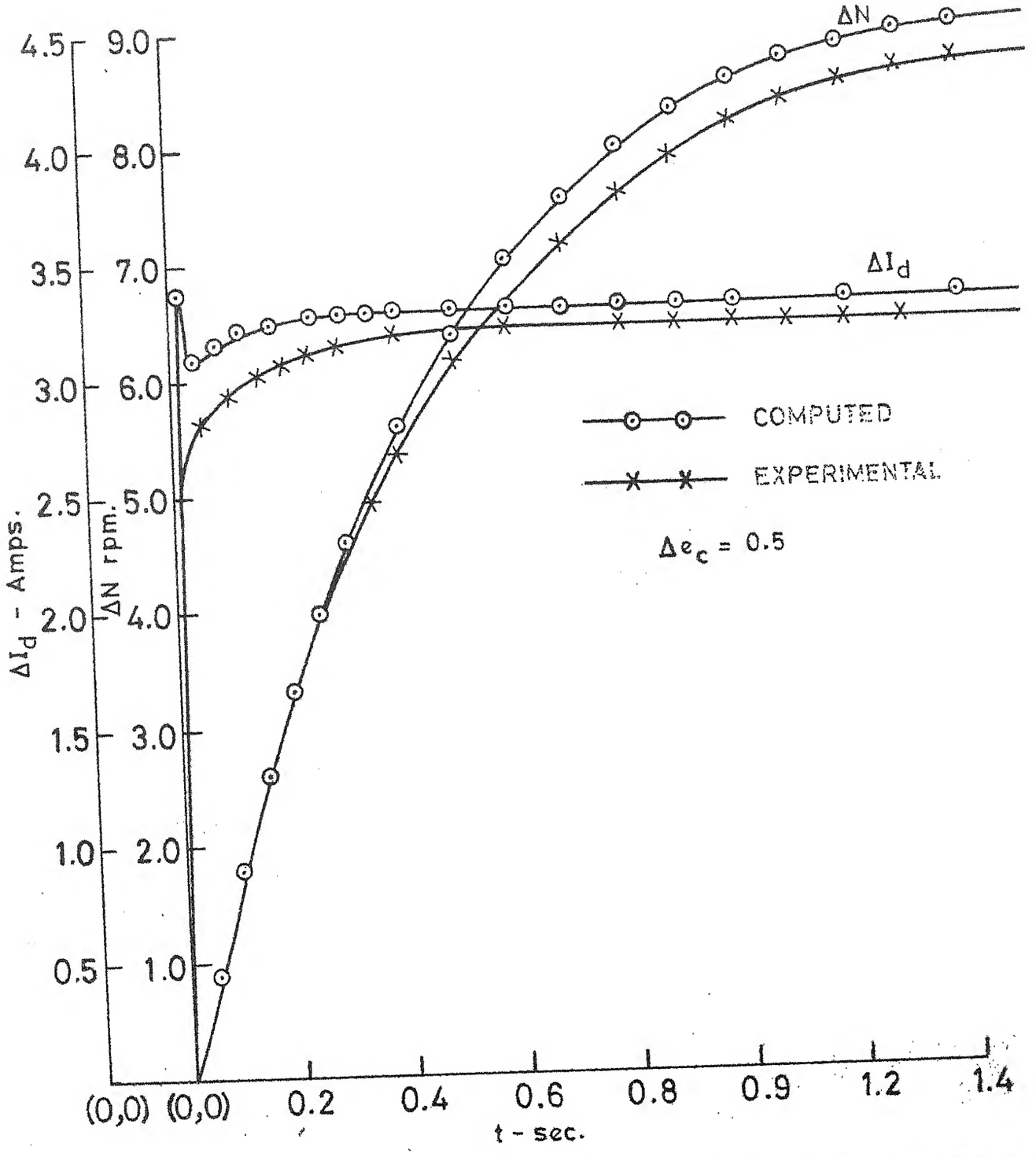

FIG. 3.7 SLIP POWER RECOVERY-SPEED AND CURRENT RESPONSE WITH CURRENT FEEDBACK ONLY

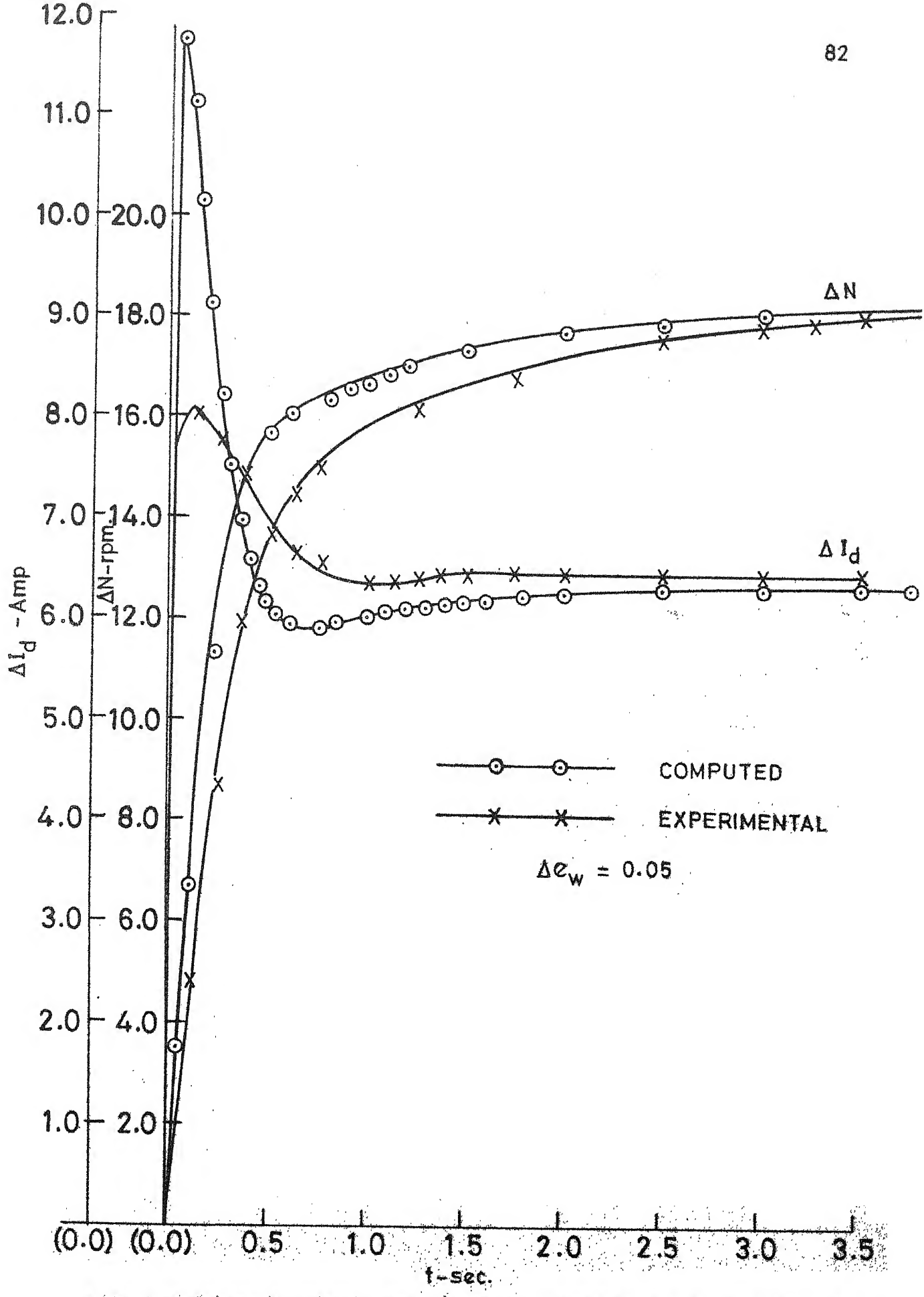

FIG.3.8 SLIP POWER RECOVERY-SPEED AND CURRENT RESPONSE WITH SPEED AND CURRENT FEEDBACK

Figures 3.1, 3.2 and 3.3), transfer functions for open and closed loop controller are written in state variable form as given below.

Let $X_1 = \Delta\omega$

$X_2 = \Delta I_d$

$X_3 = -\Delta V_d$

X_4 = average current feedback signal

X_5 = current controller output = Δe_i

X_6 = speed feedback signal

X_7 = speed controller output = Δe_c

Δe_ω = speed control loop reference signal.

The system equations are

$$\frac{d}{dt} X_1 = \frac{E}{\omega_s f} \frac{X_2}{T_m} - \frac{\Delta T_L}{f T_m} - \frac{X_1}{T_m} \qquad (3.33)$$

$$\frac{d}{dt} X_2 = \frac{X_3}{R T_d} - \frac{E}{\omega_s} \frac{X_1}{R T_d} - \frac{X_2}{T_d} \qquad (3.34)$$

$$\frac{d}{dt} X_3 = \frac{k_r X_5 - X_3}{T_c}$$

$$\frac{d}{dt} X_4 = \frac{H_c X_2 - X_4}{T_s} \qquad (3.36)$$

$$\frac{d}{dt} X_5 = k_1(X_7 - X_4) - k_1 T_{c1} \frac{d}{dt}\left(X_7 - X_4\right) \qquad (3.37)$$

$$\frac{d}{dt} X_6 = \frac{H_\omega X_1 - X_6}{T_g} \qquad (3.38)$$

$$\frac{d}{dt} X_7 = k_2(\Delta e_\omega - X_6) - k_2 T_{c2} \frac{d}{dt} X_6 \qquad (3.39)$$

The Runge-Kutta fourth order approximation method was used to solve these equations simultaneously.

Using this program the small signal response for motor speed and rotor current is obtained for the following cases:

i) open loop

ii) closed loop with current feedback only

iii) closed loop with speed and current feedback.

The first three equations are used to study the dynamic response of the open loop drive. Where $X_5 = \Delta e_1$ is input to the controller. Similarly, equations (3.33) - (3.37) are used for studying the system response when only current feedback is effective. In this case $X_7 = \Delta e_c$ is input to the system. For studying the response when both the feedbacks are effective, equations (3.33) - (3.39) are used and Δe_ω is input to controller.

The transient response is computed for the same operating point around which transfer functions are computed in the previous sections. The initial values of the system variables are assumed to be zero as the

system is in steady state before the disturbance. The same program can be used to compute transient response for load perturbations.

Comparison of computed and experimentally obtained transient response is given in Figures 3.6, 3 7 and 3.8.

3.11 CONCLUSIONS

For small perturbations of input signals around a given operating point, the small signal model developed gives good accuracy. The same model is useful in designing a closed loop controller with predictable performance.

This model holds good over a wide range of speed and torque. The controller characteristics imposes a limitation due to which this model does not hold good during motor retardation.

A slipring motor with closed loop control can be used in many industrial applications where precise speed control is required. This drive is economical compared to dc motor or variable frequency induction motor drive.

CHAPTER 4

CHOPPER CONTROLLED SLIPRING INDUCTION MOTOR

4.1 INTRODUCTION

At a given speed, torque developed by induction motor can be varied by changing the effective rotor resistance. This technique is commonly used for starting the slipring motor. When this method is applied for speed control of slipring motor its major drawback, like stator voltage control, is poor efficiency at low speed. Therefore, this method is used for low or medium power drives only. The advantages of this scheme over stator voltage control are

i) wide range speed control is possible, irrespective of the load speed torque characteristics, and

ii) pullout torque is independent of rotor resistance (refer Figure 4.1).

Conventionally, external resistance connected in the rotor circuit is controlled manually in descrete steps. Using power semiconductors, the conventional resistance control can be eliminated by using 3-phase rectifier bridge and chopper controlled external resistance. The simple arrangement of resistance and

chopper in the rotor circuit cause highly distorted waveforms of rotor winding currents. A filter circuit between 3-phase rectifier and chopper is incorporated to obtain ripple free rectified rotor current.

The other alternatives of controlling effective rotor resistance are i) short circuiting rotor circuit through phase controlled thyristors [23,24] or ii) using controlled bridge rectifier with external R-L load on dc side [22]. Since both of these circuits operate on variable frequency source from sliprings, the wide range phase angle control requires elaborate firing circuits and/or rotating transducer mounted on the motor shaft[8].

The chopper control scheme is simple and economical for small and medium power slipring motor. The drawback of open-loop control with rotor resistance control scheme is its poor regulation. Slipring induction motor may now be applied in closed loop regulated drives with a degree of precision fully acceptable in many cases, by the use of fast response thyristor chopper controllers. A one percent regulation for a wound rotor motor by using feedback and chopper is easy. A 0.5 percent regulation is practical. But achieving better regulation requires close examination and consideration of many drive parameters. The

design of chopper controlled slipring motor drive - using filter on the rotor side - complete with closed loop speed control and inner current control loop is given in this chapter.

4.2 BASIC CHOPPER CIRCUIT

Figure 4.2 gives a basic chopper circuit. A chopper is a power switch electronically monitored by a control circuit. When the chopper is in the ON mode all the time the equivalent external resistance R_{eq} in the rotor circuit is R_1. When the chopper is in the Off mode all the time equivalent external resistance R_{eq} in the rotor circuit is $(R_1 + R_2)$. The speed torque characteristics corresponding to $R_{eq} = R_1$ and $R_{eq} = (R_1 + R_2)$ are given in Figure 4.1. If the chopper is periodically regulated so that, in each chopper period, it is ON for some time but is OFF for the rest, it is possible to obtain variation of R_{eq} between R_1 and $(R_1 + R_2)$. Thus the chopper electronically alters the external resistance R_2, and hence corresponding speed torque characteristic of motor is varied in a continuous and contactless manner [25]. The waveform of rectified current and voltage across switch for this simple chopper arrangement are also given in Figure 4.2. Effect of ripple in the bridge output on current waveform is neglected.

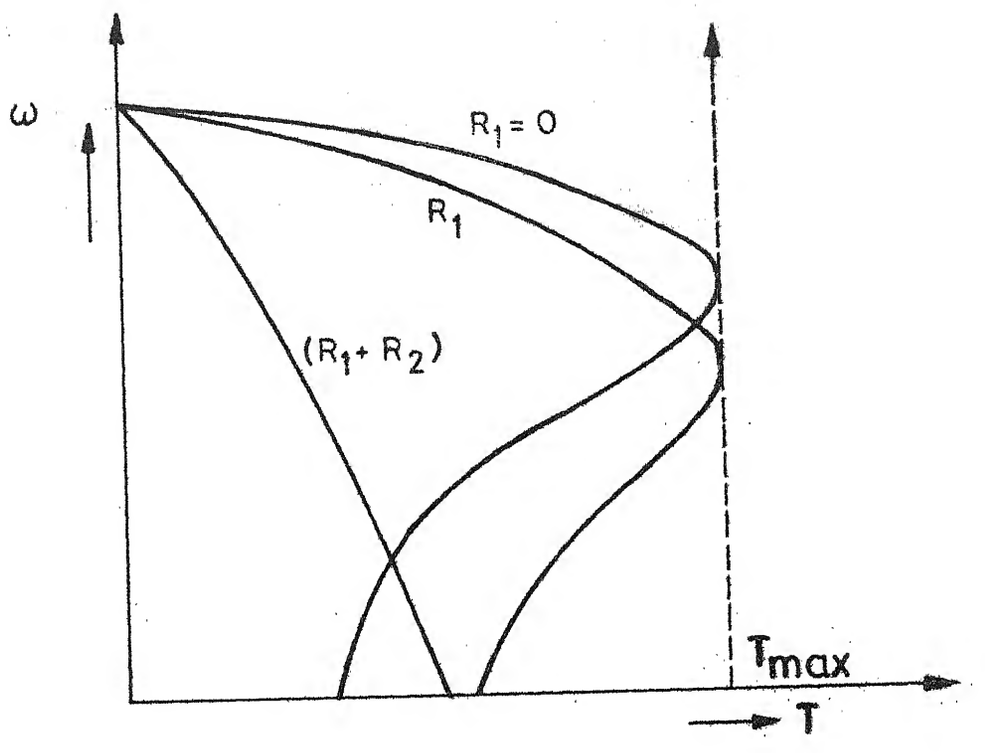

FIG. 4.1 SPEED-TORQUE CHARACTERISTICS FOR ROTOR RESISTANCE CONTROL

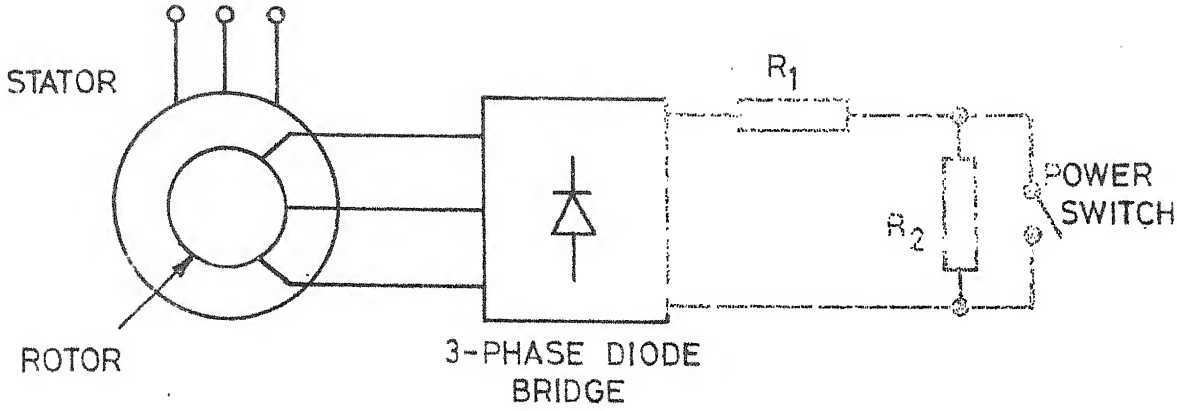

(a) BASIC CHOPPER SCHEMATIC DIAGRAM

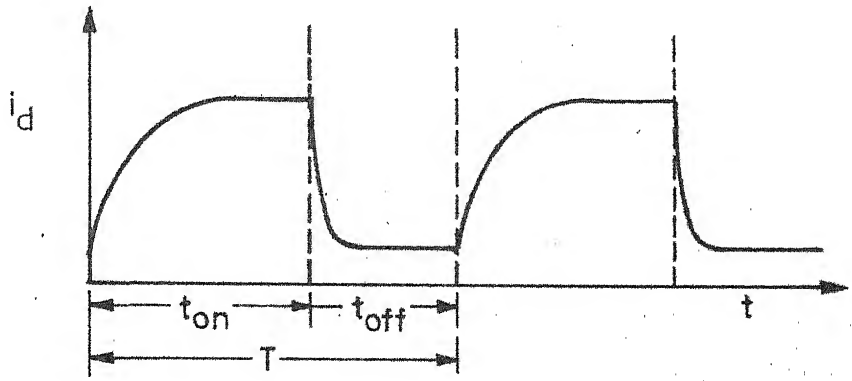

(b) RECTIFIED CURRENT WAVEFORM

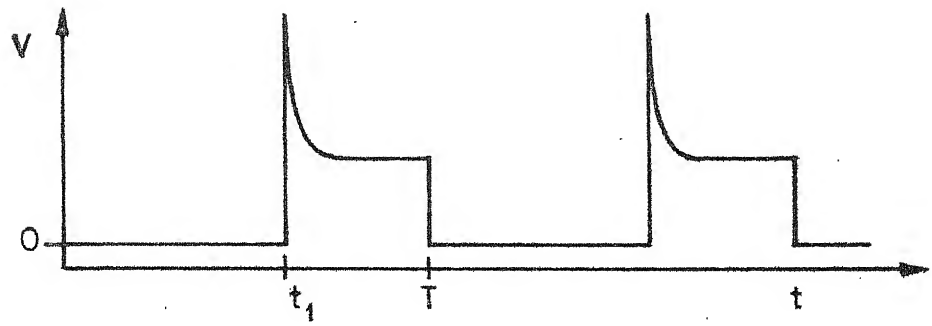

(c) VOLTAGE ACROSS POWER SWITCH

FIG. 4.2 BASIC CHOPPER CIRCUIT

In this arrangement no external inductor is used. Only inductance in the circuit is the rotor leakage reactance. This offers very small time constants during ON and OFF periods. Due to this, current reaches to steady state during ON and OFF periods. R_2 should be chosen as large as possible to obtain lower speeds. However, this will increase the voltage spike across the switch, which will require a thyristor with excessively high voltage.

Using such a simple chopper circuit for controlling the average value of resistance (rotor current) introduces the additional problems such as discontinuity in the rotor winding currents, and voltage spikes across the chopper thyristor. Highly distorted waveforms of currents within the rotor cause excessive heating of the windings. This requires considerable derating of the motor capacity. To certain extent this heating can be reduced if chopping frequency is much lower than the supply frequency. However, chopping at such low frequency may cause fluctuations in the motor speed for low inertia loads.

Increasing the chopper frequency will certainly give speed output without any fluctuations. But this will increase the amplitude of current harmonics and hence, heating of the motor. This problem can be taken care of by introducing a filter in the rotor circuit

as shown in Figures 4.3 or 4.4. With a filter in the rotor circuit current waveforms can be made continuous and ripple in d.c. current can be reduced to a very small value by selecting the appropriate chopper frequency and corresponding parameters of the filter circuit. This improvement permits application of motors with a derating factor of almost 90 percent [26].

Figure 4.3(a) gives a chopper circuit with L-R filter. The current and voltage waveforms are also given in the same figure.

In the next section it will be shown that to reduce the ripple in the d.c. current it is necessary that

$$\tau_2 \approx \tau_1$$

and

$$\tau_1 > T$$

where

τ_1 - time constant during ON period

τ_2 - time constant during OFF period

and $\frac{1}{T}$ is chopper frequency.

This restricts R_2 to a very small value resulting in not so wide variation and in the speed-torque characteristics. This problem is taken care of if we use 2nd order filter as shown in Figure 4.4. The presence

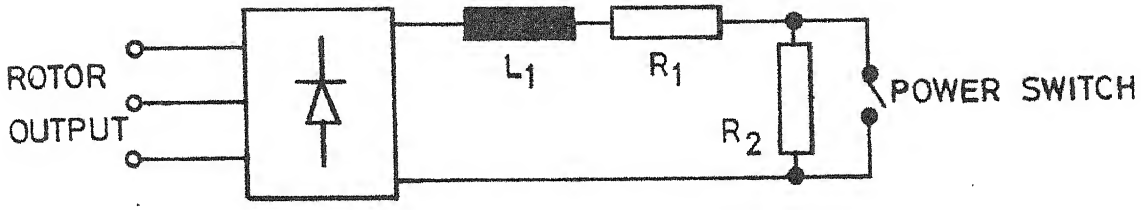

(a) CHOPPER WITH I^{st} ORDER FILTER

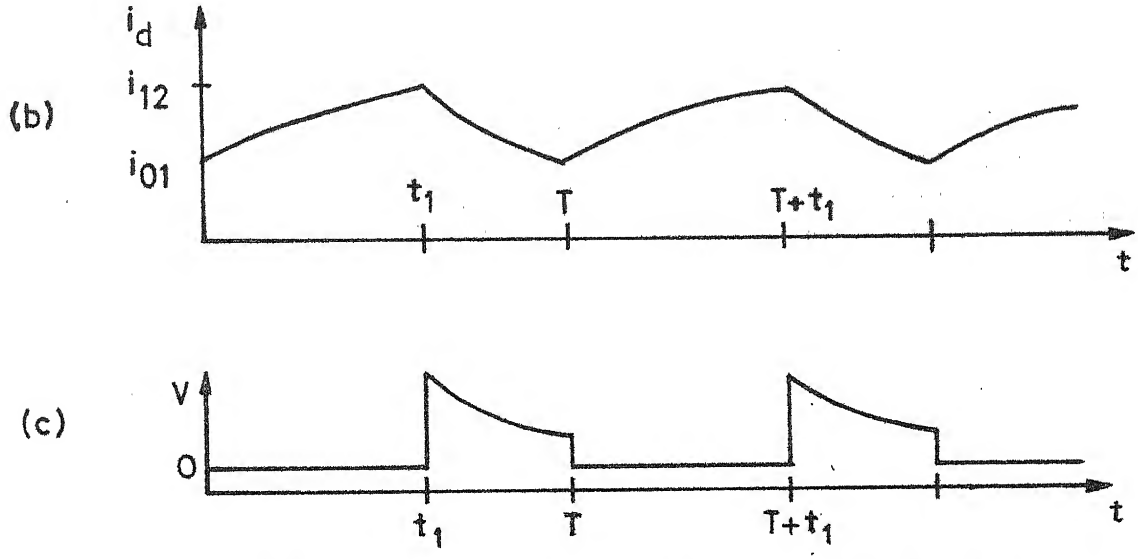

(b),(c) RECTIFIED CURRENT AND SWITCH VOLTAGE WAVEFORMS

FIG. 4.3 IMPROVED CHOPPER CIRCUIT

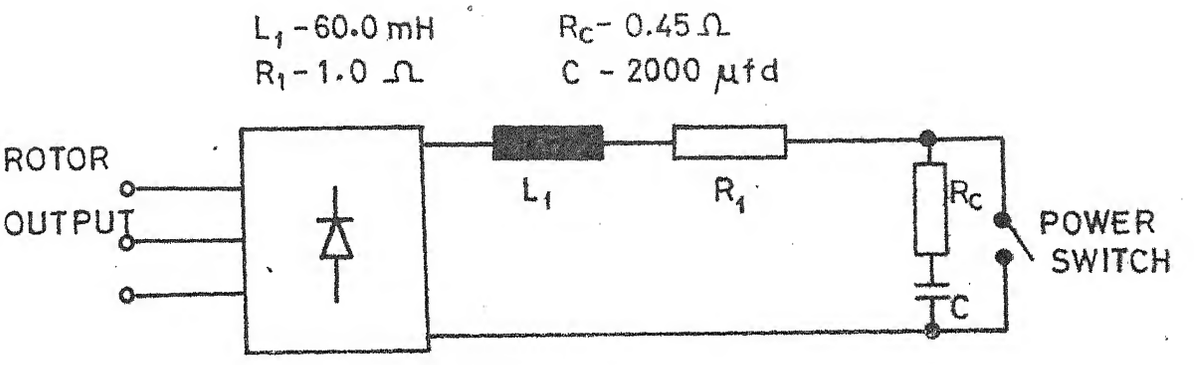

(a) CIRCUIT DIAGRAM

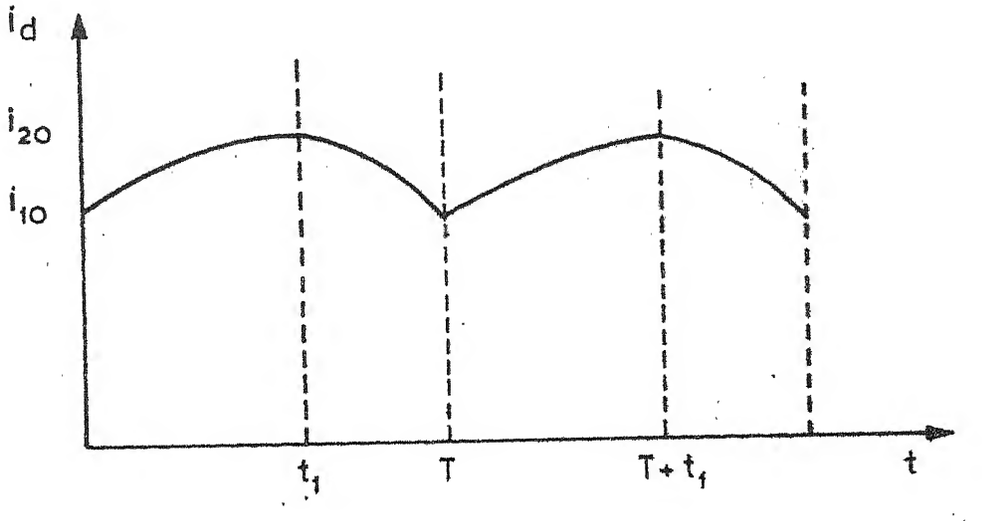

(b) RECTIFIED CURRENT WAVEFORM

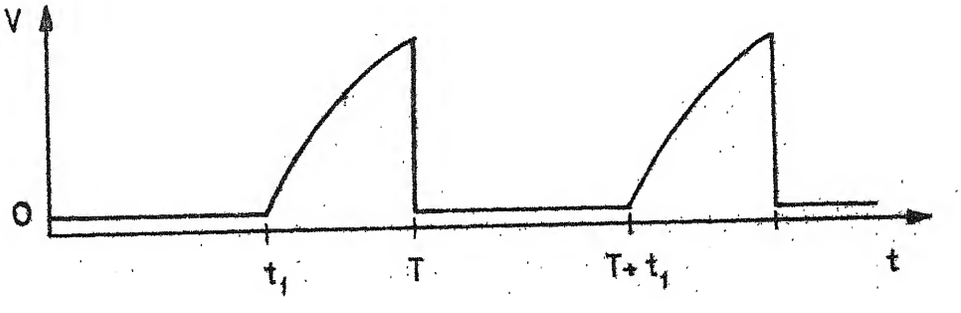

(c) VOLTAGE ACROSS SWITCH

FIG. 4.4 CHOPPER WITH 2^{nd} ORDER FILTER

of capacitor C in this circuit prevents voltage spikes across the switch. Moreover, under steady-state, R_{eq} becomes infinity when switch is OFF all the time. This will give wider variation in the speed-torque characteristics and also reduced ripple in the rotor current. The resistance R_c is used to limit the capacitor discharge current through the switch.

4.3 DERIVATION OF CIRCUIT MODELS

The problems associated with the analysis of chopper controlled slipring motor are similar to that of slip power recovery scheme given in Section 2.5. For chopper circuit when filter is used, current in dc link could be assumed continuous and ripple free. Thus the circuit models will also become similar to that of slip power scheme. Consequently, the discussion on merits of dc circuit model over that of ac circuit model given in Section 2.5 is also applicable to chopper control scheme. With the help of dc circuit model given here, the relation between equivalent external resistance R_{eq} and chopper duty cycle is obtained for first order filter only. It is observed that for second order filter relation between R_{eq} and chopper duty cycle is highly nonlinear.

The per phase ac equivalent circuit of induction motor referred to rotor is given in Figure 2.3(a). The dc circuit model is derived for 3-phase system.

If for the given chopper frequency filter components are chosen such that ripple in the current i_d is negligible then rotor current is composed of alternating square pulse of $2\pi/3$ duration. Hence the relation given by eqn. (2.2)

$$I_2 = \sqrt{\frac{3}{2}} \cdot I_d$$

for slip power recovery scheme holds good for chopper controller as well, where

I_2 - rotor rms current,

I_d - average value of i_d.

The power loss in the stator and rotor resistance for all three phases is $2I_d^2(S\, r_1 + r_2)$ in the d.c. side. Because of leakage reactance of the motor windings there is a voltage reduction of $(3\omega/\pi).\ (\ell_1 + \ell_2)$ in the output voltage of the rectifier bridge.

If the voltage drops across slipring brushes and diodes are neglected, the system is represented by the d.c. equivalent circuit as shown in Figure 4.5. The configuration for external components depends on the type of filter used. For this circuit model

$$E = \frac{3\sqrt{6}}{\pi} E_2$$

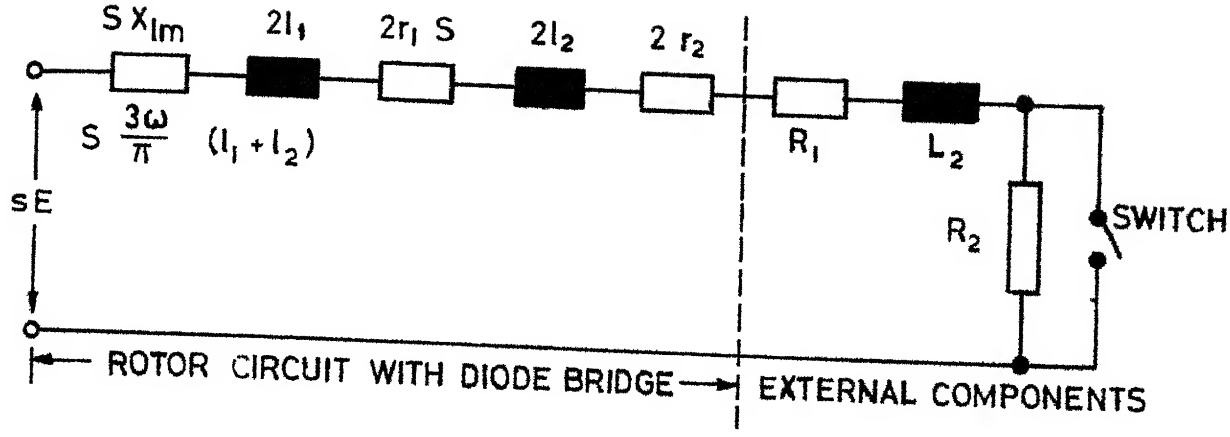

FIG. 4.5 D C CIRCUIT MODEL

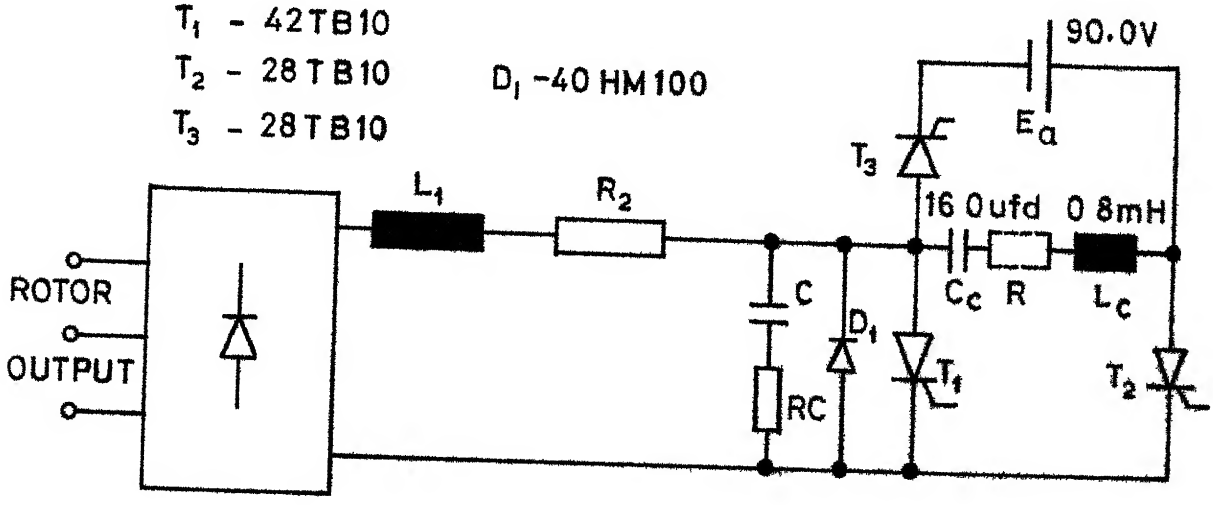

FIG. 4.6 CHOPPER CONTROL SYSTEM

where E - average value of rectified rotor voltage at stand-still

E_2 - rotor voltage per phase in rms at stand-still.

The different parameters used in the figure are

$\ell_1+\ell_2$ - total leakage inductance per phase referred to rotor

r_1 - stator resistance per phase referred to rotor

r_2 - rotor resistance per phase

R_1, R_2 - external resistances

L_1 - external inductor

$$X_{\ell m} = \frac{3\omega_s}{\pi}(\ell_1 + \ell_2)$$

ω_s - supply frequency in rad/sec.

S - motor slip.

The torque developed by motor at given slip can be determined if steady-state average current is known. The nature of current waveform and its average value will depend on the type of filter used and chopper duty cycle. With first order filter, i.e., circuit given in Figures 4.3 it is easy to obtain the relation between I_d and chopper duty cycle, under certain simplifying assumption [14]. The detailed analysis with second order filter is given in the next section.

With first order filter, let

t_1 - On period

t_2 - OFF period

$R_{11} = R_1 + S.2r_1 + 2r_2$

$1/T$ = chopper frequency

$R_{22} = R_{11} + R_2$

$L_{11} = L_1 + 2(\ell_1 + \ell_2)$

$\tau_1 = L_{11}/R_{11}$

$\tau_2 = L_{11}/R_{22}$

$I_1 = S\ E/R_{11}$

$I_2 = S\ E/R_{22}$

If we neglect the voltage drop due to commutation in the diode bridge, current during ON mode is given by

$$i_1 = I_1(1 - e^{-t/\tau_1}) + i_{10}\, e^{-t/\tau_1} \qquad (4.1)$$

and during OFF mode

$$i_2 = I_2(1 - e^{-t/\tau_2}) + i_{20}\, e^{-t/\tau_2} \qquad (4.2)$$

where i_{10} and i_{20} are initial values of current for ON and ~~of~~OFF mode, respectively.

Assuming that the chopper frequency and filter inductor are such that

$$t_1/\tau_1 \ll 1$$

and $t_2/\tau_2 \ll 1$

it can be shown that [14]

$$I_d = SE/[R_{11} + (t_2/T)\, R_2] \qquad (4.3)$$

Therefore,

$$R_{eq} = R_2(t_2/T) \qquad (4.4)$$

This equation shows that R_{eq} is proportional to the OFF period of the chopper circuit. This is how the external resistance in the rotor circuit can be varied by controlling the duty cycle of the chopper circuit.

The rotor copper loss is given by

$$SP_2 = (SE - SX_{\ell m}\, i_d)I_d - S2r_1I_d^2 \qquad (4.5)$$

where P_2 is airgap power or torque in synchronous watts and

$(S\,E - S\,X_{\ell m}\,I_d)$ is the effective d.c. voltage available in the rotor circuit

While $S\,X_{\ell m}\,I_d$ is only reduction in voltage due to commutation and it does not account for power loss in the rotor circuit. Therefore, torque in synchronous watts

$$P_2 = [E - (X_{\ell m} + 2r_1)I_d]I_d \qquad (4.6)$$

Equations (4.3) and (4.6) can be used to obtain torque versus slip characteristic for different duty cycles of the chopper.

4.4 CHOPPER WITH SECOND ORDER FILTER

4.4.1 Analysis with Second Order Filter[27,28]:

It has already been pointed out that with a simple L-R filter, it is not possible to get a wide variation in the speed torque characteristics. With second order filter, it is possible to increase the speed control range of the drive. Figure 4.4 shows the configuration of the second order filter where capacitance C replaces the resistance R_2 of the first order filter. R_c is used to limit the discharge current of C during ON mode of the chopper. The dc equivalent circuit given in Figure 4.5 holds good for this arrangement also. However, external components shown in the figure will be replaced by that of second order filter.

Analysis (ON mode):

$$i_1 = I_1(1 - e^{-t/\tau_1}) + i_{10}\, e^{-t/\tau_1} \qquad (4.7)$$

where

$$I_1 = SE/R_{11}$$

$$\tau_1 = L_{11}/R_{11}$$

and i_{10} = initial value of current for ON mode.

The voltage across the capacitor v_c is zero during ON mode.

Analysis (OFF mode).

For under-damped circuit,

$$i_2 = \left(\frac{SE - i_{20} R_{11}}{\omega_d L_{11}}\right) e^{-\xi \omega_n t} \sin \omega_d t + i_{20} e^{-\xi \omega_n t} \frac{1}{\omega_d} [\omega_d \cos \omega_d t + \xi \omega_n \sin \omega_d t] \quad (4.8)$$

where

$$\omega_n = 1/\sqrt{(L_{11} C)}$$

$$\xi \omega_n = R_{11}/2L_{11}$$

$$\omega_d = \omega_n \sqrt{(1-\xi^2)}$$

$$\xi < 1$$

and i_{20} is the initial value of the current for OFF mode. Therefore, effective time constant

$$\tau_2 = 2L_{11}/R_{11}$$

and $$v_c = SE - \left(L_{11} \frac{di_2}{dt} + R_{11} i_2\right) \quad (4.9)$$

In this case it is not easy to get a closed form solution for the following reasons:

1. For the given circuit it is a tedious job to determine boundary values i_{10} and i_{20} under steady state condition.

2. Presence of leakage reactances on the ac side of the bridge rectifier makes it all the more difficult.

Hence a digital computer program was developed to determine the steady state current waveform of i_d. From the steady state current waveform average current I_d, and hence torque developed for the given speed can be determined. This program gives the static speed torque characteristics for different duty cycles of chopper. Details of this program are given in Section 4.11.

The superiority of second order filter over other arrangements is already pointed out in the previous sections. Hence design considerations, computer aided analysis and experimental investigations are given in subsequent sections for chopper control scheme with second order filter only.

4.4.2 Design Considerations for Second Order Filter:

Before deciding over filter components it is necessary to decide over chopper frequency. For a thyristor chopper, the power switch shown in Figure 4.4 is replaced by a thyristor and commutation circuit. The details are given in the next section. It is mainly

the thyristor turn-off time, commutation circuit and desirable variation in duty cycle that determine the chopper frequency. From the analysis given in the previous section, it is obvious that higher chopper frequency is desirable in order to reduce filter components size. The design considerations for determining chopper frequency are as follows:

1. Thyristor turn-off time, maximum rotor current, filter capacitor discharge current and auxiliary supply voltage will determine the values of commutating components.
2. The commutation circuit puts restriction on minimum or maximum time for which main thyristor should remain ON or OFF, respectively.
3. Now, the desirable range of duty cycle, depending on the requirements of particular drive application, will determine the maximum frequency.

Let chopper frequency be f_c. Therefore

$$T = 1/f_c.$$

Determination of Filter Components:

Choose

1. R_1 to limit the worst case rotor current
2. $L_{11}/R_{11} > T$ - to ensure that i_1 does not reach steady state during the maximum ON period.

3. C is determined such that circuit is underdamped and $1/4\ f_d > T$, here $f_d = \omega_d/2^-$.

Any higher values of L or C will reduce the ripple in the rotor current. However, these values should not be large enough to deteriorate the dynamic response of the drive.

4. R_c - 'Capacitor discharge current' limiting resistance should be large enough to protect the capacitor and the thyristor switch. However, larger values of R_c will increase the discharge time constant 'CR_c'. This requires that the thyristor, which is now carrying the rotor current and also capacitor discharge current, should be kept ON for a longer period before commutation circuit can turn it OFF.

4.5 CHOPPER CONTROL SCHEME [29,30]

Figure 4.6 shows the control circuit. T_1 is the main thyristor which acts as shunt switch. When T_1 is 'ON', external components connected in the rotor circuit are L_1 and R_1 only. During this period current builds up from i_{10} to i_{20} (see Figure 4.4(b)) through L and R_1. The turning 'OFF' of T_1 will divert rotor current into filter capacitor 'C'. This circuit configuration is a second order filter in the rotor circuit. Now, current

decreases to i_{10} (under steady state), and capacitor is charged to voltage v_c. When T_1 is turned ON again, Capacitor C discharges through T_1 while resistance R_c limits the maximum current through T_1 and dissipates most of the stored energy of capacitor C. T_1 must remain ON till the current is decreased to a value which can be commutated by T_2 and its associated commutating circuit. This period decides the minimum permissible duty cycle.

This filter operation gives almost smooth ripple free current I_d through L_1 and R_1. And corresponding rotor winding current can be assumed to be rectangular current pulse with a pulse width of $2\pi/3$.

4.5.1 Commutation Circuit:

In this chopper, impulse commutation arrangement is used to turn off the main thyristor T_1. In Figure 4.6 T_2 is the commutating thyristor. C_c and L_c are the commutating components. A resistance R shown in dotted lines takes care of Q of the circuit. T_3 is used for reversing the polarity of capacitor voltage. 'E_a' (auxiliary supply) maintains high voltage across capacitor even when rotor voltage is low.

To begin with T_3 and T_1 are triggered, the triggering of T_3 charges C_c, in positive direction to the voltage e_{c2}, and time taken for charging is $[\pi \sqrt{(L_c C_c)}]$. T_3 undergoes natural commutation. T_1 is kept ON for the period of t_1 as controlled by a PWM circuit. At the end of this thyristor T_2 is triggered. This turns T_1 OFF by sending a current impulse $I_p \sin [t/\sqrt{(L_c C_c)}]$.

I_p is the peak discharge current which is given by $e_{c2} \sqrt{(C_c/L_c)}$. For design consideration this is made equal to 1.5 times the maximum rotor current [29]. The polarity of voltage across C_c is reversed, and now voltage is e_{cr}. Once T_1 and D_1 are turned OFF, energy stored in the rotor circuit is transferred partly to the commutating capacitor C_c. This may build up capacitor voltage to excessively high value. However, when a second order filter is used this effect becomes almost negligible.

It is possible to design a commutating circuit without any auxiliary supply, i.e. $E_a = 0$. In such a case, capacitor C_c receives its charge from rotor output 'E' only. Since 'E' is proportional to motor slip, commutating capacitor voltage will also depend on the slip, and thur making it ineffective at higher speeds to commutate the specified load current. This arrangement

would restrict the speed range attainable by this control In order to overcome this problem an auxiliary supply E_a is used

4.5.2 Firing Circuit

The firing sequence of thyristors is shown in Figure 4.7. Figure 4.7(b) gives the schematic diagram of firing circuit. A triangle wave generator and a comparator forms a basic PWM circuit. And the frequency of triangle-wave generator decides the chopper frequency. The pulse width of PWM output is proportional to e_1 the control input. Since the power thyristors used require comparatively large gate currents of the order of 70-100 mA it was necessary to have drivers in each channel of the firing circuit. Since the cathode of 'T_3' is not grounded a pulse transformer is used in the firing circuit, to provide it with isolation. Thyristor T_1 receives a maintained firing pulse. While T_2 and T_3 are pulse fired. In both the channels pulses of 0.5 msec. width are derived from the one-shot circuits. It was often observed that spurious triggering of one-shots resulted in the simultaneous triggering of T_2 and T_3, hence a short circuit across the auxiliary supply. In order to prevent this a simple logic arrangement was incorporated in Channels II and III. With this

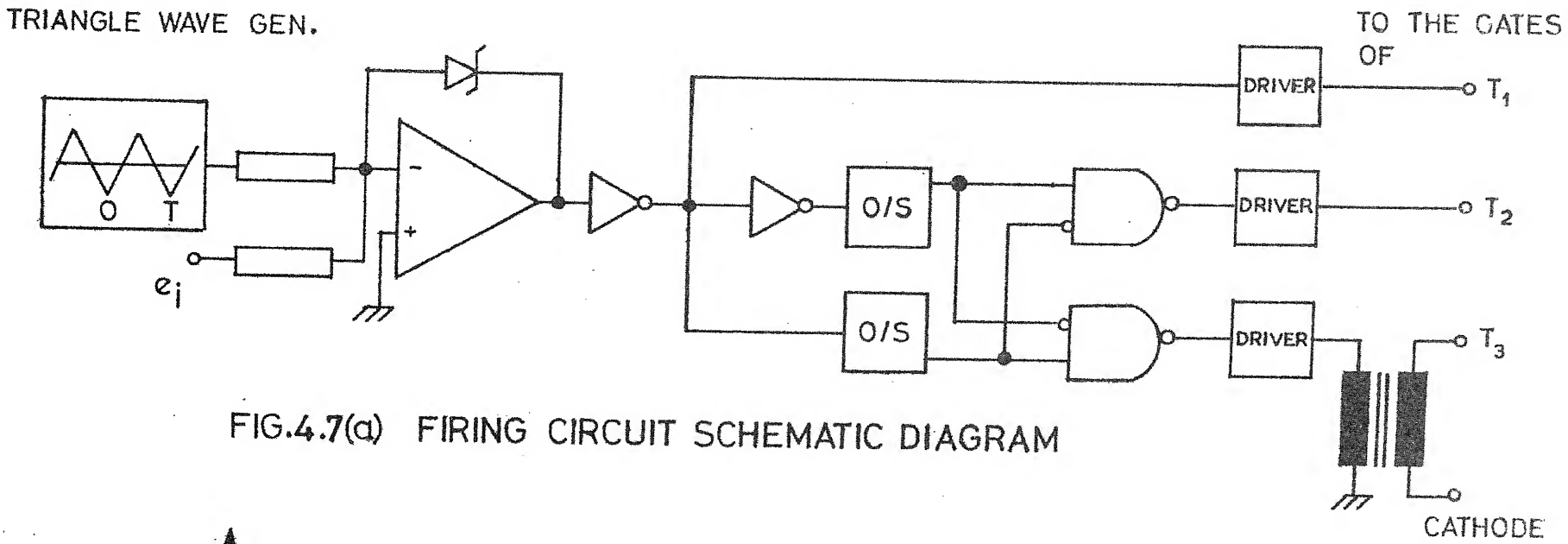

FIG.4.7(a) FIRING CIRCUIT SCHEMATIC DIAGRAM

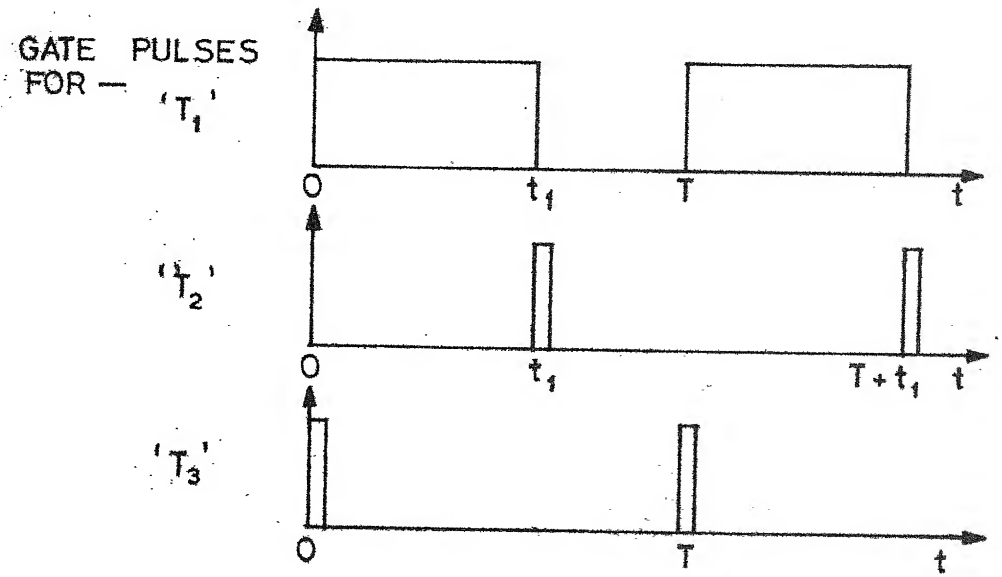

FIG.4.7 (b) FIRING SEQUENCE OF THYRISTORS

logic arrangement T_2 can receive a firing pulse only when T_3 is not receiving one Similarly T_3 gets a firing pulse when T_2 is not getting it.

4.6 CLOSED LOOP SPEED CONTROL

The rotor resistance controlled slipring IM has very poor speed regulation with open loop control. In many industrial applications, very good speed regulation of the drive is essential. In such cases, it becomes necessary to go for closed loop speed control. Precision closed loop regulators for conventional rotor resistance control are impractical. However, with a thyristor chopper, a slip ring IM may now be applied in closed loop drives, with a good degree of precision.

4.6.1 System Description:

Figure 4.8 gives a block diagram of the complete speed control system. A chopper with second order filter is connected on the rotor side of 3 phase slip-ring motor. A permanent magnet tachogenerator mounted on the same shaft is used to obtain speed feedback signal. The rotor current is sensed by connecting a small resistance in the dc circuit. The duty cycle of the chopper circuit is controlled by varying e_1, the output of current controller. An eddy current

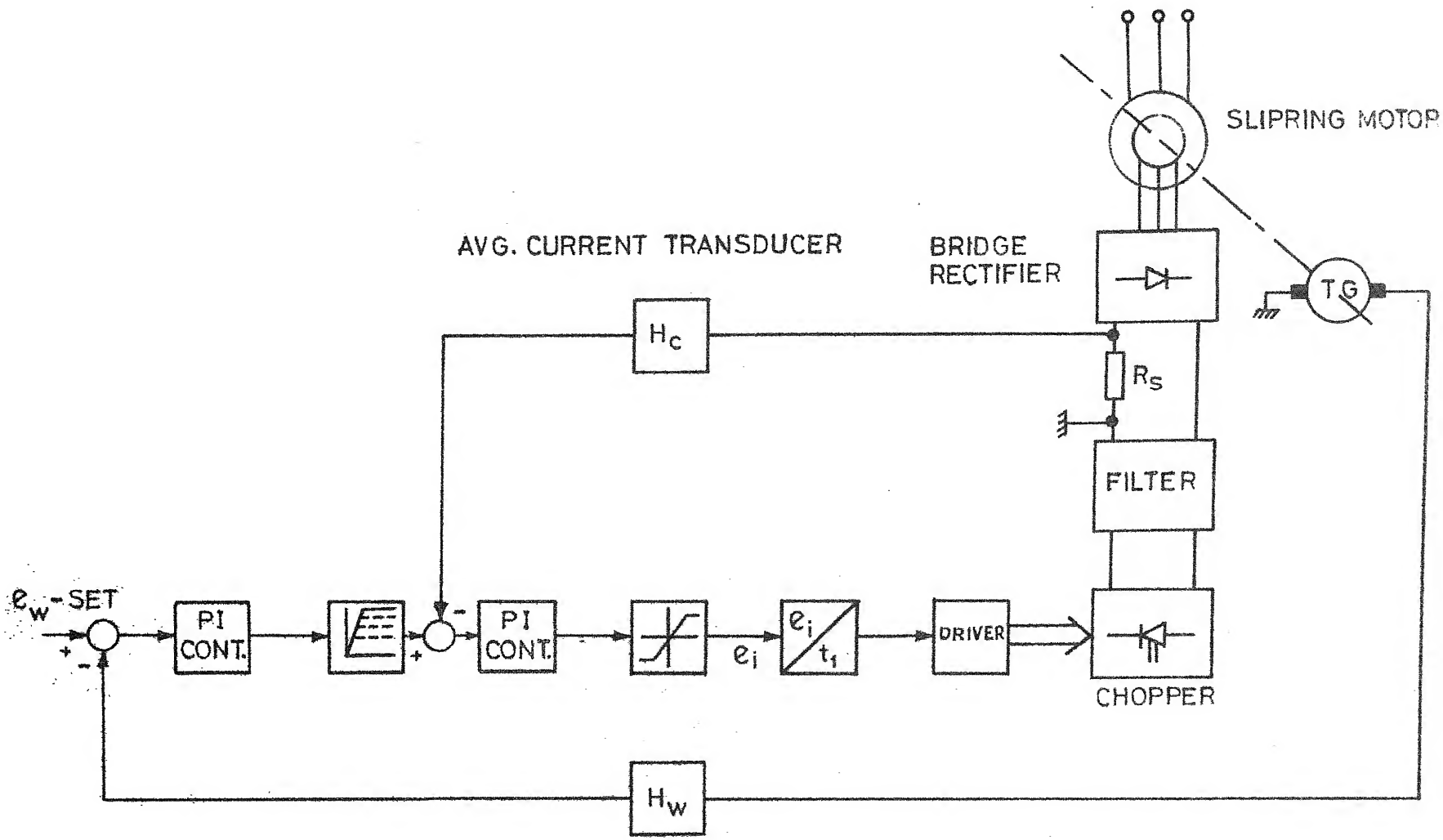

FIG.4.8 BLOCK DIAGRAM OF CLOSED LOOP CONTROL SCHEME

brake connected to the same shaft is used as load. The motor details are given in Appendix A. The equivalent circuit parameters are given in Figure 2.9.

The scheme shown in the block diagram uses PI control for speed and current control loops. The description and operation of these controllers is identical to that of slip power recovery scheme given in Section 2.8.

4.7 SPEED CONTROLLER

A permanent magnet dc tachogenerator is used to obtain a speed feedback signal. The design of attenuator and first order filter in the feedback path is identical to that of slip power recovery scheme. The detailed discussion on this is given in Section 2.8.

Figure 4.9 gives the circuit diagram of speed controller. It is essential that output of speed controller should be unidirectional and with well defined saturation level. Besides this, to make current limit adjustable it is desirable to make this saturation level rather than the feedback factor adjustable. This was achieved by using a precision 1/2 bridge limiter with adjustable limiting level. Output of this limiter is a reference for the current control loop.

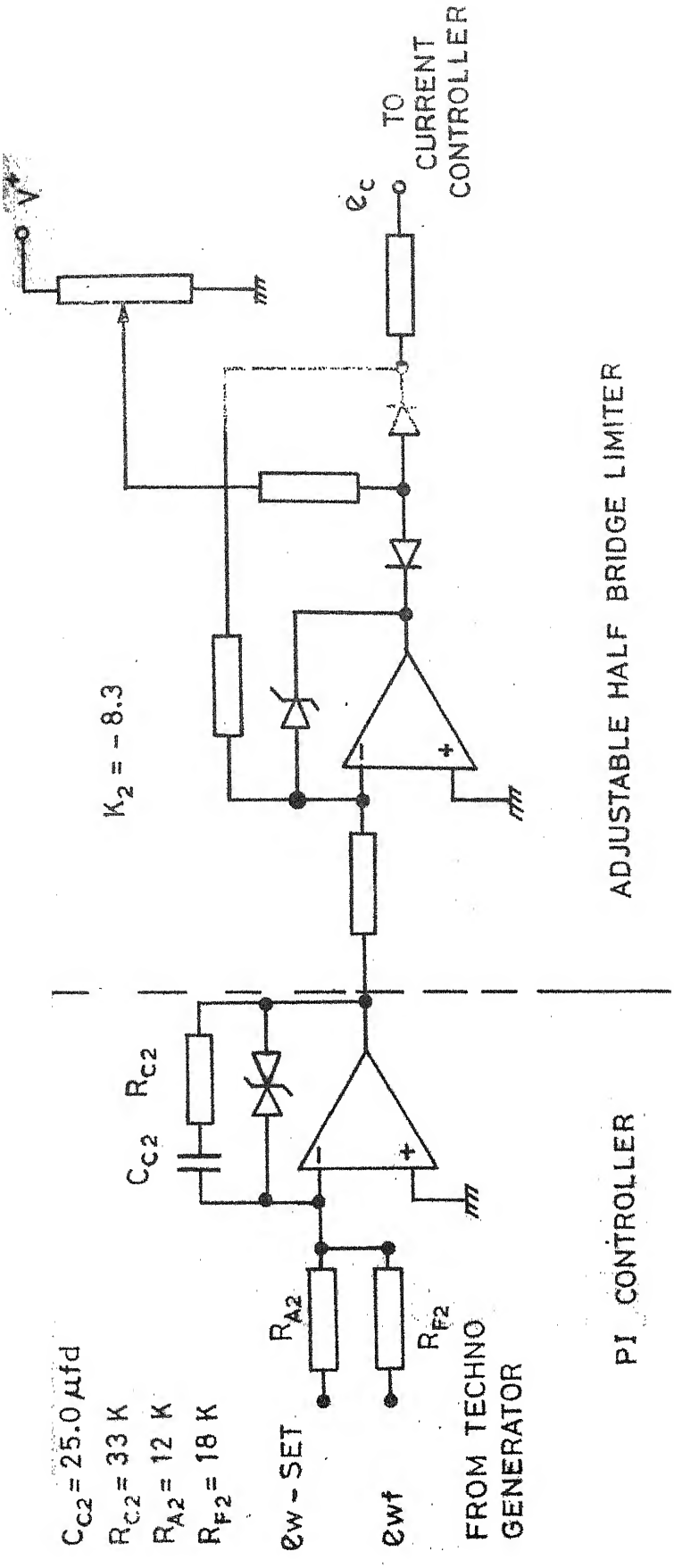

FIG.4.9 SPEED CONTROLLER

A PI controller was used to obtain zero steady state error in the speed. Design procedure is similar to that of speed controller for slip power recovery (see Section 2.9). The transfer function of PI controller is given as

$$G_{\omega c} = \frac{k_2(1 + s\, T_{c2})}{s}$$

where,

$$T_{c2} = C_{c2}\, R_{c2}$$

$$k_2 = 1/(R_{f2}\, C_{c2}) \quad \text{(gain of limiter)}$$

4.8 CURRENT TRANSDUCER

A hall effect transducer or dc current transformer can be used on the dc side of the rotor circuit to sample the rotor current I_d. Since the rotor circuit is isolated, there was no need of having a transducer which must provide isolation from the power circuit. In chopper circuit cathode of the main thyristor T_1 is grounded, and a resistance of 1.0 ohm is connected between ground and negative terminal of the bridge rectifier. The voltage across this resistance is proportional to current in the rotor circuit. The same resistance helps in limiting the short circuit current in the rotor circuit. This justifies its comparatively high value of 1.0 ohm.

The output of current transducer should be proportional to average current I_d. While designing a current transducer following considerations were taken into account. For a chopper circuit - without filter current waveform could be highly distorted. To make such current feedback signal less distorted would require a filter with large time constants. Particularly, when a chopper frequency is low. Moreover, the filter time constants would be different for different chopping frequency and also for different parameters of chopper filter. A simple filter in the current feedback path may have adverse effect on the dynamic performance of the drive.

To overcome these problems it was decided to develop a high speed average current sensing circuit. The circuit parameters would remain same whether chopper is with filter or without filter. Figure 4.10 gives the circuit diagram of a current transducer. Channel I samples the current waveform at t = 0 and holds it for the rest of the cycle. Under steady state, this gives the minimum value of current, I_{min}. In channel II capacitor C_3 stores the peak values of current, I_{max}. And it is transferred to C_2 in the beginning of the next cycle. C_3 is discharged at $t = t_1$. This keeps

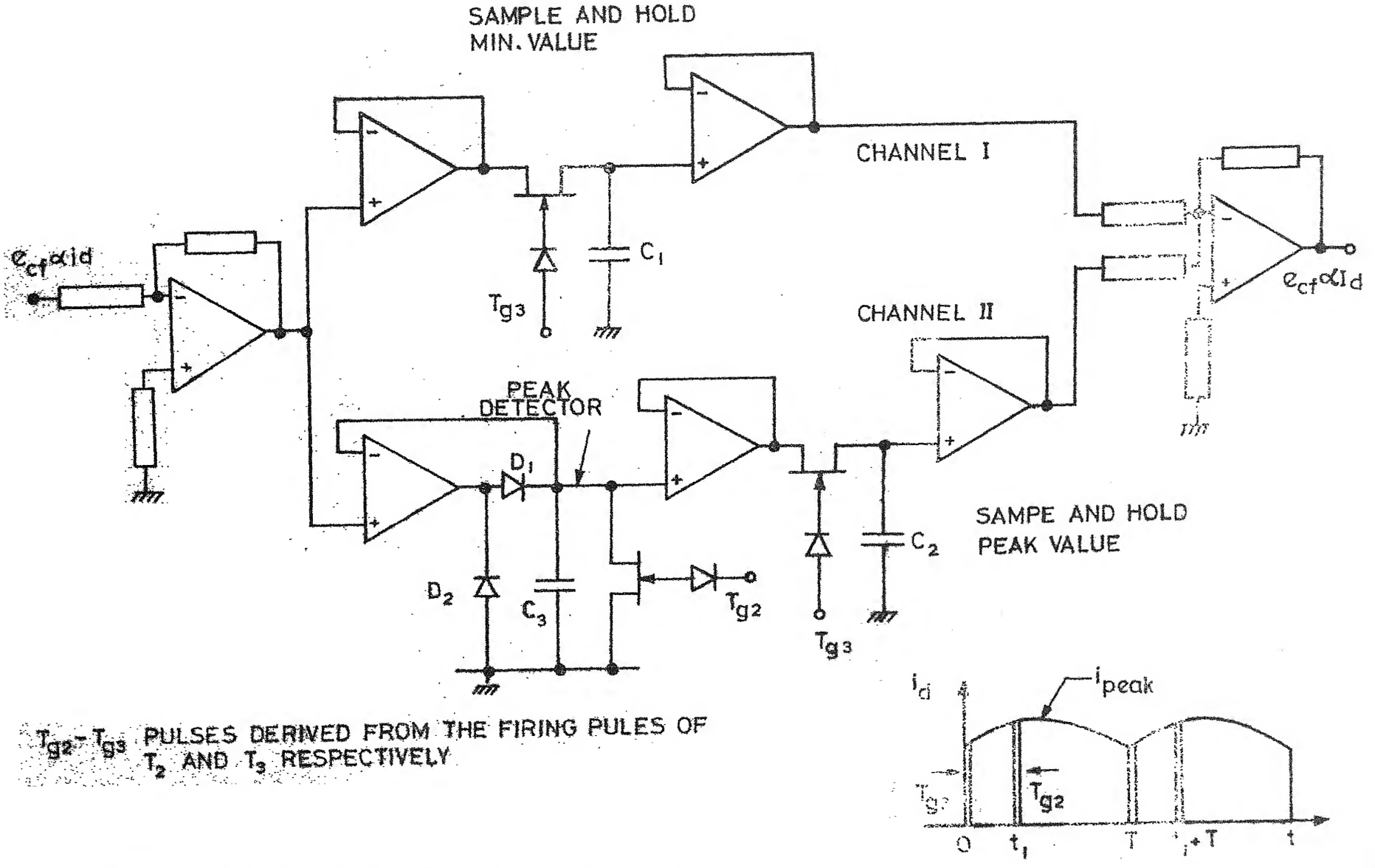

T_{g2} - T_{g3} PULSES DERIVED FROM THE FIRING PULES OF T_2 AND T_3 RESPECTIVELY

FIG.4.10 CURRENT AVERAGING CIRCUIT

it ready to store the peak value in the next cycle. The buffered output of these two channels is connected to a summer. Output of the summer is proportional to $(i_{max} + i_{min})$.

If τ_1 and τ_2 are large compared to t_1 and t_2 respectively, we can assume that average of i_{max} and i_{min} is same as I_d the average of i_d. However this condition may not be satisfied under all possibilities of chopper operation. And this may result in the non-linear transfer characteristics of current transducer. It is felt that having this nonlinearity is better than having large ripples in the current feedback path.

This circuit gives approximate value of average current within one cycle of chopping frequency.

$$\text{Current transducer gain } H_c = \frac{e_{cf}}{I_d}$$

Since this circuit responds almost instantaneously there is no time constant involved. However, this should be treated as sampled data system, due to sample and hold arrangement.

In that case,

$$H_c(s) = \frac{H_c}{1 + S\,T_c} \quad \text{where} \quad T_c = T/2,$$

and $T = 1/f_c$ - chopper period.

It was observed in the final calculations that effect of T_c on system performance can be ignored in favour of other dominating time constants.

4.9 CURRENT CONTROLLER

The circuit diagram of current controller is shown in Figure 4.11. In a previous section, it is observed that commutation circuit puts a limitation on the maximum permissible duty cycle. While minimum duty cycle is determined by 'second order filter' in rotor circuit and commutation circuit parameters. With these limitations e_1 - input to the PWM circuit should be such that

$$V_{cl} \leq e_1 \leq V_{cu}$$

where V_{cl}, V_{cu} determine the minimum and maximum duty cycle respectively.

A precision bridge limiter is used between a PI controller and PWM firing circuit. This limiter action keeps the duty cycle in the permissible range. A PI controller is used to give 'zero' steady state error. A reference signal e_c for the current control is obtained from the output of speed controller. The speed controller has adjustable saturation level. Output from the current transducer is used as current

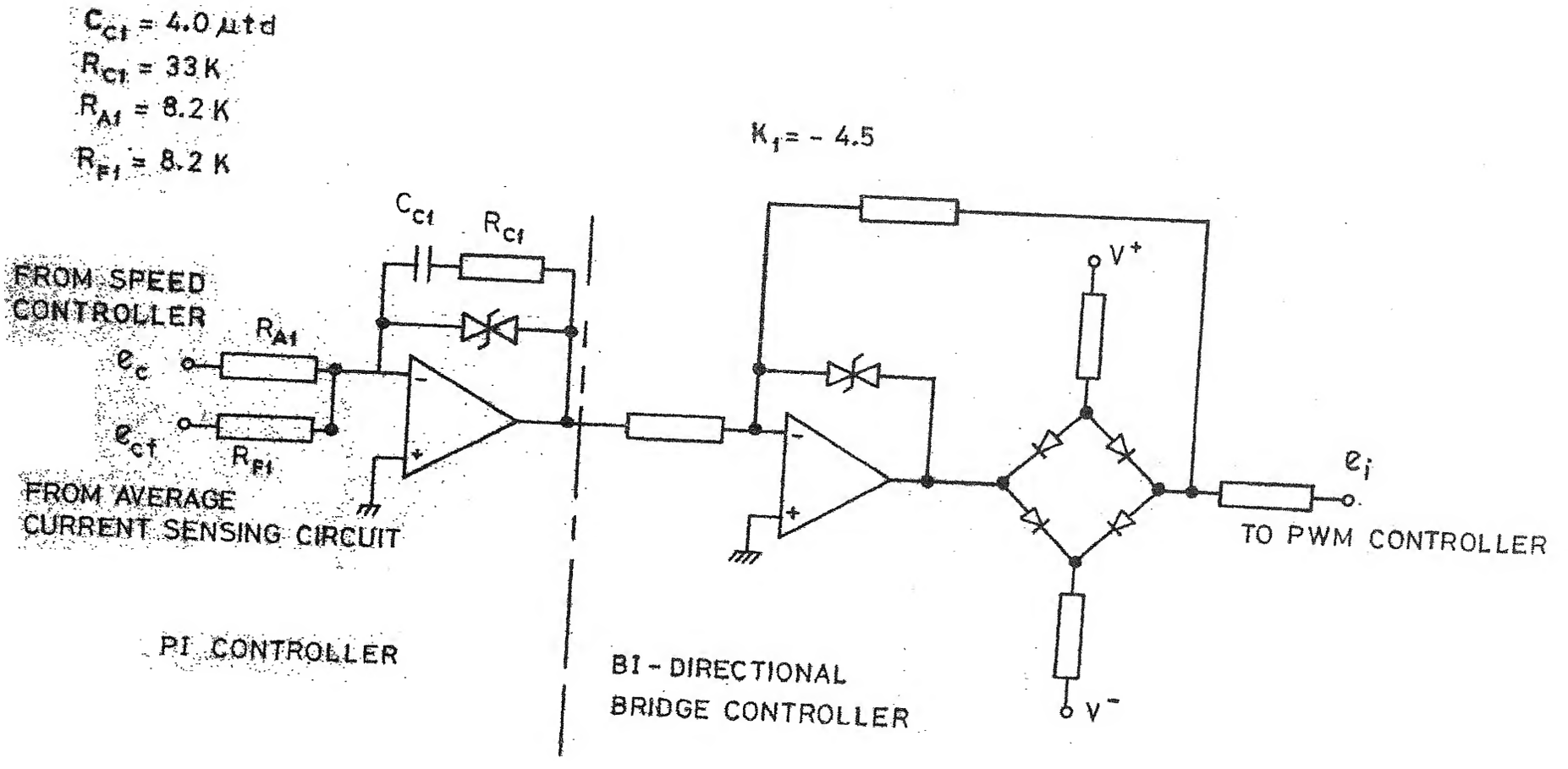

FIG. 4.11 CURRENT CONTROLLER

feedback signal e_{cf}. During starting output of speed controller will saturate because of larg error in the speed feedback loop. Hence this limits the starting current and hence torque to the preset value. Under overloading condition also similar action will take place.

The detailed description and advantages of current controller over current limit arrangement are given in Section 2.10.

The transfer function of current controller is given by,

$$G_{cc}(s) = \frac{k_1 (1 + s T_{cl})}{s}$$

where

$$T_{cl} = C_{cl} R_{cl}$$

$$k_1 = 1/(R_{fl} C_{cl}) \quad \text{(gain of the limiter)}$$

The design procedure for this controller is given in Chapter 5.

4.10 EXPERIMENTAL INVESTIGATIONS

A 3 HP slipring induction motor was used for experimental investigations. The values of chopper circuit components are given in Figure 4.4. The details of motor are given in Appendix A. Figure 2.9

gives the per phase equivalent circuit of motor referred to rotor.

The loading arrangement for the drive is identical to that given in Section 2.11, for slip power recovery scheme. A permanent magnet tacho-generator is used to provide speed feedback. A resistance connected in the dc path of the rotor circuit is used to obtain rotor current feedback signal.

Figures 4.12 and 4.13 give the open loop speed-torque characteristics without filter and with second order filter, respectively. Using second order filter ripple amplitude of rotor current I_d is considerably reduced, and thyristor is relieved of high voltage spikes. And minimum permissible ON period of T_1 is increased, for the same commutating circuit components (refer Section 4.5). However, if the inverter grade thyristors are used, it will be possible to design a commutation circuit to obtain wide range speed control, with second order filter. The computed characteristics based on the dc circuit model given in Section 4.3 are also given for the sake of comparison. The steady state speed torque characteristics with closed loop system are found to be almost flat for various set speeds and

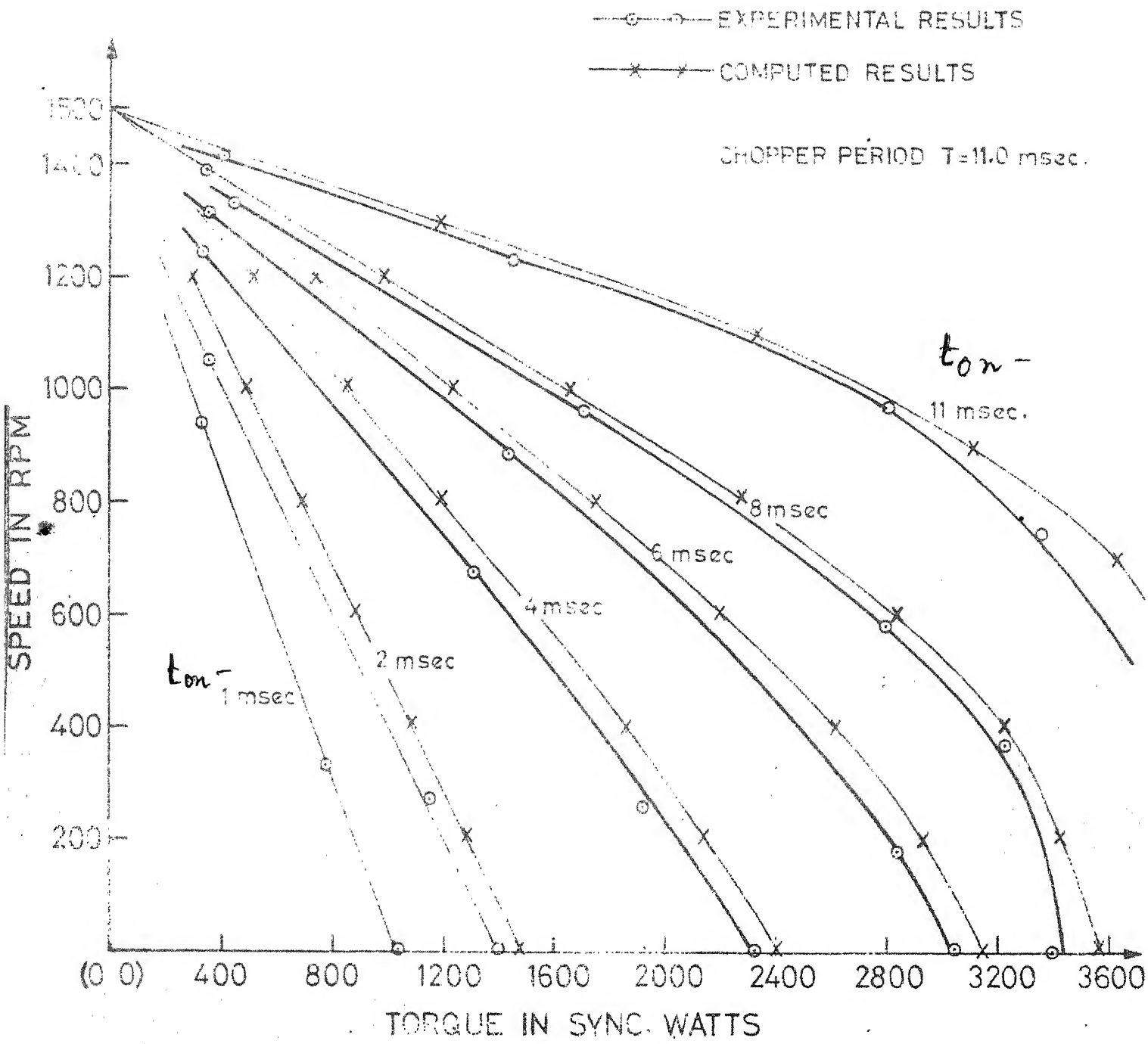

FIG.4.12 SPEED TORQUE CHARACTERISTICS WITHOUT FILTER

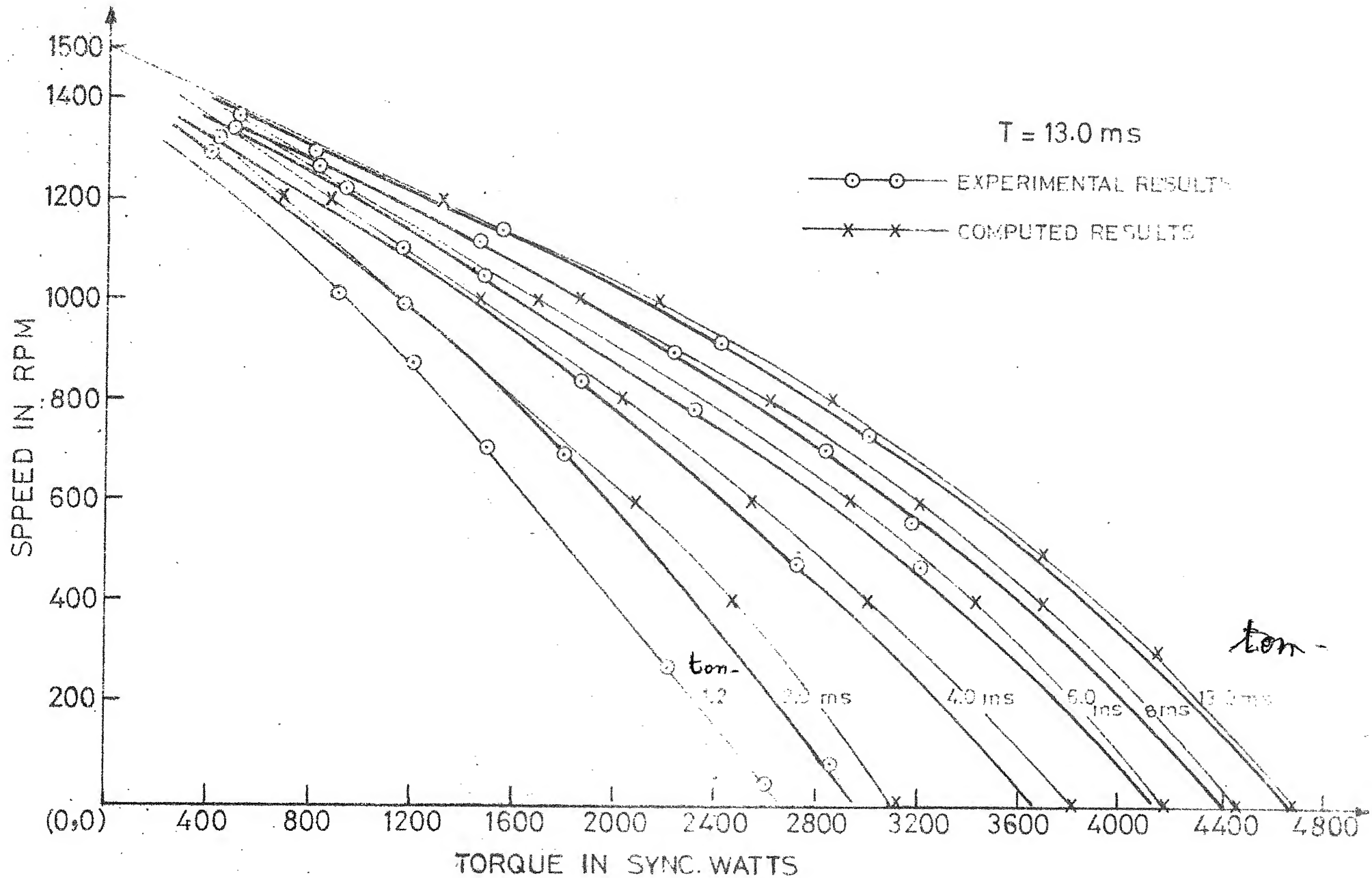

FIG.4.13 SPEED-TORQUE CHARACTERISTICS WITH 2nd ORDER FILTER

currents. The transient response of the drive is given in Chapter 5.

4.11 NUMERICAL METHOD

The reasons for using numerical techniques for determining steady state speed torque characteristics of the motor with second order filter are already discussed in the text.

From the conventional theory of rectifiers, it is known that presence of reactances on the ac side of the bridge cause current overlap during change over (i e. commutation) of conducting diodes. This results in loss of voltage during commutation period. And its average effect over a cycle is to produce equivalent d.c. voltage drop

$$V_c = X_{\ell_m} \cdot I_d$$

where,

$$X_{\ell_m} = \frac{3\omega}{\pi} (\ell_1 + \ell_2)$$

Hence, it is obvious to treat X_{ℓ_m} as resistance while considering average current under steady state. This may lead one to treat X_{ℓ_m} as resistance even when computing transients during ON or OFF modes. However, it is felt that the best way to take care of its presence would be to consider it as inductance equal to $2(\ell_1 + \ell_2)$ while computing transients during ON and OFF

periods. And the loss of voltage due to commutation is taken care by reducing the average voltage impressed on the filter and chopper circuit by $X_{\ell m} I_d$.

This may give the impression of considering the leakage reactances twice in the same circuit model. However, a close examination will show that

1. While considering it as inductance for computing transients during ON or OFF mode average voltage across inductance is zero.
2. When it is considered as resistance it takes care of decrease in voltage due to commutation effect only.

Hence, while computing steady state waveform, it becomes necessary to go for iterative procedure to determine the steady state current waveform and thereby average current and torque developed for the given motor speed.

4.11.1 Digital Computer Program

After labelling the appropriate current and voltages as state variables the differential equations for the chopper with filter were written in state variables form. The Runge-Kutta 4th order approximation method was used to solve them simultaneously. From this the steady state speed torque characteristics can be

computed for different duty cycles of the chopper. Comparison of computed and experimentally obtained, open loop performance is given in Figures 4.12 and 4.13.

4.12 CONCLUSIONS

Problems associated with simple chopper circuit such as excessive voltage across thyristor and discontinuity in the rotor current are eliminated by introducing a filter in the rotor circuit. The second order filter gives a variation in speed torque characteristics wider than that with a first order filter. The necessity for feedback to obtain better speed regulation is explained. The advantage of current controller over current limit is pointed out with regards to the speed of response. The closed loop control system discussed here used PI controllers to obtain zero steady state error. A slip-ring motor with filter and closed loop speed control can replace dc motor in many applications.

CHAPTER 5

THE TRANSIENT RESPONSE OF CHOPPER CONTROLLED SLIPRING INDUCTION MOTOR

5.1 INTRODUCTION

The thyristor chopper controlled slipring motor drive, complete with speed and current feedbacks is described in the previous chapter. In this chapter a small signal dynamic model is developed for this particular drive.

A small signal block diagram is developed for the motor from which transfer functions are derived to predict the transient response of the drive. It is shown that these transfer functions can be used for designing the closed loop controller.

It should be noted that chopper controlled slipring motor drive given in the Chapter 4 does not have the provision to provide braking torque, unless dynamic braking is used. Since dynamic braking requires switching of stator from ac to dc supply, it was not implemented. A detailed discussion on the validity of the transfer functions developed for a drive with similar limitations is given in Section 3.1.

5.2 DEVELOPMENT OF SMALL SIGNAL MODEL

The complete transient analysis of conventional induction motor is quite involved. The presence of bridge rectifier and chopper makes it all the more difficult. Therefore, it is not possible to derive analytically a transfer function that will be valid under all conditions. However, transfer functions that will be valid for small perturbations may be derived under certain simplifying assumptions, the parameters being dependent on the given steady-state operating point [20, 31].

Thus an analysis for small changes of speed about an operating point is attempted. The following simplifying assumption is made in the dc circuit model given in Section 4.3.

The voltage drop across stator impedance and voltage loss due to commutation is negligible.

With this assumption the torque developed by motor under steady state becomes

$$T = \frac{E\, I_d}{\omega_s} \qquad (5.1)$$

From eqn.(5.1), torque is the linear function of I_d. This will hold good only when motor is not heavily loaded. Now, for a given duty cycle of chopper, I_d is

is proportional to slip S and E is constant. However, for a given value of slip, current I_d is not a linear function of duty cycle, and hence of control voltage e_i (refer Section 4.3). This relation could be linear only when $\tau_1 = \tau_2$, where

τ_1 - Rotor circuit time constant during ON mode.

τ_2 - Rotor circuit time constant during OFF mode.

In a practical drive, it will not be possible to satisfy condition like $\tau_1 = \tau_2$. Numerically it can be shown and experimentally it was observed for second order filter given in Figure 4.6, that for $\tau_1 > \tau_2$ the relation between I_d and duty cycle is highly nonlinear. The I_d versus 'chopper ON period - t_1' characteristics for different motor speeds are given in Figure 5.1. From Figure 5.1, rotor current I_d is highly sensitive to duty cycle changes in lower range and insensitive in higher range. Taking into account this nonlinearity

$$I_d = \frac{E}{R} S f(e_i) \qquad (5.2)$$

where $f(e_i)$ is a nonlinear function of e_i and duty cycle is proportional to e_i. R is the total resistance in the rotor circuit when switch is ON, and S is the motor slip.

For 100 percent duty cycle $f(e_i) = 1$

Hence $I_{d(max.)} = \frac{E}{R} S$

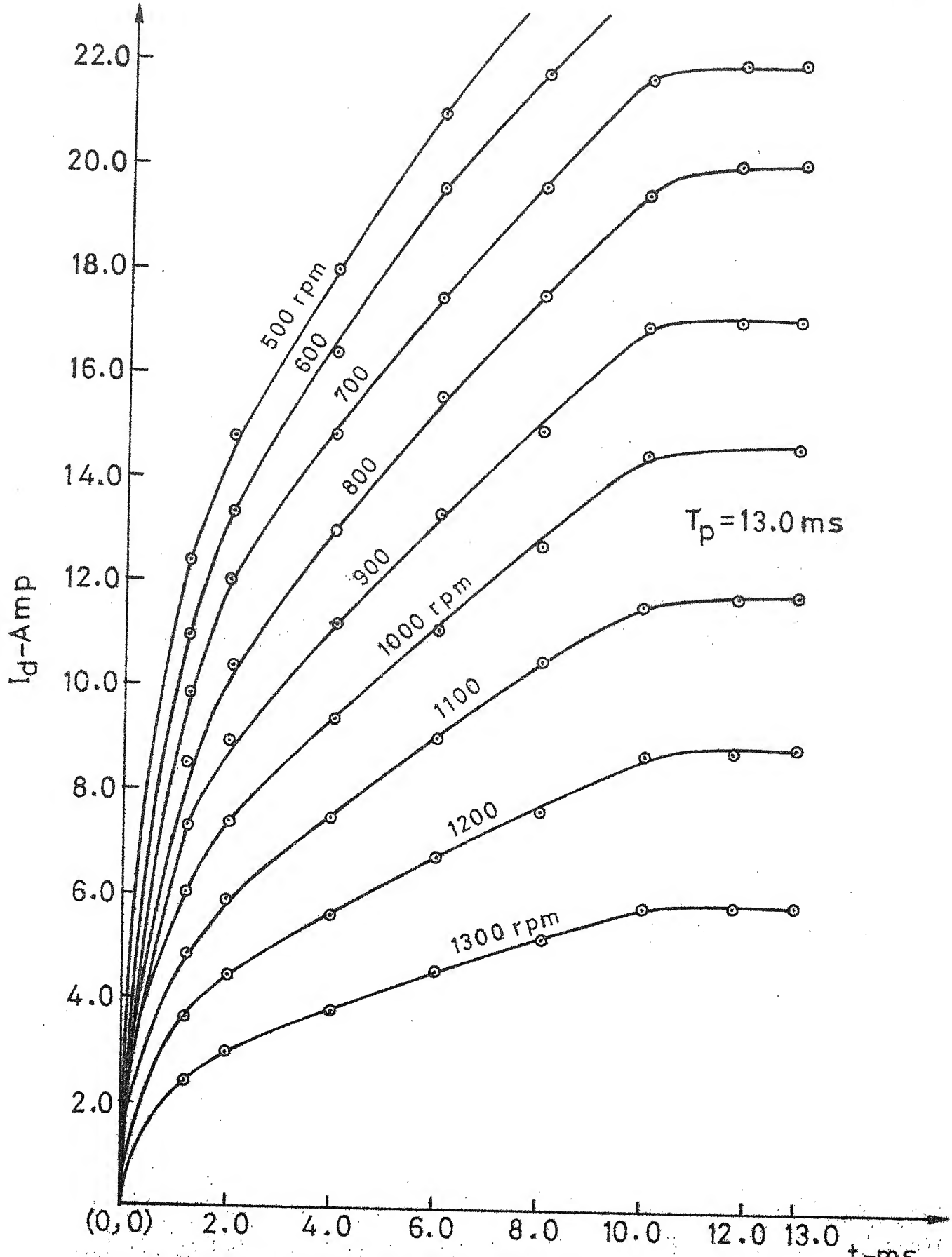

FIG. 5.1 TRANSFER CHARCTERISTICS-CHOPPER WITH FILTER

Before deriving transfer functions we will linearize this relation around a reference point.

Let operating point be such that

$$I_d = I_{do}, \quad S = S_o \quad \text{and} \quad e_1 = e_{1o}$$

Making a Taylor's series expansion of eqn.(5.2) around the given operating point, and neglecting higher order terms, we end up with the following linear relation.

$$\Delta I_d = \frac{E}{R}\left[S_o \left(\frac{df}{de_i}\right)^o \Delta e_1 + f(e_{io})\Delta S\right] \qquad (5.3)$$

where $(df/de_i)^o$ - derivative at the reference point and $\Delta I_d, \Delta e_i, \Delta S$ represent perturbations around the operating point. Since

$$S = \frac{\omega_s - \omega}{\omega_s}$$

where

ω = motor speed

$$\Delta S = -\frac{\Delta\omega}{\omega_s}$$

Let

$k_r = (df/de_1)^o$ — small signal gain

and

$K_R = f(e_{io})/e_{1o}$ — large signal gain

Substituting these relations in eqn.(5.3) gives

$$\Delta I_d = \frac{E}{R}[S_o\, k_r \Delta e_1 - K_R\, e_{1o} \Delta\omega / \omega_s] \qquad (5.4)$$

From eqn. (5.2),

$$f(e_{1o})\ \frac{E}{R} = \frac{I_{do}}{S_o} \qquad (5.5)$$

From equations (5.3), (5.4) and (5.5),

$$\Delta I_d = \frac{E}{R}(S_o\, k_r \Delta e_1) - \frac{I_{do}\Delta\omega}{S_o\omega_s}$$

Let

$$f_1 = S_o k_r \frac{E}{R}$$

and ΔI_d can be written as

$$\Delta I_d = f_1 \Delta e_1 - \frac{I_{do}\Delta\omega}{S_o\ \omega_s} \qquad (5.6)$$

Now, $\Delta T = E\Delta I_d/\omega_s$, from eqn. (5.1). If the perturbation in load torque T_L is $\Delta T_L = 0$ the perturbation in motor speed is given by

$$\Delta\omega = \frac{\Delta T}{f} = \frac{E\Delta I_d}{\omega_s\, f} \quad \text{(under steady state)}$$

where f - coefficient of linear (viscous) friction of load.

Substituting the value ΔI_d from eqn.(5.6), gives

$$\Delta\omega = \frac{E}{\omega_s\, f}[f_1 \Delta e_1 - \frac{I_{do}}{S_o}\ \frac{\Delta\omega}{\omega_s}] \qquad (5.7)$$

From equations (5.6) and (5.7), under steady state

$$\Delta I_d / \Delta e_1 = f_1/(1+k_{eb})$$

$$\Delta\omega / \Delta e_1 = (E/\omega_s) f_1/(1+k_{eb}) \qquad (5.8)$$

where $k_{eb} = (E/\omega_s^2 f)(I_{do}/S_o)$ represents the effect of internal speed feedback.

5.3 BLOCK DIAGRAM AND TRANSFER FUNCTIONS

Before developing a block diagram the presence and effect of various time constants in the system is investigated.

5.3.1 Chopper Time Constant:

Although the duty cycle is proportional to e_1, the triggering of the thyristors is not instantaneously corrected. There is certain delay in the actual change in the duty cycle and change in the control signal. Hence, this system should be treated as a sampled-data system. The triggering of the main thyristor corresponds to sampling of e_1. The amplitude of e_1 at that instant determines the duty cycle. And chopper does not respond to any changes in e_i till the next cycle. This corresponds to zero-order hold arrangement. Analysis can be simplified by considering it as simple first-order system with a time constant $T_c = T/2$ [21], where $1/T$ is chopper frequency.

Let

$$e_1'(s) = \frac{e_1(s)}{1+s\ T_c} \qquad (5.9)$$

Now, the delayed change in duty cycle is represented by e_1'.

5.3.2 Filter Time Constant:

A filter connected in the rotor circuit, to reduce the heating of rotor windings, could be a 'first order filter' or a 'second order filter'. However, during ON mode of main thyristor both of them will act as first order filter with time constant τ_1. It is only during OFF period that second order filter circuit will act as second order filter. Let the filter parameters be adjusted such that its effective time constant during OFF period is τ_2 (refer Section 4.4).

$$\tau_1 = L_{11}/R_{11}$$

$$\tau_2 = L_{11}/R_{22} \quad \text{for 1st order filter}$$

$$\simeq 2L_{11}/R_{11} \quad \text{for 2nd order filter}$$

where,

R_1, R_2 are external resistances

$L_{11} = L_1 + 2(\ell_1 + \ell_2)$

$R_{11} = R_1 + S_o\ 2r_1 + 2r_2$

$R_{22} = R_{11} + R_2$

with this, effective time constant of filter will be

$$T_f = T \frac{\tau_1 \tau_2}{t_1 \tau_2 + t_2 \tau_1} \qquad (5.10)$$

where

t_1 - ON period

t_2 - OFF period, and

$T = t_1 + t_2$.

The chopper time constant T_c comes into picture only when the change in e_i being considered. However, filter time constant T_f is to be considered for changes in ω and also in e_i. Considering these time constants, equations (5.4) and (5.6) could be rewritten as

$$\Delta I_d(s) = \frac{E}{R(1+sT_f)}\left[\frac{S_o k_r}{1+sT_c} \Delta e_i(s) - e_{io} K_R \frac{\Delta\omega\ (s)}{\omega_s}\right] \qquad (5.11)$$

$$\Delta I_d(s) = \frac{f_1 \Delta e_i(s)}{(1+sT_f)(1+sT_c)} - \frac{I_{do}}{s_o} \frac{\Delta\omega(s)}{\omega_s(1+sT_f)} \qquad (5.12)$$

Considering the perturbations in speed and torque

$$\Delta\omega(s) = \frac{\Delta T - \Delta T_L}{f(1+ sT_m)}$$

where

$T_m = J/f$ - mechanical time constant of load and motor.

J = moment of inertia of motor and load.

If $\Delta T_L = 0$

$$\Delta\omega(s) = \frac{(E/\omega_s)\,\Delta I_d(s)}{f(1 + sT_m)} \qquad (5.13)$$

Block diagram corresponding to equations (5.11), (5.12) and (5.13) is given in Figure 5.2.

5.3.3 Derivation of $\Delta I_d(s)/\Delta e_1(s)$ and $\Delta\omega(s)/\Delta e_i(s)$:

From the block diagram of Figure 5.2,

$$\frac{\Delta I_d}{\Delta e_1}(s) = \frac{f_1(1+sT_m)}{[(1+sT_f)(1+sT_m)+k_{eb}](1+sT_c)}$$

where

$$k_{eb} = \frac{E}{\omega_s^2 f}\,\frac{I_{do}}{s_o}$$

Therefore,

$$\frac{\Delta I_d}{\Delta e_1}(s) = \frac{f_1(1+sT_m)}{T_fT_m[s^2+(\frac{1}{T_f}+\frac{1}{T_m})s + \frac{1}{T_fT_m}(1+k_{eb})](1+sT_c)} \qquad (5.14)$$

The roots of

$$s^2 + (\frac{1}{T_f}+\frac{1}{T_m})s + \frac{1}{T_mT_f}(1+k_{eb}) = 0$$

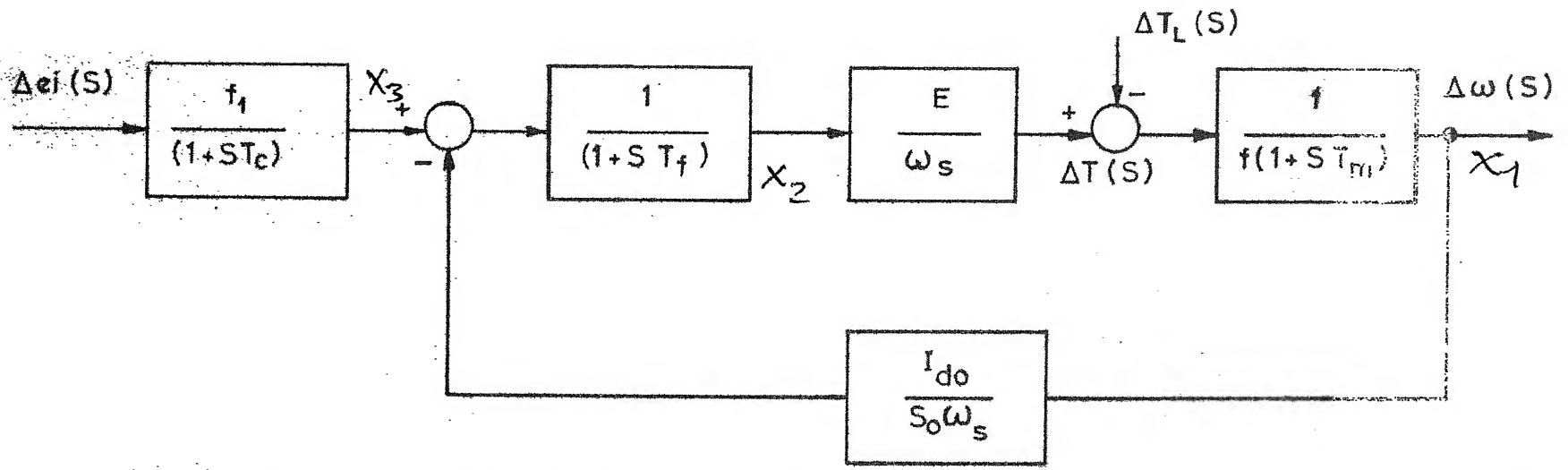

FIG.5.2 CHOPPER CONTROLLED SR-IM-SMALL SIGNAL BLOCK DIAGRAM

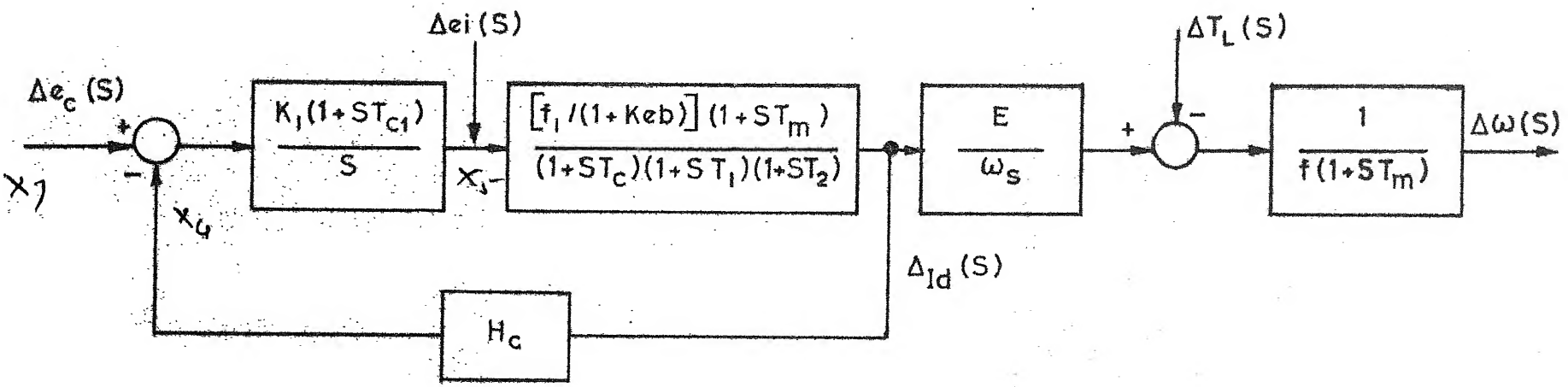

FIG.5.3 BLOCK DIAGRAM-CURRENT CONTROL LOOP

are given by

$$s_{1,2} = -\frac{1}{2}\left(\frac{1}{T_f}+\frac{1}{T_m}\right) \pm \left[\frac{1}{4}\left(\frac{1}{T_f}+\frac{1}{T_m}\right)^2 - \frac{1}{T_f T_m}(1+k_{eb})\right]^{\frac{1}{2}} \tag{5.15}$$

Let $T_1 = -1/s_1$ and $T_2 = -1/s_2$.

Substituting this in equation (5.14) gives

$$\frac{\Delta I_d}{\Delta e_i}(s) = \frac{[f_1/(1+k_{eb})](1+sT_m)}{(1+sT_1)(1+sT_2)(1+sT_c)} \tag{5.16}$$

Now

$$\frac{\Delta\omega}{\Delta e_i}(s) = \frac{\Delta I_d}{\Delta e_i}(s)\,\frac{E}{\omega_s f(1+sT_m)}$$

from the block diagram.

From eqn.(5.16), we get

$$\frac{\Delta\omega}{\Delta e_i}(s) = \frac{(E/\omega_s f)[f_1/(1+k_{eb})]}{(1+sT_1)(1+sT_2)(1+sT_c)} \tag{5.17}$$

Effect of ΔT_L:

From the block diagram, if ΔT_L is not zero

$$\frac{\Delta\omega}{\Delta T_L}(s) = \frac{(1/f)(1+sT_f)}{(1+sT_f)(1+sT_m)+k_{eb}}$$

$$= \frac{[1/f(1+k_{eb})](1+sT_f)}{(1+sT_1)(1+sT_2)} \tag{5.18}$$

Equations (5.16) to (5.18) are the transfer functions for the perturbations around the operating point.

From the block diagrams developed, it can be observed that

i) It is the internal speed feedback factor k_{eb} that tends to make current response more oscillatory,

ii) If $k_{eb} << 1$, $T_1 \simeq T_m$ and $T_2 \simeq T_f$ with this approximation,

$$\frac{\Delta I_d}{\Delta e_i}(s) = f_1/[(1+sT_f)(1+sT_c)] \qquad (5.19)$$

and

$$\frac{\Delta \omega}{\Delta T_L}(s) = \frac{1/f}{(1+sT_m)} \qquad (5.20)$$

5.4 TRANSFER FUNCTIONS - CLOSED LOOP SYSTEM

The open loop transfer functions and block diagram are given in the previous section. To study the transient response of closed loop system around the given operating point, the same transfer functions can be used. The closed loop control scheme for chopper controlled slipring motor complete with speed and current feedback is given in Figure 4.8, and system description is given in Section 4.6. In this section, block diagrams, and transfer functions for the same scheme will be developed. Subsequent sections give the design of various blocks of the closed loop controller.

5.4.1 Current Control Loop.

In the linear analysis of current loop, it is assumed that

i) The limiter in the current loop is operating in the linear mode.

ii) The limiter in the speed control loop in the saturated mode. This makes speed feedback ineffective.

Figure 5.3 gives the block diagram of current loop. The PI controller transfer function is

$$G_{cc}(s) = k_1(1+sT_{c1})/s$$

where

$$T_{c1} = R_{c1}C_{c1}$$

$$k_1 = \frac{\text{gain of limiter}}{C_{c1}R_{f1}}$$

If the time constant of current averaging circuit is neglected in favour of other time constants in the loop, the loop gain will be

$$G_c G_{cc} H_c(s) = \frac{[f_1/(1+k_{eb})](1+sT_m)(1+sT_{c1})k_1 H_c}{s(1+sT_c)(1+sT_1)(1+sT_2)} \quad (5.21)$$

where H_c is current feedback factor. From equation (5.15), the values of T_1 and T_2 are functions of k_{eb}

and T_f and T_m. Let the operating point be such that

$$T_1 \simeq T_m \qquad \text{and} \qquad T_c << T_{c2} \text{ or } T_2.$$

The validity of the assumptions is shown in Section 5.7. With this assumption,

$$G_c G_{cc} H_c(s) = \frac{[k_1 H_c f_1/(1+k_{eb})](1+sT_{c1})}{s(1+sT_2)} \qquad (5.22)$$

The closed loop transfer function for current control loop, is given by

$$G_c^*(s) = \frac{\Delta I_d}{\Delta e_c}(s) = \frac{G_c G_{cc}(s)}{1+G_c G_{cc} H_c(s)}$$

where Δe_c is input signal to current control loop.

From eqn.(5.22)

$$G_c^*(s) = \frac{\Delta I_d}{\Delta e_c}(s) = \frac{[k_1 f_1/(1+k_{eb})](1+sT_{c1})}{s(1+sT_2)+[k_1 f_1 H_c/(1+k_{eb})](1+sT_{c1})}$$

$$= \frac{(1/H_c)(1+sT_{c1})}{(1+sT_a)(1+sT_b)} \qquad (5.23)$$

where $-1/T_a$ and $-1/T_b$ are the roots of equation

$$s^2+s\left[\frac{1}{T_2}+\frac{k_1 H_c f_1 T_{c1}}{(1+k_{eb})T_2}\right]+\frac{k_1 H_c f_1}{(1+k_{eb})}\frac{1}{T_2} = 0$$

5.4.2 Speed Control Loop:

While analyzing the behaviour of speed controller, it is assumed that both the limiters are operating in the linear mode.

The speed control loop block diagram in Figure 5.4 incorporates the approximate transfer function given by equation (5.23). In the block diagram $k_2(1+sT_{c2})/s$ is PI controller transfer function. $G_{\omega c}(s)$ and tacho-generator transfer function is $H_\omega/(1+sT_g)$ A first order filter in the speed feedback path was necessary to reduce the effect of ripples in the tacho-generator output (refer Section 2.8). From Figure 5.4, loop gain

$$G_{\omega c}(s)\,\frac{\Delta I_d}{\Delta e_c}(s)\,\frac{E}{\omega_s}\,\frac{1}{f(1+sT_m)}\,\frac{H_\omega}{(1+sT_g)}$$

$$= \frac{(k_2E/H_c\omega_s f)(1+sT_{c1})(1+sT_{c2})}{s(1+sT_a)(1+sT_b)(1+sT_m)} \qquad (5.24)$$

5.5 DETERMINATION OF OPERATING POINT PARAMETERS

In the small signal model discussed so far, some of the parameters are functions of operating point. This operating point and associated parameters could be calculated either graphically or numerically. Once, the performance curves of the chopper controlled slip-ring motor giving the steady state values of speed and torque for various duty cycles, and speed torque characteristics of load are available, we can determine the operating point. That is we can find S_o and I_{do} for the given t_{10} and since $\Delta t_1/\Delta e_1$ is constant for the PWM

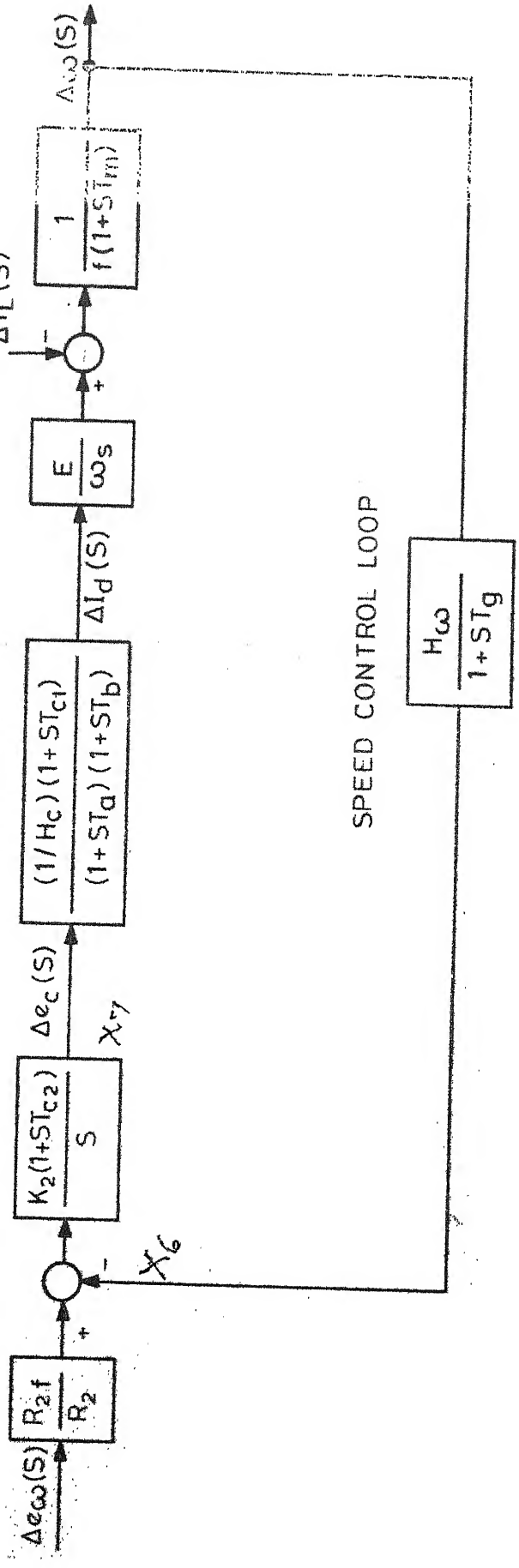

FIG.5.4 BLOCK DIAGRAM-SPEED CONTROL LOOP

circuit we can determine e_{10}. These performance curves could be plotted from the actual experiments conducted on the motor or from numerically obtained results using a simplified dc circuit model.

For studying transient response experimentally, the following operating point was selected.

Motor speed N_o	= 900 rpm
Motor slip S_o	= 0.4
Rotor current in dc path	= 13.3 Amp
Chopper ON period t_{10}	= 6.0 mS

The controller power circuit and rotor circuit parameters are given in Figures 4.6 and 4.5 respectively. The machine parameters and load characteristic are given in Appendix A. This information is used to determine the open loop transfer functions of the drive.

5.6 TRANSFER FUNCTION EVALUATION - OPEN LOOP

For second order filter given in Figure 4.6, L_{11} = 59.0 mH, R_{11} = 3.45 ohms and R = 3.0 ohms. The filter time constants during ON and OFF modes will be,

$$\tau_1 = L_{11}/R = 19.65 \text{ mS}$$

$$\tau_2 = 2L_{11}/R_{11} = 34.2 \text{ mS}$$

where L_{11} - Total inductance in the rotor circuit

R_{11} - Total resistance in the rotor circuit when main thyristor is OFF

R - Total resistance in the rotor circuit when main thyristor is ON.

Hence, the effective time constant of filter at the given operating point will be,

T_f = 25.5 mS, from eqn. (5.10).

The chopper time constant

$T_c = T/2 = 6.5$ mS

The loading generator field current is adjusted such that the coefficient of linear (viscous) friction around the given operating point is

$f = 4.0$ Watts-sec^2.

The mechanical time constant of the set-up is

$T_m = 437.5$ mS

For the PWM control circuit cycle length

$T = 13.0$ mS and

$t_1 = 6.5 + 1.3\ e_1$ mS

Therefore,

$\Delta t_1/\Delta e_1 = 1.3$ mS/volt.

Figure 5.1 gives I_d versus t_1 curves for different values of motor speed. From these curves f_1 at the given operating point is

$$f_1 = \frac{\Delta I_d}{\Delta t_1} \frac{\Delta t_1}{\Delta e_1} = 1.3 \text{ A/volt}$$

and

$$k_r = f_1 \frac{R}{S_o E} = 0.0513$$

where E = 190 volts for stator supply of 400 volts.

Similarly,

$$\frac{I_{do}}{s_o} = \frac{13.3}{0.4} = 33.3$$

Consequently,

$$k_{eb} = \frac{R}{\omega_s^2 f} \frac{I_{do}}{s_o} = 0.064$$

and

$$f_1/(1+k_{eb}) = 1.22$$

Substituting the values of T_f, T_m, and k_{eb} in the characteristic equation (5.15) gives

$$T_1 = 408 \text{ mS}, \quad T_2 = 25.6 \text{ mS}.$$

where $-1/T_1$, $-1/T_2$ are the roots of the characteristic equation.

Therefore, from equations (5.16) and (5.17)

$$\frac{\Delta I_d}{\Delta e_i}(s) = \frac{1.22\ (1+sT_m)}{(1+sT_1)(1+sT_2)(1+sT_c)} \qquad (5.25)$$

Similarly, from eqn.(5.18),

$$\frac{\Delta \omega}{\Delta T_L}(s) = \frac{0.235(1+sT_f)}{(1+sT_1)(1+sT_2)} \qquad (5.26)$$

where,

T_1 = 408 mS, T_2 = 25.6 mS

T_m = 437.5 mS, T_c = 6.5 mS and

T_f = 25.5 mS.

5.7 TRANSFER FUNCTION EVALUATION - CLOSED LOOP:

5.7.1 Current Control Loop:

The derivation of transfer function of current control loop is given in the previous section. Neglecting the time constant of current transducer, current feedback factor is

H_c = 0.1 V/Amp.

The design considerations for $H_c(s)$ are given in Section.3.8. The transfer function of a PI controller in this loop is

$$G_{cc}(s) = \frac{k_1(1+sT_{c1})}{s}$$

where T_{c1} = 108 mS and k_1 = 139 , includes the gain of a limiter.

The design procedure for current controller is similar to that of slip power recovery scheme given in Section 3.8. In this case PI controller gain k_1 is chosen to keep phase margin of atleast 60°. With the help of Nocols chart it is observed that system response is not oscillatory [19]. The Bode plots of $G_c(s)$ and $G_{cc}H_c(s)$ are given in Figure 5.5. Since $T_1 = T_m$ (refer Section 5.6) cut-off frequencies at $1/T_1$ and $1/T_m$ are not indicated in the Bode plots. Consequently eqn.(5.25) is rewritten as

$$G_c(s) = \frac{\Delta I_d}{\Delta e_i}(s) = 1.22/[(1+sT_2)(1+sT_c)] \quad (5.27)$$

Therefore, loop gain

$$G_c G_{cc} H_c(s) = \frac{17.0(1+sT_{cl})}{s(1+sT_2)(1+sT_c)} \quad (5.28)$$

The closed loop transfer function of current control loop is given by

$$G_c^*(s) = \frac{\Delta I_d}{\Delta e_c}(s) = \frac{G_c G_{cc}(s)}{1+ G_c G_{cc} H_c(s)}$$

Since T_c is very small compared to T_2 or T_{cl}, it is ignored while calculating the transfer function $G_c^*(s)$. With this assumption, from equation (5.25),

$$G_c^*(s) = \frac{10.0(1+sT_{cl})}{(1+sT_a)(1+sT_b)} \quad (5.29)$$

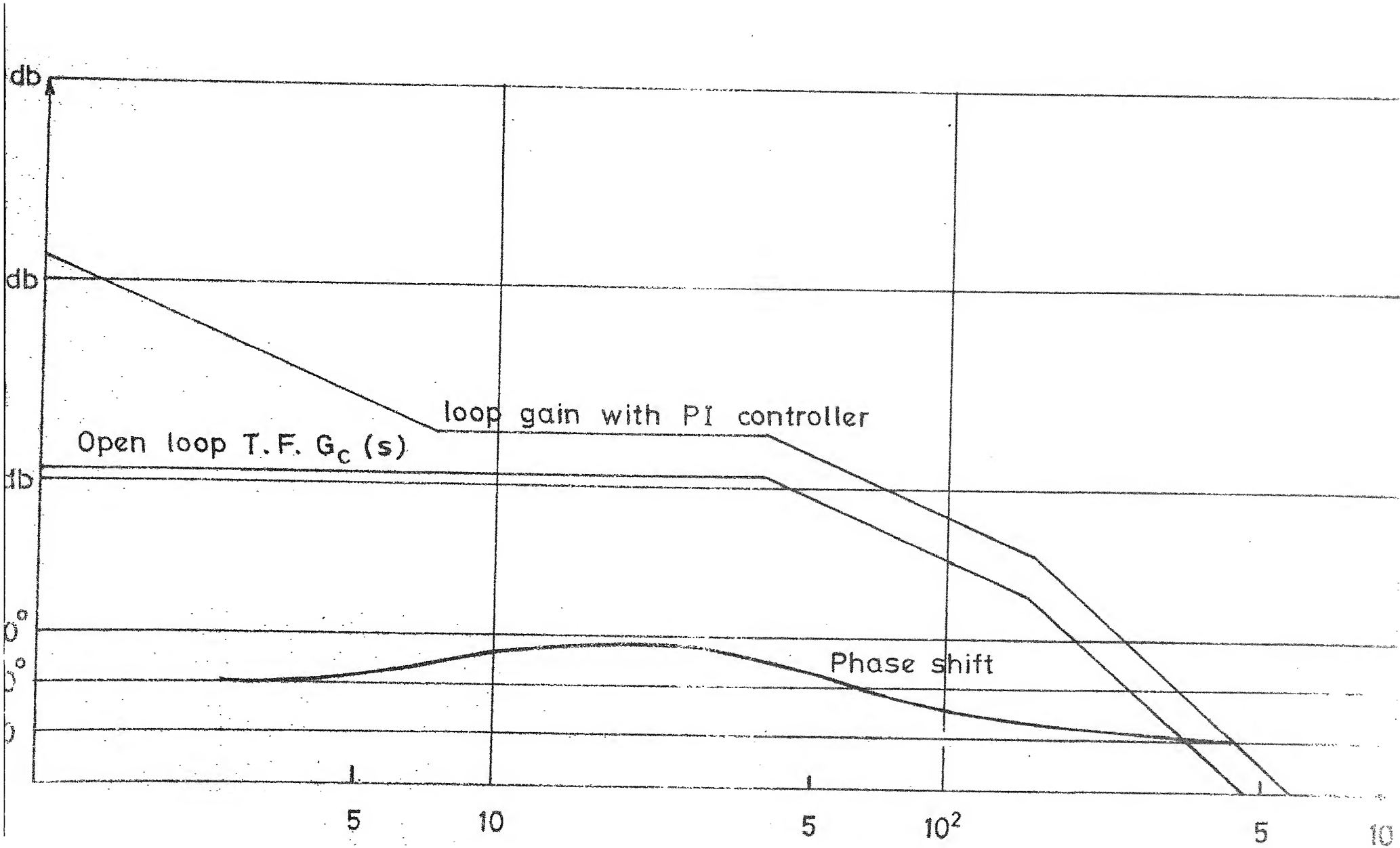

FIG.5.5 FREQUENCY RESPONSE-CURRENT CONTROL LOOP

where $-1/T_a$ and $-1/T_b$ are the roots of equation

$$s^2 + \frac{1}{T_2}(1 + 17.0\,T_{c1})s + \frac{17.0}{T_2} = 0$$

This gives

$$T_a = 180 \text{ mS} \quad \text{and} \quad T_b = 8.2 \text{ mS}.$$

5.7.2 Speed Control Loop:

This simplified transfer function $G_c^*(s)$ of current loop is used for studying the speed control loop. This loop has a PI controller with transfer function

$$G_{\omega c}(s) = \frac{k_2(1+sT_{c2})}{s}$$

where $T_{c2} = 825$ mS and

$k_2 = 18.45$, includes the gain of a limiter.

The design procedure for k_2 and T_{c2} is similar to that of current control loop (refer Section 3.8).

The tacho-generator filter and potential divider are adjusted such that

$$H_\omega(s) = 0.0386/(1+sT_g)$$

where $T_g = 62.0$ mS. The design procedure for $H_\omega(s)$ is given in Section 2.8.

The transfer function,

$$G_{\omega}(s) = \frac{\Delta\omega}{\Delta I_d}(s) = \frac{E}{\omega_s f}\,\frac{1}{1+sT_m} = \frac{0.303}{1+sT_m} \qquad (5.30)$$

and consequently, loop gain

$$G_{\omega c}G_c^{*}G_{\omega}H_{\omega}(s) = \frac{18.45(1+sT_{c2})}{s}\,\frac{10.0(1+sT_{c1})}{(1+sT_a)(1+sT_b)}\,\frac{0.303}{1+sT_m}\,\frac{0\ 0386}{1+sT_g} \qquad (5.31)$$

Expressing loop gain = A(s) B(s)

where

$$A(s) = \frac{3.03(1+sT_{c1})}{(1+sT_a)(1+sT_b)(1+sT_m)(1+sT_g)}$$

and

$$B(s) = \frac{18.45 \times 0.0386(1 + sT_{c2})}{s} \qquad (5.33)$$

Figure 5.6 gives Bode plots of A(s),B(s) and A(s).B(s). From bode plots it is observed that the cut-off frequency, $1/T_g$ of $H_{\omega}(s)$ is greater than the gain cross-over frequency of them system. This ensures that the presence of filter in the feedback path does not affect the system performance. The loop gain plot indicates that the system has phase margin of 60°. With the help of Nicols chart [19] it was observed that the system is stable and response is not oscillatory.

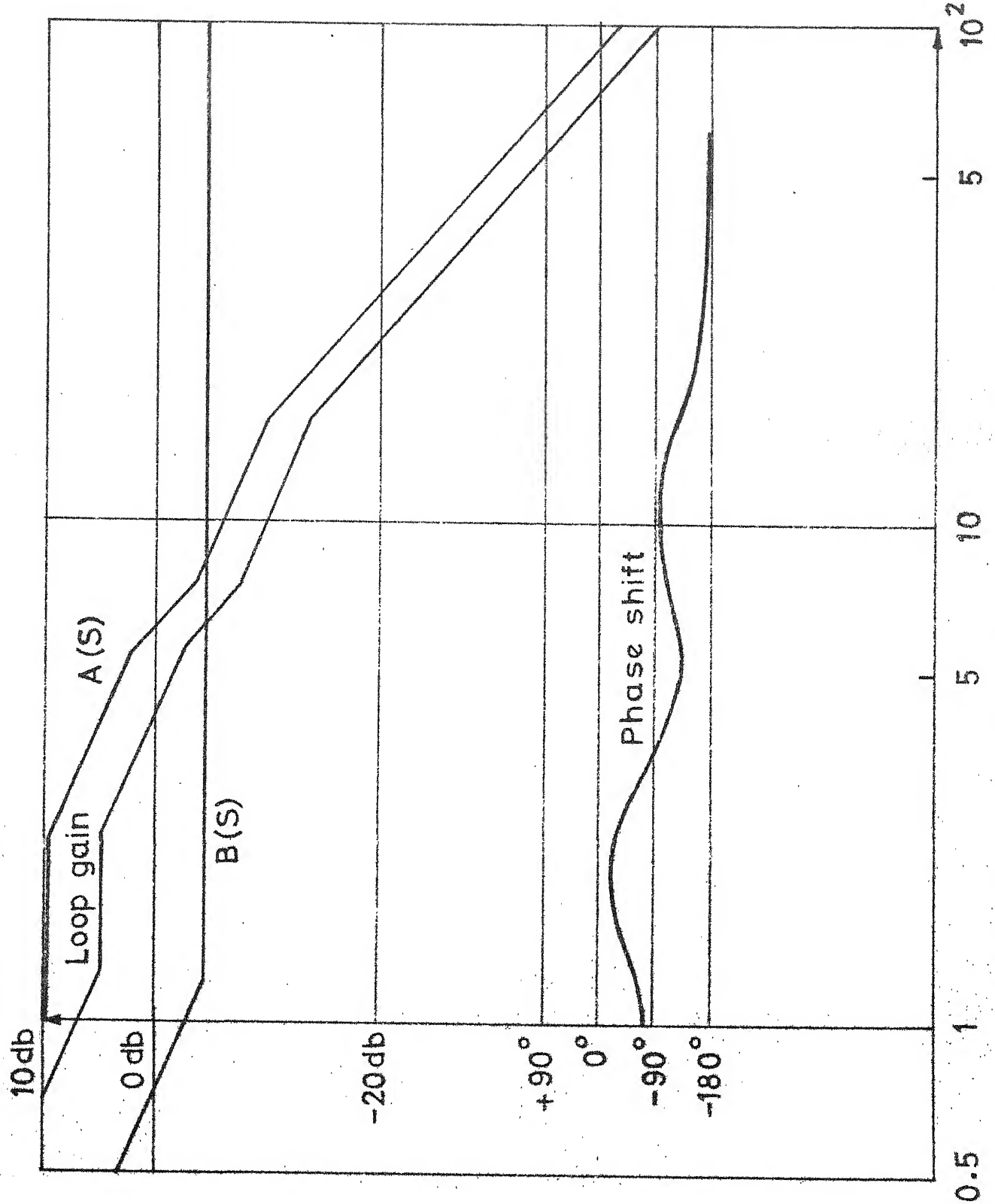

FIG.5.6 FREQUENCY RESPONSE-SPEED CONTROL LOOP

5.8 EXPERIMENTAL INVESTIGATIONS

The loading and testing arrangement for the drive is same as given in Section 2.9. Details of Induction Motor are given in Appendix A. The steady state characteristics of the drive (refer Section 4.10) with second order filter are given in Figure 4.13.

The initial condition of the drive is kept same as the operating point given in Section 5.5. And a step input is applied to the controller at different input points in order to obtain transient response of the motor speed, and rotor current. The response is recorded on the strip-chart recorder.

The open loop speed and current responses for 2.0 mS change in the ON period, t_1 are given in Figures 5.7(a) and 5.7(b) respectively.

Similarly Figure 5.8 gives the closed loop transient response with current feedback only. The step change in the current loop reference signal $\Delta e_c = 0.4V$.

The transient responses with speed and current feedbacks are given in Figure 5.9. The step change in speed control loop reference signal is $\Delta e_\omega = +0.02V$.

Since the controller does not have the provision to provide braking torque during retardation, only positive step inputs are applied as test signals.

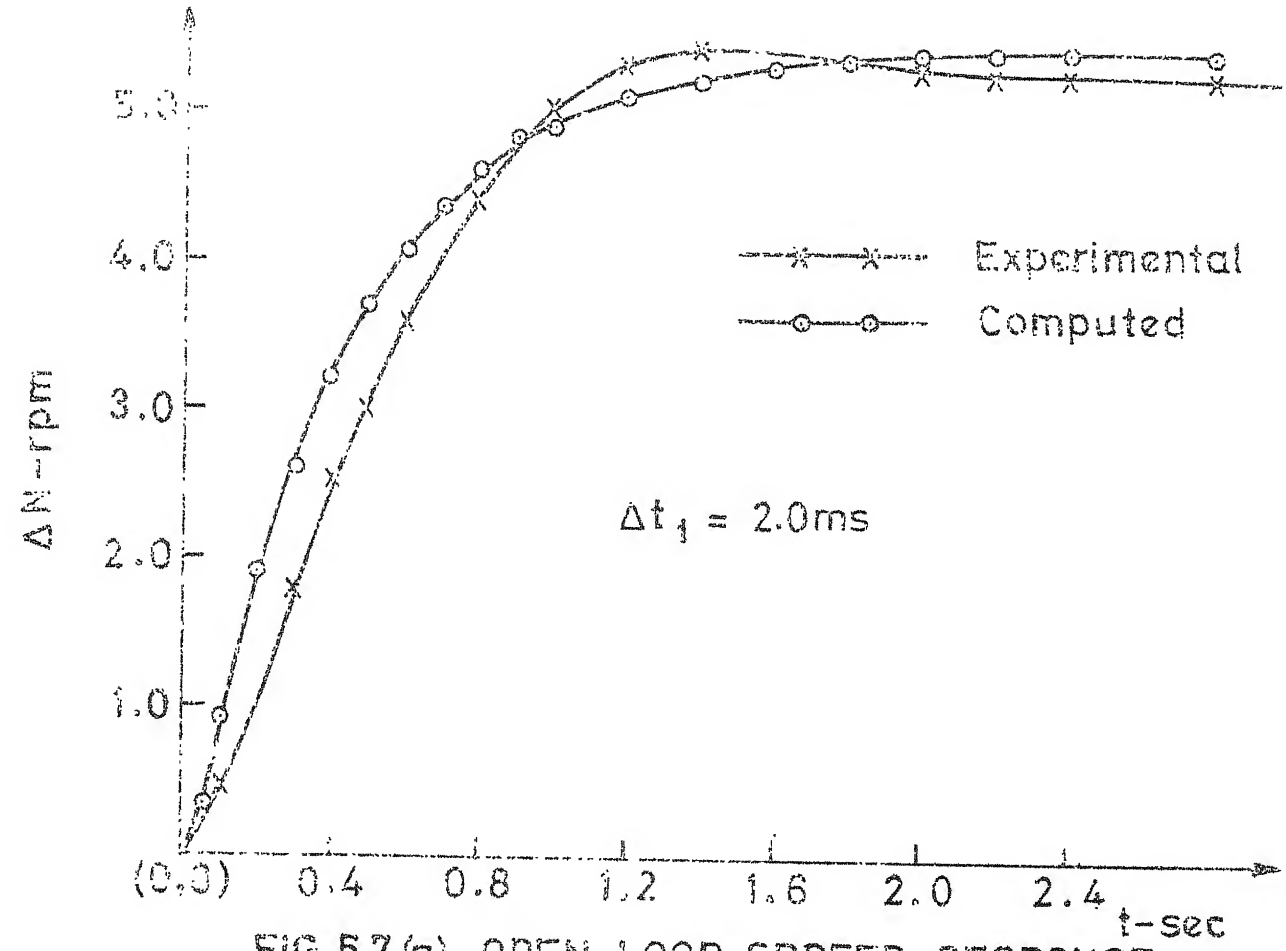

FIG. 5.7 (a) OPEN LOOP SPPEED RESPONSE

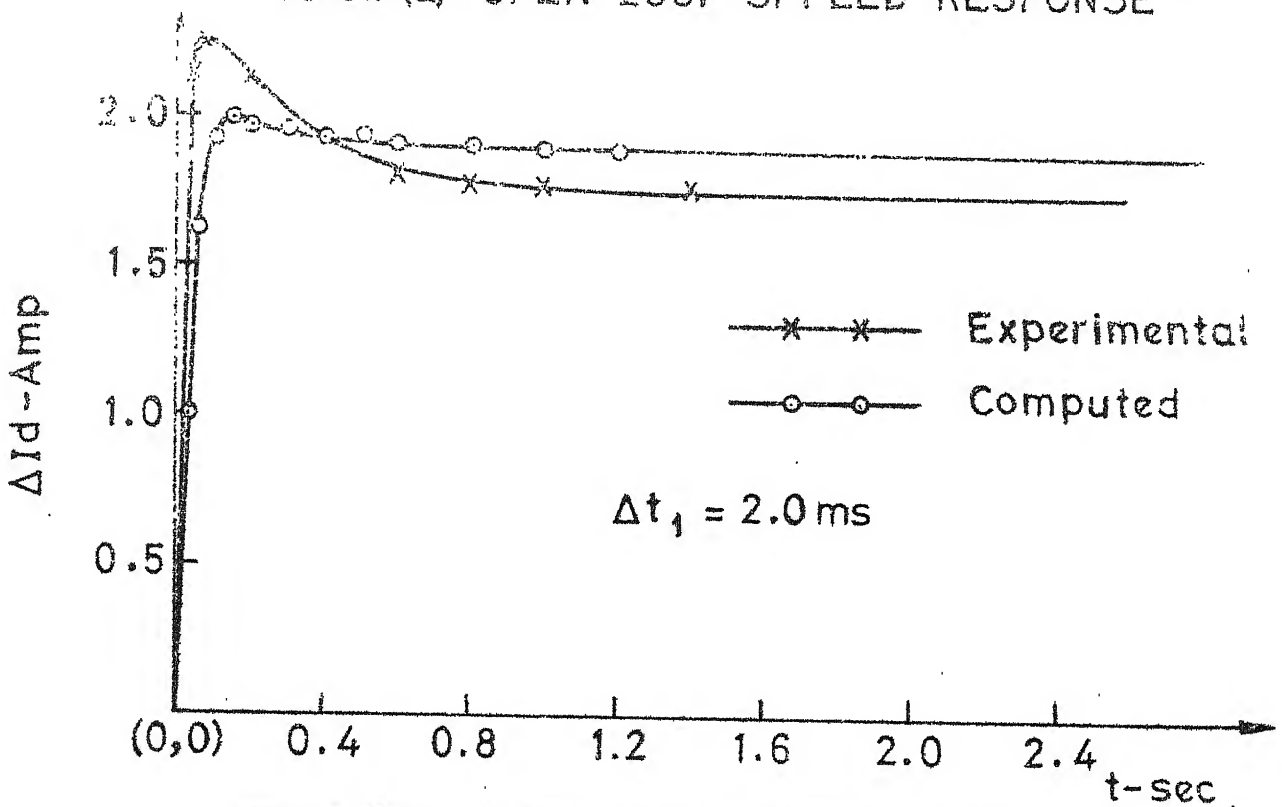

FIG. 5.7 (b) OPEN LOOP CURRENT RESPONSE

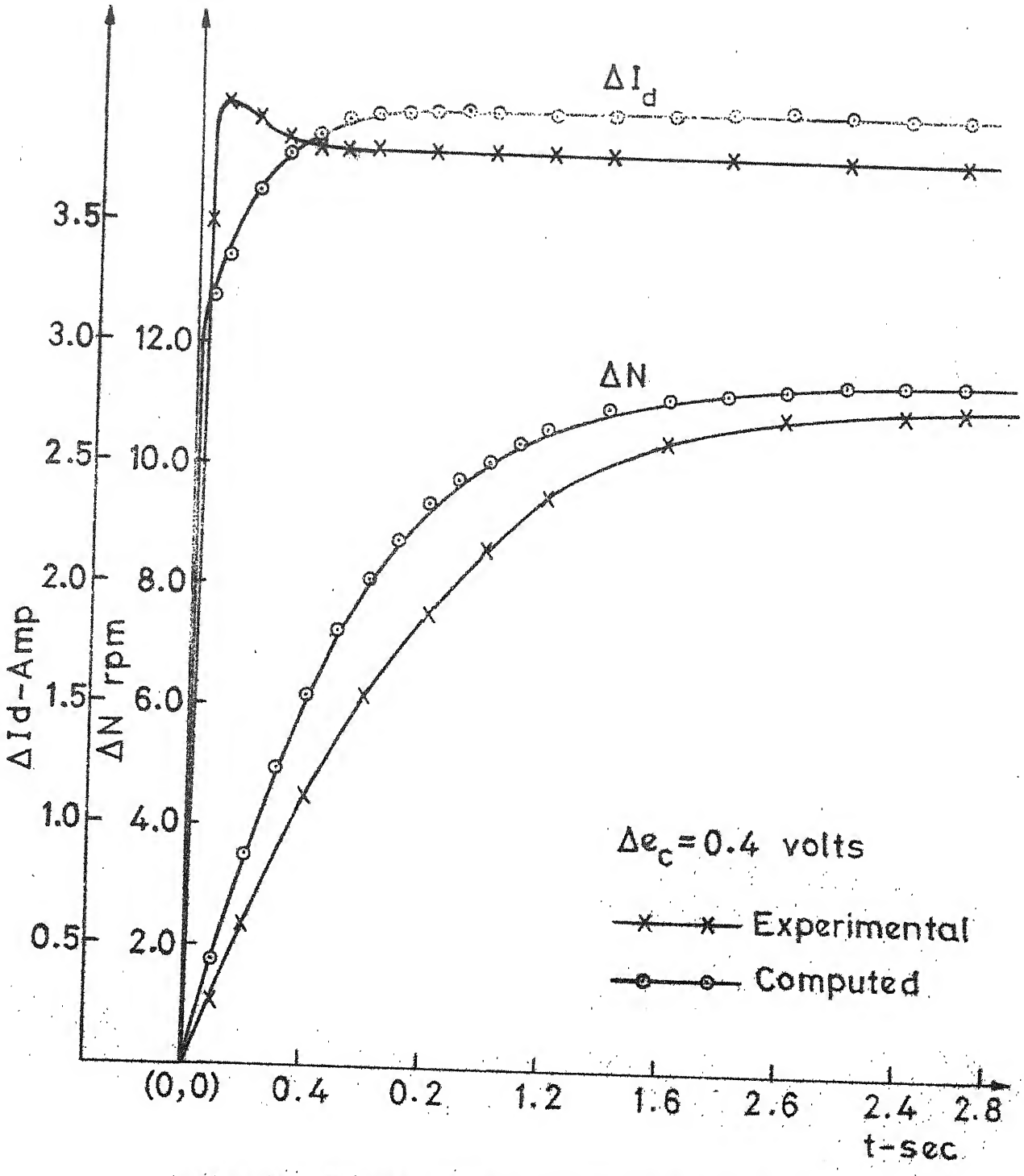

FIG.5.8 SPEED AND CURRENT RESPONSE WITH CURRENT FEEDBACK ONLY

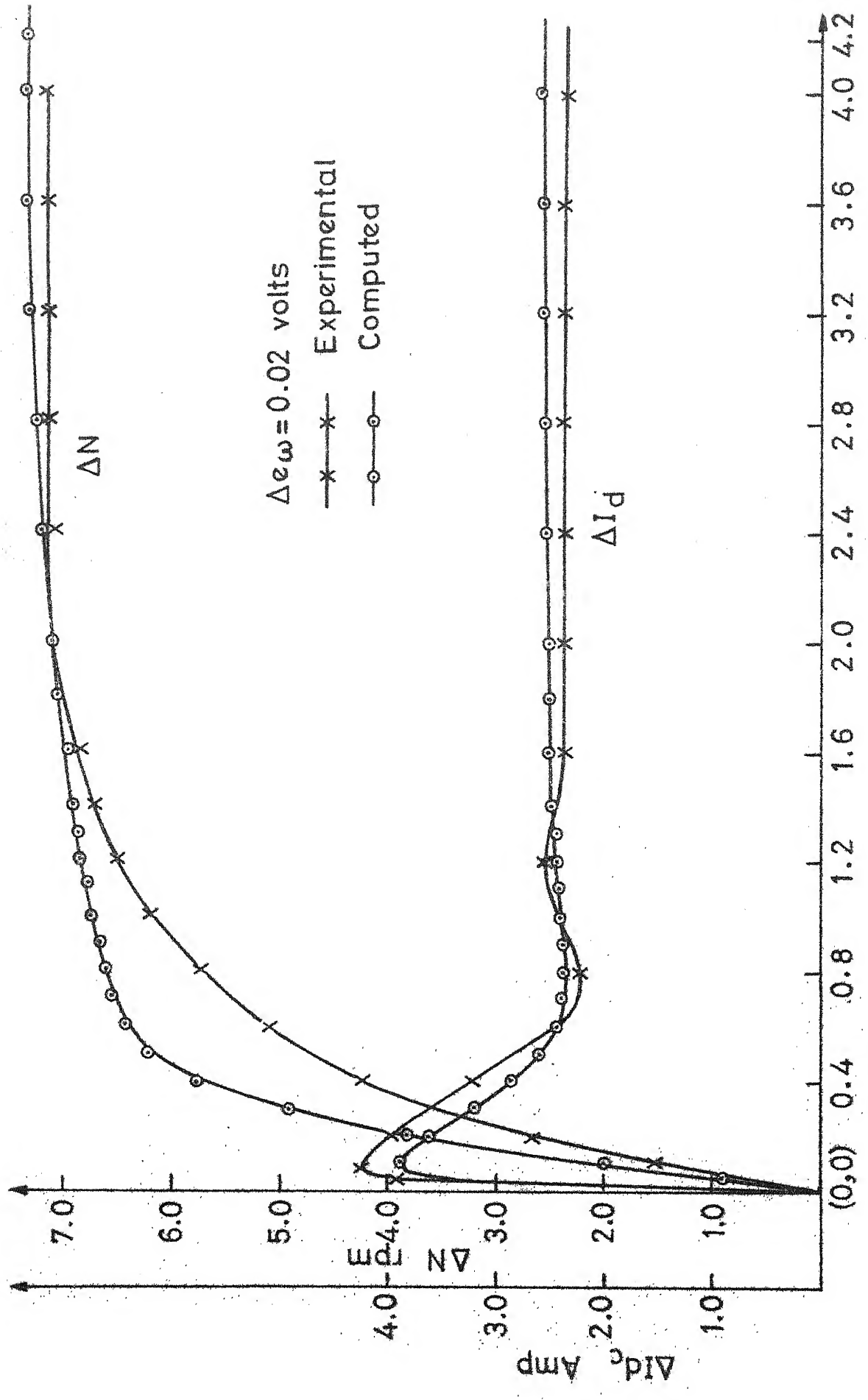

FIG.5.9 SPEED AND CURRENT RESPONSE WITH SPEED AND CURRENT FEEDBACK

5.9 DIGITAL COMPUTER PROGRAM

After labelling the appropriate current, speed and controller output voltages as state variables (refer Figures 5.2, 5.3 and 5.4), transfer functions for open and closed loop controller are written in state variable form as given below. Let

$X_1 = \Delta\omega$

$X_2 = I_d$

X_3 = Delayed change in rotor current due to chopper time constant.

X_4 = Average current feedback signal.

X_5 = Current controller output = Δe_1

X_6 = Speed feedback signal

X_7 = Speed controller output = Δe_c

Δe_ω = Speed control loop reference signal.

The system equations are

$$\frac{d}{dt} X_1 = \frac{E}{\omega_s f} \frac{X_2}{T_m} - \frac{\Delta T_L}{f T_m} - \frac{X_1}{T_m} \qquad (5.34)$$

$$\frac{d}{dt} X_2 = \frac{X_3}{T_f} - \frac{I_{do}}{S_o \omega_s} \frac{X_1}{T_f} - \frac{X_2}{T_f} \qquad (5.35)$$

$$\frac{d}{dt} X_3 = \frac{f_1 X_5 - X_3}{T_c} \qquad (5.36)$$

$$\frac{d}{dt} X_4 = \frac{H_c X_2 - X_4}{T_c} \qquad (5.37)$$

$$\frac{d}{dt} X_5 = k_1(X_7 - X_4) + k_1 T_{c1} \frac{d}{dt}(X_4 - X_7) \qquad (5.38)$$

$$\frac{d}{dt} X_6 = \frac{H_\omega X_1 - X_6}{T_g} \qquad (5.39)$$

$$\frac{d}{dt} X_7 = k_2(\Delta e_\omega - X_6) - k_2 T_{c2} \frac{d}{dt} X_6 \qquad (5.40)$$

The Runge-Kutta fourth order approximation method was used to solve these equations simultaneously.

Using this program the small signal response for mooor speed and rotor current is obtained for the following cases:

i) open loop

ii) closed loop with current feedback only

iii) closed loop with speed and current feedback.

Equations (5.34), (5.35) and (5.36) are used to study the dynamic response of the open loop drive, where $X_5 = \Delta e_1$ is input to the controller. Similarly, equations (5.34) to (5.38) are used for studying the system response when only current feedback is effective. In this case $X_7 = \Delta e_c$ is input to the system. For studying the response when both the feedbacks are effective, equations (5.34) to (5.40) are used and Δe_ω is input to controller.

The transient response is computed for the same operating point around which transfer functions are computed in the previous sections. The initial values of the system variables are assumed to be zero as the system is in steady state before the disturbance. The same program can be used to compute transient response for load perturbations.

Comparison of computed and experimentally obtained transient response is given in Figures 5.7, 5.8 and 5.9.

5.10 CONCLUSIONS

For small perturbations of input signals around a given operating point, the small signal model developed gives good accuracy. The same model is useful in designing a closed loop controller with predictable performance.

Analytically it can be shown, and experimentally it was observed that for $\tau_2 >> \tau_1$ the relation between I_d and duty cycle is highly nonlinear. This makes it highly sensitive to duty cycle changes in lower range and insensitive in higher range.

A slipring motor with filter and closed loop speed control can replace dc motor in some of the applications.

CHAPTER 6

CONCLUSION

The detailed analysis and design of thyristor controllers for slipring induction rotor is given in the previous chapters. This study is limited to i) sub-synchronous slip power recovery scheme, and ii)chopper controlled rotor resistance technique. These methods are simple, economical and give wide range speed control compared to the other methods of speed control for slipring induction motor. The summary of work done and concluding remarks are given in this chapter.

6.1 REVIEW OF THE WORK DONE AND CONCLUSIONS

The aim of the present thesis as mentioned in Chapter 1 is to study the slip power recovery and rotor resistance control methods applicable to the slipring motor, and propose mathematical models of the drive system for the analysis of steady state and dynamic performance.

The slip power recovery scheme discussed in this thesis has a provision of returning slip power to the supply lines. This makes the drive highly

efficient compared to when stater voltage control or rotor resistance control methods are used. The power circuit and associated control circuits for sub-synchronous operation are simple and economical compared to stator voltage and frequency control. Hence slip power controller is a highly economical alternative for controlling high power (100 kW and above) drives. The recovered rotor power causes overall reduction in the motor power factor. However, alternative arrangements giving improved power factor give higher distortion factor.

The other method of controlling slipring motor discussed in the thesis, is by thyristor chopper control on rotor side. Though this method of control is simple its application is limited to low and medium power drives due to its poor efficiency at low speeds of operation. With this type of controller, unlike stator voltage control method, there is no reduction in maximum torque developed by motor. The problems associated with simple chopper circuit on rotor side are highly distorted rotor current waveforms and high voltage spikes across thyristor switch. A second order filter between rectifier and chopper gives ripple free winding currents and relieves thyristor of high voltage

spikes and at the same time gives wider variation in th speed torque characteristics of the drive. However, in practice introduction of second order filter increases the minimum permissible ON period of the chopper, the reason being commutation circuit limitations. If inverter grade thyristors are used it will be easier to realise the advantages of second order filter.

For slip power controller speed torque characteristics are similar to that of separately excited dc motor. Therefore, it is easy to obtain linear transfer functions that will hold good over a wide range of operation. For chopper controlled slipring motor, rotor current versus duty cycle characteristics are highly nonlinear. Hence the transfer functions are obtained only for small perturbations around the given operating point. The closed loop control system, complete with speed and current feedbacks is designed for slip power recovery and chopper controlled drive.

The following are the contributions made in this thesis.

1. A DC circuit model is developed for the slip power recovery scheme. It is observed that this model gives better accuracy compared to ac circuit

model. The reason being, in ac circuit model, it is not possible to take into account commutation effect of converters. (13)

2. Complete design of closed loop controller for slip power recovery scheme is given. A PI controller is used in speed control loop. This loop contains another inner loop with PI controller for current control. The closed loop speed torque characteristics of the drive are almost flat giving speed regulation better than 0.5 percent.

3. A dynamic model for slip power recovery based on certain simplifying assumptions is developed. This model is used for the analysis and design of closed loop controller, with predictable accuracy.

4. For chopper controlled drive without filter or with first order filter, the permissible variation in speed torque characteristics is limited by high voltage spikes across thyristor. The superior arrangement of using second order filter is given. With this method it is possible to obtain the wide variation in speed-torque characteristics.

5. A dc circuit model for chopper controlled drive is similar to that of slip power recovery scheme. A procedure for determining steady state current waveform

based on this model is given. The motor winding leakage reactance is treated as inductance while computing transients during ON or OFF mode of chopper operation and as equivalent resistance for computing the loss in terminal voltage due to commutation overlap.

6. A novel high speed current averaging circuit is developed. This circuit samples and holds the minimum and maximum values of rotor current for each cycle and outputs the average value for that cycle. This circuit gives average current feedback signal without introducing large time constant in the feedback path.

7. Since rotor circuit time constants are different for ON and OFF modes of operation, the relation between rotor current I_d and chopper duty cycle is highly nonlinear. The transfer functions are obtained by linearizing this relation for small perturbations around the given operating point. These transfer functions are used for the analysis and design of closed loop controller. The design of closed loop controller for chopper controlled slipring motor is similar to that of slip power recovery scheme.

LIST OF REFFRENCES

1. D.A. Paice, 'Induction motor speed control by stator voltage control', IEEE Transactions on Power Apparatus and Systems, Vol. PAS-87, pp. 585-590, Feb. 1968.

2. B. Ilango, 'Analysis of thyristor controlled DC and AC motors', Ph.D. Thesis, August 1971, I.I.T. Kanpur.

3. M. Ramamoorty, Thyristors and Their Applications, East West Press, 1977.

4. E.E. Ward, 'Inverter suitable for operation over a range of frequency', Proceedings IEE, Vol.111, pp. 1423-1434, August 1964.

5. K.P. Phillips, 'Current source inverter for ac motor drives', IEEE Transactions on Industry Applications, Vol. IA-8, pp. 679-683, Nov./Dec.1972.

6. H. Warutani, Y. Jifuku and N. Hirawa, '2100 kW Thyristor Scherbius set for Osaka City Water Works Bureau', Hitachi Review, Vol. 19, No.4, pp.146-152, 1970.

7. W. Shepherd and J. Stanway, 'Slip power recovery in an induction motor by the use of a thyristor inverter', IEEE Transactions on Industry and General Applications, Vol. IGA-5, pp. 74-82, Jan./Feb. 1969.

8. E. Ohno and M. Akamatsu, 'Secondary Excitation of an induction using a self controlled inverter (Super-synchronous thyristor Scherbius system)', Electrical Engineering in Japan, Vol.88, No.10, pp. 76-86, October 1968.

9. H. Kazuno, 'A wide-range speed control on an induction motor with static Scherbius and Kramer systems', Electrical Engineering in Japan, Vol.89, No.2, pp. 10-19, Feb. 1969.

10. P.N.Miljanic, 'The through-pass inverter and its application to the speed control of wound rotor induction machines, IEEE Transactions on Power Apparatus and Systems, Vol.87, pp. 234-239, Jan.1968.

11. W. Shepherd and A.Q. Khalil, 'Capacitive compensation of thyristor controlled slip-energy-recovery system', Proceedings IEE, Vol.117, p 948, May 1970.

12. D.A. Paice, 'Speed control of large induction motors by thyristor converters, IEEE Transactions on Industry and General Applications, Vol.IGA-5, pp. 545-551, Sept./Oct. 1969.

13. A. Lavi and R.I. Polge, 'Induction motor speed control with static inverter in the rotor', IEEE Transactions on Power Apparatus and Systems, Vol.PAS-85, pp.76-84, January 1966.

14. P.C. Sen and K.H.J.Ma, 'Rotor chopper control for induction motor drive: TRC Strategy', IEEE Transactions on Industry Applications, Vol. IA-11, pp.43-49, Jan./Feb.1975.

15. Moltgen Gottfried, Line Commutated Thyristor Converters, Pitman Publishing, 1972.

16. B.R. Pelly, 'Thyristor Phase-Controlled Converters and Cycloconverters. Operation, Control and Performance, Wiley Inter-science, 1971.

17. T. Krishnan and B. Ramaswamy, 'A Fast-Response DC motor speed control systems', IEEE Transactions on Industry Applications, Vol.IA-10, p. 643, Sept./Oct. 1974.

18. H. Elger and M.A. Weiss, 'A sub-synchronous static converter cascade for variable speed boiler feed pump drives', Siemens Review, Vol.35, p. 405-1968.

19. B.C.Kuo, 'Automatic Control System, Prentice Hall 1967.

20. M. Ramamoorty and B. Ilango, 'The transient response of a thyristor controlled series motor', IEEE Transactions on Power Apparatus and Systems, Vol. PAS-90, pp. 289-297, 1971.

21. F.A. Parrish and E.S. McVey, 'A theoretical model for single phase silicon controlled rectifier systems', IEEE Transactions on Automatic Control, pp. 577-579, Oct. 1967.

22. M. Arunachalam, 'Solid State Control of induction motors', Ph.D. Thesis, Nov. 1977, I.I.T.Kanpur.

23. P.R. Basu, 'Variable speed induction motor using thyristors in the secondary circuit', IFFE Transactions on Power Apparatus and Systems, Vol. PAS-90, pp. 509-514, March/April 1971.

24. M. Ramamoorty and M. Arunachalam, 'A solid state controller for slipring induction motors', IEEE Annual Meeting on Industry Applications, 1977.

25. K. Heumann, 'Pulse control of dc and ac motors by silicon-controlled rectifiers, IEEF Transactions on Communication and electronics, Vol.83, pp.390-399, July 1964.

26. B.I. Doyle and R.J. Woodall, 'Adjustable speed drives using AC wound rotor motors', Control Engineering, pp. 48-50, June 1973.

27. N.S. Wani and M. Ramamoorty, 'Chopper controlled slipring induction motor with closed loop control', IEEE Transactions on Industrial Electronics and Control Instrumentation, Vol. IFCI-24, pp. 153-161, May 1977.

28. M. Ramamoorty, Waltman and N.S.Wani, 'Chopper controlled slipring induction motor', Journal of Institution of Engineers, India, p.206, 1976.

29. B.D. Bedford and R.G.Hoft, Principle of Inverter Circuits, Wiley, 1964.

30. G.K. Dubey, S.K. Pillai and P.P. Reddy, 'Analysis and design of doubly fed chopper for speed control of slipring induction motors - Part I and II, IEEE Transactions on Industrial Electronics and Control Instrumentation, Vol.IECI-22, pp.522-538, 1975.

31. N.S. Wani and M. Ramamoorty, 'The transient response of chopper controlled slipring induction motor', A paper accepted for publication by IEFE Transactions on Industrial Electronics and Control Instrumentation.

APPENDIX A

THE DETAILS OF INDUCTION MOTOR AND LOAD

3-Phase Slipring Induction Motor -

3 HP, 1440 rpm, 400V

Rated stator current - 5.0A

Rated rotor voltage - 145.0V

Rated rotor current - 10.0A

Stator/rotor turns ratio n = 2.76

The per phase equivalent circuit parameters referred to stator and rotor are given given in Figure 2.9.

The moment of inertia of the set-up

$$J = 1.75 \text{ Kg-m}^2.$$

The coefficient of linear (viscous) friction around the given operating point is function of operating speed and the type of braking arrangement used. For this set-up, DC generator and eddy-current brake are available as load.

55705

Thesis
621.462
W186t

Date Slip A 55705

This book is to be returned on the date last stamped

CD 6 72 9

EE-1970-D-WAN-THY